AD_____

AWARD NUMBER: W81XWH-16-1-0188

TITLE: Ovarian Granulosa Cell Tumor: New Insights into the Clinical Challenge of Late Relapse

PRINCIPAL INVESTIGATOR: Dr. David B. Wilson

Contracting Organization: Washington University
St. Louis, MO 63130-4862

REPORT DATE: November 2018

TYPE OF REPORT: Final

PREPARED FOR: U.S. Army Medical Research and Materiel Command
Fort Detrick, Maryland 21702-5012

R□□□R□D□□□M□□□□□□□□□□□□□□□	Form Approved OMB No. 0704-0188

□R□□□R□D□□□□	□□R□□□R□□□□□□	3□D□□□□□□□□R□D□
November 2018	Final	15 Jul 2016 - 14 Jul 2018

□□□□□□□□□□D□□□□□□□□□

Ovarian Granulosa Cell Tumor: New Insights into the Clinical Challenge of Late Relapsee

□□□□R□□□□□M□□R□

□□□□R□□□□□M□□R□

W81XWH-16-1-0188

□□□□□R□□R□M□□□□M□□□□□□M□□R□

□□□□□□□R□□□

Dr. David Wilson

E-Mail: Wilson_d@wustl.edu

□d□□□R□□□□□□□M□□R□

□□□□□□□□□□M□□R□

□□□□□ □R□□□□□□□□M□□R

□□□□R□□RM□□□□□R□□□□□□□□□R□□□R□ □□M□□R

Washington University, The
One Brookings Drive
St. Louis, MO 63110-4862

□□□□□□□□□R□□□□M□□□□□R□□□□□□□□□□□□M□□□□□□□D□□DDR□□□□□□□□

□□□□□□□□□□R□M□□□□□R□□□□□□□□□□R□□□M□□□

U.S. Army Medical Research and Materiel Command
Fort Detrick, Maryland 21702-5012□

□□□□□□□□□□R□M□□□□□R□□□R□□□R□ □□M□□R□□□

□□□D□□□R□□□□□□□□□□□□□□□□□□□□□□□□□□□□□□□□M□□□

Approved for Public Release; Distribution Unlimited

□3□□□□□□□M□□□□R□□□□□□□

□□□□□□□□R□□□

Adult granulosa cell tumor (AGCT) is a unique subtype of ovarian cancer that accounts for 5% of all ovarian malignancies. AGCTs are diagnosed typically in perimenopausal women, suggesting that elevated serum gonadotropin levels may contribute to tumor development. The 5-year survival is 90-97% for patients with Stage I AGCT but is significantly worse for patients with higher stage or recurrent disease. The ostensibly favorable 5-year survival for individuals with low stage AGCT belies the major clinical problem of late relapse; one-third of women with Stage Ic AGCT suffer a relapse 6-8 years after initial diagnosis. Given the propensity for AGCT to relapse years after the initial diagnosis, more effective adjuvant therapies and surveillance strategies are needed. The objective of this two-year Ovarian Cancer Research Program (OCRP) Pilot Award was to explore whether hormonal modulation therapy may be beneficial in treatment of ACGT. Aim 1 of the project focused on development of a new xenograft model to assess the impact of estrogen replacement therapy and gonadotropin suppression therapy on the growth of AGCTs. Unfortunately, technical obstacles were encountered xenograft growth, limiting the conclusions that could be drawn from this portion of the study. Aim 2 used a large database of clinical specimens to evaluate the expression of druggable hormone targets in samples from patients with AGCT. We found that: 1) follicle stimulating hormone receptor (FSHR) is widely expressed in AGCTs, 2) serum follicle stimulating hormone (FSH) and inhibin B levels correlated inversely, suggesting that tumor-derived inhibin B affects pituitary FSH secretion, 3) CYP19A1 is expressed in a subset of AGCTs, and 4) ERβ is the main estrogen receptor in AGCTs and its expression is higher in recurrent tumors. Our study cohort was larger than any reported in the medical literature. The knowledge gleaned from this research should facilitate the design of future clinical trials and enhance the quality of life for women with AGCT, including military personnel and their family members.

□□□□□□□□□□□□RM□

Granulosa cell tumor; ovarian cancer; estrogen; gonadotropin; xenograft

□□□□□□□R□□□□□□□□□□□□□□□□□□□□□□□□			□□□□□M□□□□□□□ □□□□□□□R□□□	□□□□□□M□□R□ □□□□□□□□	□□□□□□□M□□□□R□□□□□□□□□□□□R□□□
□R□□□R□	□□□□□□□R□□□	□□□□□□□□□□□			□□□□□□□□□□□□□□□□□M□□R□ *(include area code)*
Unclassified	Unclassified	Unclassified	Unclassified		USAMRMC

1. **INTRODUCTION:** Narrative that briefly (one paragraph) describes the subject, purpose and scope of the research.

Adult granulosa cell tumor (AGCT) is a unique subtype of ovarian cancer that accounts for 5% of all ovarian malignancies. AGCTs are diagnosed typically in perimenopausal women, suggesting that elevated serum gonadotropin levels may contribute to tumor development. The 5-year survival is 90-97% for patients with Stage I AGCT but is significantly worse for patients with higher stage or recurrent disease. The ostensibly favorable 5-year survival for individuals with low stage AGCT belies the major clinical problem of late relapse; one-third of women with Stage I_c AGCT suffer a relapse 6-8 years after initial diagnosis. Given the propensity for AGCT to relapse years after the initial diagnosis, more effective adjuvant therapies and surveillance strategies are needed. The objective of this two-year Ovarian Cancer Research Program (OCRP) Pilot Award was to explore whether hormonal modulation therapy may be beneficial in treatment of ACGT. Our approach combined a preclinical mouse model with a clinical study. The specific aims of the grant were to: 1) use a new xenograft mouse model to assess the impact of estrogen replacement therapy (ERT) and gonadotropin suppression therapy on the growth of AGCTs, and 2) evaluate the expression of druggable hormone targets in samples from patients with AGCT, and determine whether these targets are associated with clinical outcomes.

2. **KEYWORDS:** Provide a brief list of keywords (limit to 20 words).

Granulosa cell tumor; ovarian cancer; estrogen; gonadotropin; xenograft

3. **ACCOMPLISHMENTS:** The PI is reminded that the recipient organization is required to obtain prior written approval from the awarding agency Grants Officer whenever there are significant changes in the project or its direction.

   What were the major goals of the project?
   List the major goals of the project as stated in the approved SOW. If the application listed milestones/target dates for important activities or phases of the project, identify these dates and show actual completion dates or the percentage of completion.

	Proposed completion date	Completion date or % completed
Major Task 1: Secure ACURO approval for animal studies	Oct 2016	Oct 2016
Specific Aim 1: Use a xenograft mouse model to assess the impact of ERT and gonadotropin suppression therapy on ACGT growth.		
Major Task 2: Assess xenograft tumor growth in response to OVX and hormone manipulation		
Subtask 1: Label the KGN cell line indelibly with luciferase + GFP	Nov 2016	Nov 2016
Subtask 2: Perform OVX or sham surgery on immunodeficient mice, initiate hormone manipulation therapy, and inoculate mice with KGN cells.	Feb 2017	Jan 2017
Subtask 3: Measure xenograft tumor growth with bioluminescent imaging (BLI) and analyze results.	July 2017	July 2018
Subtask 4: Perform qualitative validation (presence of estrogenic changes, IHC for markers, tumor analysis).	Sept 2017	25% (poor xenograft growth precluded completion)
Subtask 5: Measure and analyze serum hormone levels (E_2, FSH, LH, inhibin B, & AMH), tumor apoptosis via TUNEL assays, and tumor proliferation based on Ki-67 IHC.	Sept 2017	0% (poor xenograft growth precluded completion)
Major Task 3: Secure HRPO approval or exempt finding	Aug 2016	Sept 2016
Specific Aim 2: Evaluate the expression of druggable hormone targets in samples from patients with AGCT, and determine whether these targets are associated with clinical outcomes.		

Activity	Proposed completion date	Completion date or % completed
Major Task 4: Complete molecular profiling of AGCT specimens and correlate expression patterns and related data with clinical outcomes		
Subtask 1: Measure the expression patterns of hormone receptors and key enzymes linked to treatment responses. Perform intra-tissue steroid profiling.	July 2017	80% (intra-tissue steroid profiling pending)
Subtask 2: Analyze coded patient data to determine whether receptor and steroidogenic enzyme expression are associated with patient survival.	May 2018	July 2018
Subtask 3: Using coded patient data, evaluate the associations of receptor expression and serum hormone levels with tumor recurrence and response to treatment.	Jan 2018	July 2018
Subtask 4: Investigate whether ERT use before or after AGCT diagnosis is associated with recurrence using logistic regression.	Nov 2017	July 2018

What was accomplished under these goals?
For this reporting period describe: 1) major activities; 2) specific objectives; 3) significant results or key outcomes, including major findings, developments, or conclusions (both positive and negative); and/or 4) other achievements. Include a discussion of stated goals not met. Description shall include pertinent data and graphs in sufficient detail to explain any significant results achieved. A succinct description of the methodology used shall be provided. As the project progresses to completion, the emphasis in reporting in this section should shift from reporting activities to reporting accomplishments.

1) Major activities:

2) Specific objectives:

Specific Aim 1: Use a new xenograft mouse model to assess the impact of ERT and gonadotropin suppression therapy on the growth of AGCTs.

Specific Aim 2: Evaluate the expression of druggable hormone targets in samples from patients with AGCT, and determine whether these targets are associated with clinical outcomes.

3) Significant results or key outcomes:

Aim 1.

*Background***:** There is no consensus as to whether AGCT patients benefit from ERT or gonadotropin suppression therapy. The objective was to use a mouse xenograft model to assess the impact of these therapies on tumor growth.

*Goals***:** Determine the impact of ovariectomy (OVX), gonadotropin suppression therapy, or ERT on the growth of xenografts an immortalized human AGCT line (KGN).

*Methods***:**

- Assign mice randomly to OVX or intact groups.
- Beginning at 5 weeks of age (1 week prior to xenografting), randomize intact or OVX mice to treatment with either an inert placebo pellet, a slow-release E_2 pellet, or serial injections of a GnRH agonist (leuprorelin).
- One week later, inoculate the mice with a suspension of KGN cells that have been labelled with luciferase + GFP.

Accomplishments and key conclusions:

- The KGN cell line was labelled indelibly with luciferase + GFP.
- Mice were ovariectomized and subjected them to the aforementioned hormone treatments.
- We qualitatively validated the impact of hormonal manipulations (e.g.,estrogenic changes) in target organs such as uterine epithelium (Fig 1). Despite being immunodeficient, the mice tolerated OVX and hormonal manipulations.

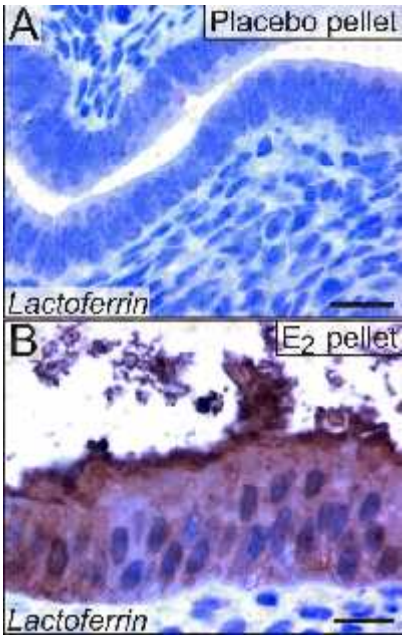

Fig 1. Impact of E_2 pellet on uterine morphology and gene expression. Lactoferrin, an estrogen-responsive gene, was used to validate the efficacy of hormonal manipulations. Bars = 15 µm.

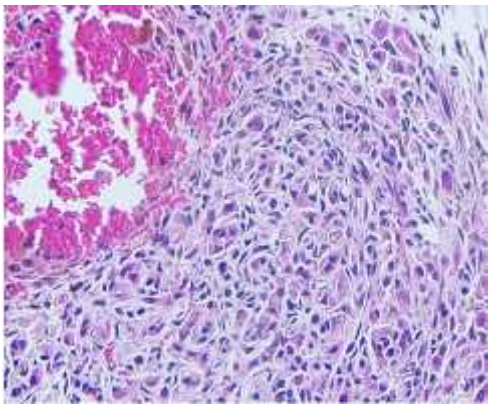

Fig 2. Histology of a 1 mm nodule resected from an immunodeficient mouse inoculated 3 months earlier with KGN cells. This nodule was located in the near the resected oviduct. ISH with a human-specific FOXL2 probe, showed that this was not a KGN-derived xenograft. We surmise that this nodule reflected ectopic mouse ovarian tissue.

Roadblocks encountered:

- The KGN xenografts did not grow under the initial conditions tried. In an effort to circumvent this obstacle, we systematically varied the inoculation conditions (e.g., cell passage number, dose of the inoculum, etc.) and extended the monitoring time. Despite these measures, we were to achieve consistent KGN xenograft growth in either ovariectomized or intact mice. On rare occasions, small nodules were seen in ovarietomized mice that had been inoculated with KGN cells (Fig 2); however, histological analysis of these nodules, including *in situ* hybridization with a human-specific FOXL2 probe, showed that these were not bona fide KGN-derived xenografts.
- Due to the lack of xenograft growth, we were unable to complete the BLI studies or the biochemical analysis of the xenografts and mouse serum samples.
- This technical hurdle with KGN xenografts was unanticipated, because prior reports in the literature had suggested that it was feasible to grow such xenografts (Jiang C et al., J Clin Endocrinol Metab. 2015;100:E852-860; Bilandzic M et al., *Cancer Lett*. 2014;354:107-114). We reached out to independent investigators in the field who, like use, were attempting to grow KGN xenografts in intact and ovariectomized mice; they encountered the same difficulties as we did. We conclude that, despite published reports, the KGN cell line is not amenable to xenografting.

Aim 2.

Background: There is no consensus as to whether AGCT patients benefit from ERT or gonadotropin suppression therapy.

Goals: Use tissue microarrays (TMAs) to characterize hormone receptor expression levels in tumors from a cohort of patients and look for possible clinical correlations (hormone receptors as prognostic or predictive markers).

Methods:

- Prepare TMAs on 175 tumor specimens
- Perform immunohistochemistry (IHC) on TMAs for key markers, including ERβ, GPER, CYP19AI, and ERα.
- Perform RNA ISH for FSH receptor (FSHR) and other key markers on these same TMAs.
- Use qPCR to measure mRNA expression levels on a limited number of tumor specimens (n ~ 30).
- Perform intra-tissue steroid profiling.
- Collect clinical data on hormone concentrations (FSH, LH, E_2, inhibin B, AMH) in patient sera, so as to correlate serum and tissue expression levels.

Accomplishments and key conclusions:

- *FSHR is widely expressed in AGCTs*. Since gonadotropins are speculated to play a role in AGCT progression, we characterized the expression of FSHR using RNA ISH on a TMA of 175 AGCTs. FSHR mRNA was detected in 90% of AGCTs (Fig 3), and the signal was strong or moderate in 60% of the tumors. *FSHR* expression was lower in tumors with high mitotic activity (p=0.01), but expression did not correlate with other clinical parameters such as tumor size, stage, or risk of recurrence.

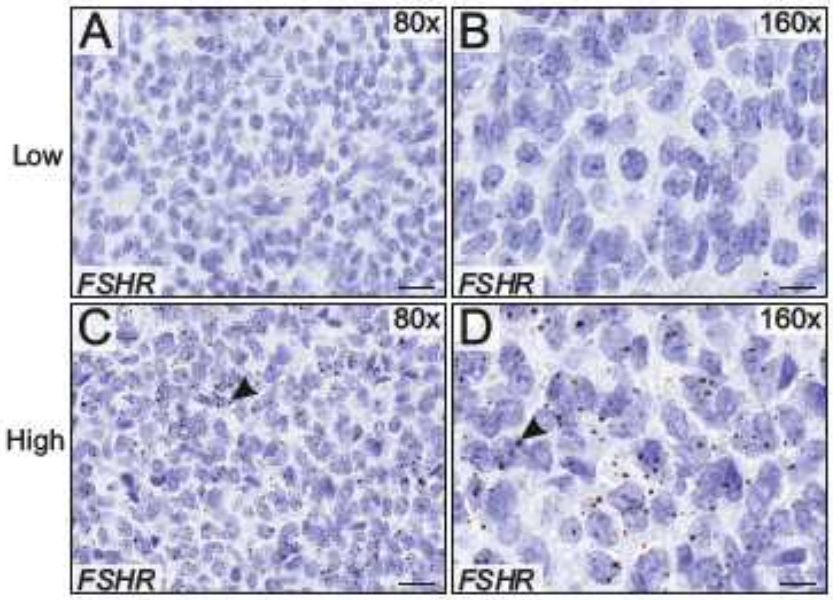

Fig 3. RNA in situ hybridization was used to quantify FSHR expression in the AGCT TMA. Representative images of low (A,B) and high (C,D) staining patterns. Original magnification 80 x and 160 x; bars = 20 µm.

- *Serum FSH and inhibin B levels correlated inversely, suggesting that tumor-derived inhibin B affects pituitary FSH secretion*. We analyzed FSH, E2 and inhibin B levels in 51 preoperative serum samples. FSH levels were generally low in AGCT patients, with median levels of 1.55 IU/l (range 0.05-15.3 IU/l) and 6.6 IU/l (range 0.1-60.3 IU/l) in premenopausal and postmenopausal patients, respectively. For E2 the median level was 0.125 nM (range 0.01-0.48 nM) in premenopausal patients and 0.15 nM (range 0.04-1.05 nM) in postmenopausal patients. Serum FSH levels were significantly lower in patients with large (>10 cm) vs. small tumors (p=0.001). FSH and E2 levels did not correlate with one other; however, FSH and inhibin B levels showed a strong inverse correlation (Spearman´s rho -0.75, p<0.0001), consistent with the suppressive effect of circulating inhibin B on FSH secretion from the pituitary. Inhibin B levels were higher in patients with larger tumors (p=0.01). Additionally, we assessed the preoperative serum FSH levels from synchronous samples of 36 AGCT patients whose tumors were represented in the TMA. We observed significantly increased tumor ERβ expression in patients with low serum inhibin B levels (p=0.04), suggesting diminished inhibin B – FSH feedback in high ERβ expressing AGCTs. We found no significant correlations between serum FSH or E2 levels and other estrogen receptors.

- *CYP19A1 is expressed in a subset of AGCTs.* Aromatase inhibitors have been used anecdotally in the treatment of relapsed AGCT. These drugs inhibit the synthesis of estrogens from androgen precursors by binding to aromatase (CYP19A1). To assess the expression of *CYP19A1* in AGCTs, we performed IHC and RNA ISH on the TMA. CYP19A1 immunoreactivity was detected in 48% of the tumors, and 17% showed moderate or strong staining (Figure 4E-H). CYP19A1 mRNA was detected in 15% of the tumor specimens by RNA ISH (Figure 4A-D). CYP19A1 mRNA expression correlated significantly with the moderate/high CYP19A1 protein expression ($p<0.0001$). CYP19A1 protein expression also correlated positively with ERβ expression ($p=0.009$). There were no correlations between CYP19A1 expression and clinical parameters such as tumor size, stage, or recurrence rate. Interestingly, CYP19A1 expression in the tumor tissue did not correlate with circulating E2, FSH, or inhibin B levels.

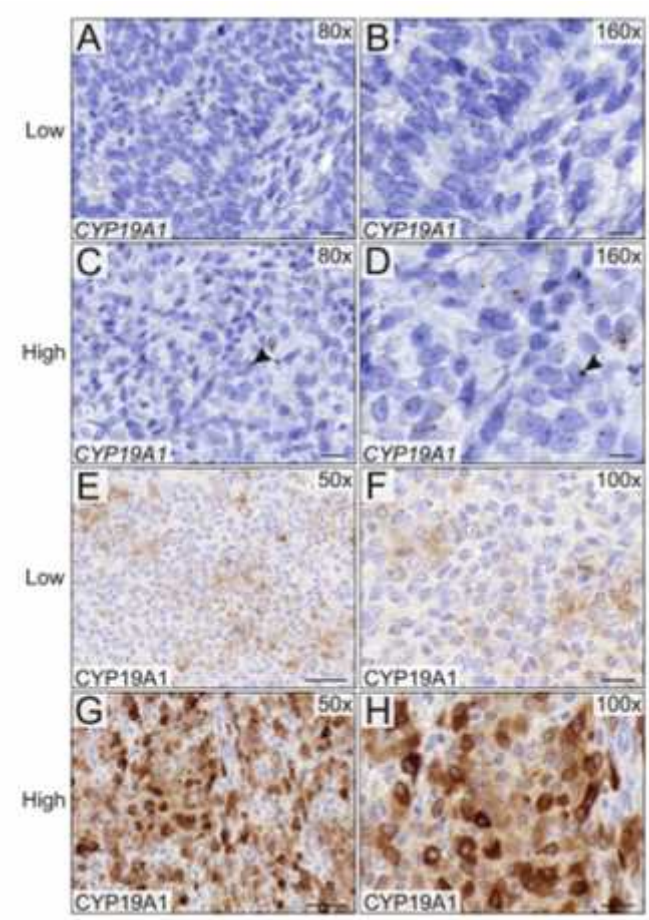

Fig 4. CYP19A1 expression was assessed in the TMA by RNA ISH (A-D) and IHC (E-H). Representative images of low (A-B, E-F) and high (C-D, G-H) staining AGCTs. Magnifications 80 x and 160 x; bars = 20 µm. Arrows indicate positively stained cells.

- *ERβ is the main estrogen receptor in AGCTs and its expression is higher in recurrent tumors.* We characterized estrogen receptor expression in the AGCT TMA using IHC or RNA ISH. ERα immunoreactivity was observed in 33% of the tumors, and ERβ protein was detected in 94% (Figure 5A-H). In the ERα-positive tumors, the staining pattern was nuclear in 59% and cytoplasmic in 48% of the tumors. ERβ immunoreactivity was exclusively nuclear and classified as moderate or strong in 67% of the tumors. *GPER1* mRNA expression was detected only in 14 % of the tumors by RNA ISH (Figure 5I-L). ERβ expression levels were significantly higher in recurrent AGCTs when compared to primary tumors (p=0.001). Furthermore, paired analysis of primary and recurrent samples from same patients demonstrated a significantly stronger ERβ immunoreactivity in the recurrent AGCTs (p = 0.0013) compared to the primary tumor (Figure 6A). A similar pattern between primary and recurrent samples was noted for GPER1 mRNA expression, although the levels of expression were low (Figure 6B). We found no correlation between any of the estrogen receptor expression patterns and tumor size, stage at primary diagnosis, recurrence rate, or menopause status at the time of sample retrieval. None of the estrogen receptors had prognostic significance in terms of disease-free or overall survival.

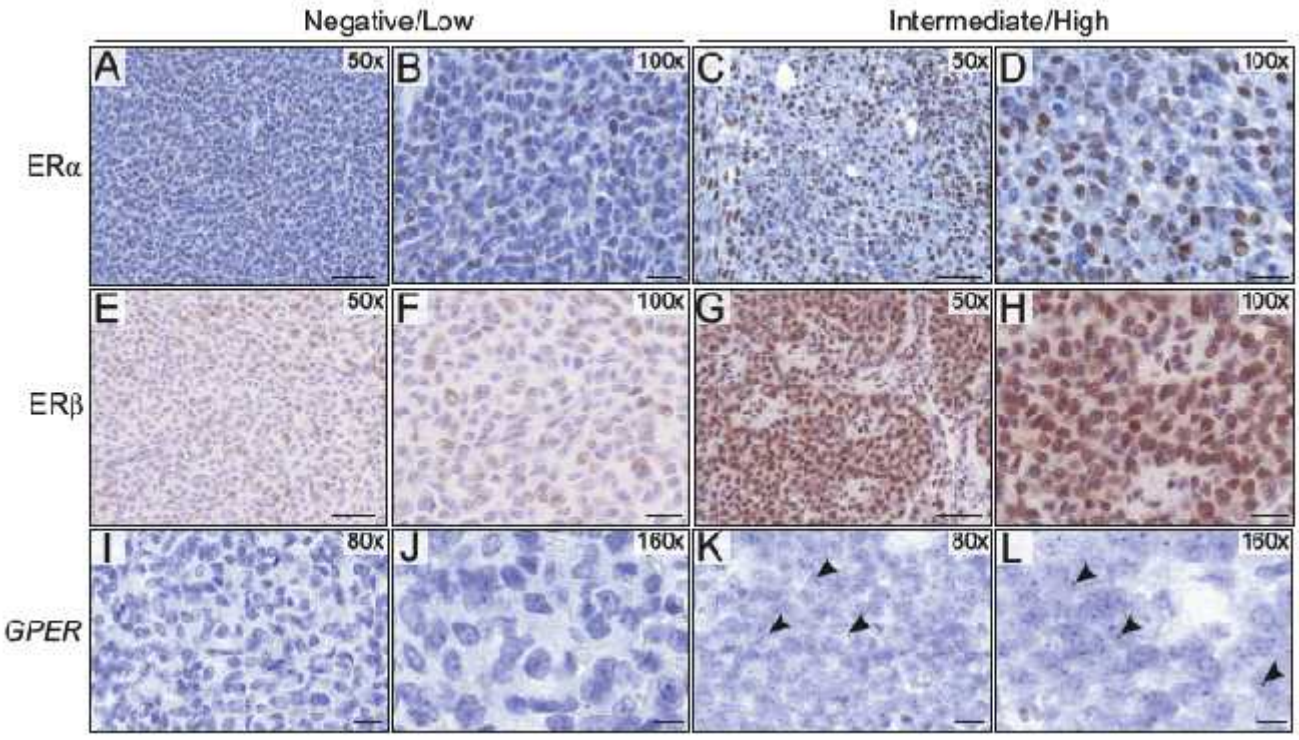

Fig 5. Expression of ERα and ERβ was assessed by IHC (A-H), and expression of GPER1 was determined by RNA ISH (I-L) using AGCT TMA. Representative images of low and high staining patterns, magnification 80 x and 160 x; bars = 20 µm.

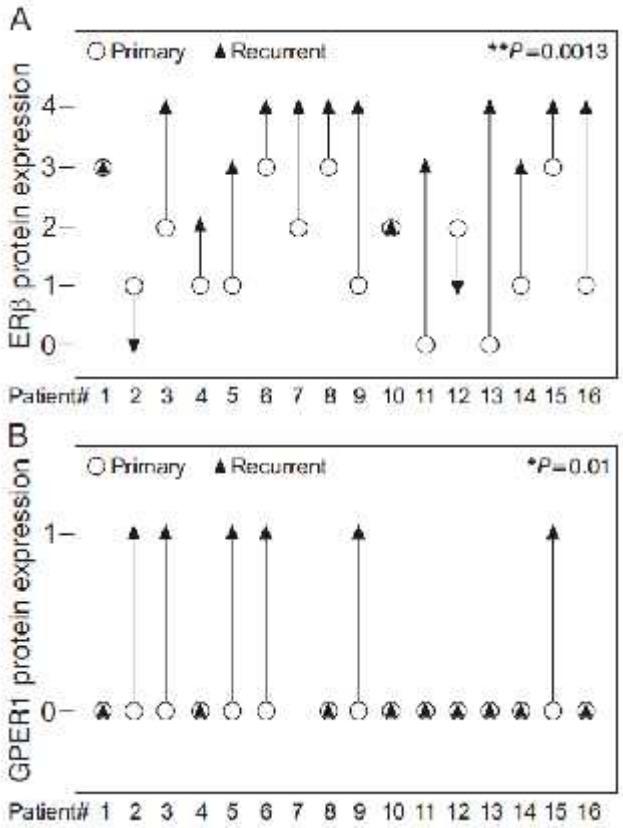

Fig 6. Paired analysis of the expression of estrogen receptors ERβ (A) and GPER1 (B) in 16 patients with both primary and recurrent tumor samples in the TMA. Both ERβ immunoreactivity and GPER1 mRNA expression were significantly increased in recurrent AGCTs compared with primary tumors.

What opportunities for training and professional development has the project provided?
If the project was not intended to provide training and professional development opportunities or there is nothing significant to report during this reporting period, state "Nothing to Report."

Describe opportunities for training and professional development provided to anyone who worked on the project or anyone who was involved in the activities supported by the project. "Training" activities are those in which individuals with advanced professional skills and experience assist others in attaining greater proficiency. Training activities may include, for example, courses or one-on-one work with a mentor. "Professional development" activities result in increased knowledge or skill in one's area of expertise and may include workshops, conferences, seminars, study groups, and individual study. Include participation in conferences, workshops, and seminars not listed under major activities.

Nothing to report.

How were the results disseminated to communities of interest?
If there is nothing significant to report during this reporting period, state "Nothing to Report."

Describe how the results were disseminated to communities of interest. Include any outreach activities that were undertaken to reach members of communities who are not usually aware of these project activities, for the purpose of enhancing public understanding and increasing interest in learning and careers in science, technology, and the humanities.

Nothing to report. We have submitted a manuscript for publication (see below).

What do you plan to do during the next reporting period to accomplish the goals?
If this is the final report, state "Nothing to Report."

Describe briefly what you plan to do during the next reporting period to accomplish the goals and objectives.

Nothing to report.

4. **IMPACT:** Describe distinctive contributions, major accomplishments, innovations, successes, or any change in practice or behavior that has come about as a result of the project relative to:

What was the impact on the development of the principal discipline(s) of the project?
If there is nothing significant to report during this reporting period, state "Nothing to Report."

Describe how findings, results, techniques that were developed or extended, or other products from the project made an impact or are likely to make an impact on the base of knowledge, theory, and research in the principal disciplinary field(s) of the project. Summarize using language that an intelligent lay audience can understand (Scientific American style).

The overarching goal of this project was to garner preclinical and clinical data to support the use of adjuvant therapy in patients with AGCT. The preclinical studies (Aim 1) entailed a novel mouse xenograft model that relied on OVX to recapitulate to the menopausal hormonal milieu present in patients with AGCT. As detailed elsewhere in this report, technical hurdles (poor growth of KGN cell-derived xenografts) limited the conclusions that could be drawn from this part of the study. Our original hope was that the xenograft model could be used and adapted to test the impact of pharmacologic agents on tumor progression. Unfortunately, this was not feasible. It is possible that patient-derived xenografts might grow better than KGN-derived cells in our OVX model, and future experiments may explore this possibility. Although difficulties were encountered with the preclinical model, our clinical studies (Aim 2) were successful. We were able to leverage a rich clinical database coupled to patient blood and tissue samples to gain insights into molecular characteristics in AGCT and to correlate these findings with clinical outcomes. Our study cohort is larger than any reported in the medical literature. The knowledge gleaned from this research should facilitate the design of future clinical trials and enhance the quality of life for women with AGCT, including military personnel and their family members.

What was the impact on other disciplines?
If there is nothing significant to report during this reporting period, state "Nothing to Report."

Describe how the findings, results, or techniques that were developed or improved, or other products from the project made an impact or are likely to make an impact on other disciplines.

Nothing to report

What was the impact on technology transfer?
If there is nothing significant to report during this reporting period, state "Nothing to Report."

Describe ways in which the project made an impact, or is likely to make an impact, on commercial technology or public use, including:

- *transfer of results to entities in government or industry;*
- *instances where the research has led to the initiation of a start-up company; or*
- *adoption of new practices.*

Nothing to report

What was the impact on society beyond science and technology?
If there is nothing significant to report during this reporting period, state "Nothing to Report."

Describe how results from the project made an impact, or are likely to make an impact, beyond the bounds of science, engineering, and the academic world on areas such as:

- *improving public knowledge, attitudes, skills, and abilities;*
- *changing behavior, practices, decision making, policies (including regulatory policies), or social actions; or*
- *improving social, economic, civic, or environmental conditions.*

Nothing to report

5. **CHANGES/PROBLEMS:** The Project Director/Principal Investigator (PD/PI) is reminded that the recipient organization is required to obtain prior written approval from the awarding agency Grants Officer whenever there are significant changes in the project or its direction. If not previously reported in writing, provide the following additional information or state, "Nothing to Report," if applicable:

Changes in approach and reasons for change
Describe any changes in approach during the reporting period and reasons for these changes. Remember that significant changes in objectives and scope require prior approval of the agency.

Nothing to report

Actual or anticipated problems or delays and actions or plans to resolve them
Describe problems or delays encountered during the reporting period and actions or plans to resolve them.

As detailed elsewhere in this report, technical hurdles (poor growth of KGN cell-derived xenografts) limited our ability to test the impact of pharmacologic agents on tumor progression. Patient-derived xenografts might grow better than KGN-derived cells in our OVX model, and future experiments may explore this possibility. Alternatively, primary cultures of AGCTs could be used to study the impact of E2 and other agents on tumor cell growth *in vitro*.

Changes that had a significant impact on expenditures

Describe changes during the reporting period that may have had a significant impact on expenditures, for example, delays in hiring staff or favorable developments that enable meeting objectives at less cost than anticipated.

Nothing to report

Significant changes in use or care of human subjects, vertebrate animals, biohazards, and/or select agents

Describe significant deviations, unexpected outcomes, or changes in approved protocols for the use or care of human subjects, vertebrate animals, biohazards, and/or select agents during the reporting period. If required, were these changes approved by the applicable institution committee (or equivalent) and reported to the agency? Also specify the applicable Institutional Review Board/Institutional Animal Care and Use Committee approval dates.

Significant changes in use or care of human subjects

N/A

Significant changes in use or care of vertebrate animals.

None

Significant changes in use of biohazards and/or select agents

None

6. PRODUCTS: List any products resulting from the project during the reporting period. If there is nothing to report under a particular item, state "Nothing to Report."

) **Publications, conference papers, and presentations**

Report only the major publication(s) resulting from the work under this award.

Journal publications. *List peer-reviewed articles or papers appearing in scientific, technical, or professional journals. Identify for each publication: Author(s); title; journal; volume: year; page numbers; status of publication (published; accepted, awaiting publication; submitted, under review; other); acknowledgement of federal support (yes/no).*

Dörner J, Rodriguez VM, Ziegler R, Röhrig T, Cochran RS, Götz RM, Levin MD, Pihlajoki M, Heikinheimo M, Wilson DB. $GLI1^{+}$ progenitor cells in the adrenal capsule of the adult mouse give rise to heterotopic gonadal-like tissue. *Mol Cell Endocrinol*. 2016;441:164–175; status of publication (published); acknowledgement of federal support (yes).

Penny GM, Cochran RB, Pihlajoki M, Kyrönlahti A, Schrade A, Häkkinen M, Toppari J, Heikinheimo M, Wilson DB. Probing GATA factor function in mouse Leydig cells via testicular injection of adenoviral vectors. *Reproduction* 2017;154:455–467; status of publication (accepted); acknowledgement of federal support (yes).

Haltia U-M, Pihlajoki M, Andersson N, Mäkinen L, Tapper J, Horlings HM, Turpeinen U, Anttonen M, Bützow R, Unkila-Kallio L, Carpén O, Wilson DB, Heikinheimo M, Färkkilä A. Functional profiling of FSH and estradiol in ovarian granulosa cell tumors; status of publication (submitted); acknowledgement of federal support (yes).

Books or other non-periodical, one-time publications. *Report any book, monograph, dissertation, abstract, or the like published as or in a separate publication, rather than a periodical or series. Include any significant publication in the proceedings of a one-time conference or in the report of a one-time study, commission, or the like. Identify for each one-time publication: Author(s); title; editor; title of collection, if applicable; bibliographic information; year; type of publication (e.g., book, thesis or dissertation); status of publication (published; accepted, awaiting publication; submitted, under review; other); acknowledgement of federal support (yes/no).*

Wilson DB, Pihlajoki M. Physiology of the adrenal cortex. In: Martini L, Huhtaniemi I, eds. *Reference Module in Biomedical Sciences* ISBN 9780128012383, http://dx.doi.org/10.1016/B978-0-12-801238-3.95735-0: Elsevier; 2016; status of publication (published); acknowledgement of federal support (yes).

Pihlajoki M, Heikinheimo M, Wilson DB. Regulation of adrenal steroidogenesis. In: Levine AC, eds. *Adrenal Disorders: Physiology, Pathophysiology and Treatment* New York: Springer; 2017; status of publication (published); acknowledgement of federal support (yes).

Other publications, conference papers, and presentations. *Identify any other publications, conference papers and/or presentations not reported above. Specify the status of the publication as noted above. List presentations made during the last year (international, national, local societies, military meetings, etc.). Use an asterisk (*) if presentation produced a manuscript.*

None.

Website(s) or other Internet site(s)
List the URL for any Internet site(s) that disseminates the results of the research activities. A short description of each site should be provided. It is not necessary to include the publications already specified above in this section.

Research activities will be disseminated through Researchgate, a widely used website. Articles and datasets may be uploaded to this site.

https://www.researchgate.net/profile/David_Wilson33

Technologies or techniques
Identify technologies or techniques that resulted from the research activities. In addition to a description of the technologies or techniques, describe how they will be shared.

None

Inventions, patent applications, and/or licenses
Identify inventions, patent applications with date, and/or licenses that have resulted from the research. State whether an application is provisional or non-provisional and indicate the application number. Submission of this information as part of an interim research performance progress report is not a substitute for any other invention reporting required under the terms and conditions of an award.

None

Other Products

Identify any other reportable outcomes that were developed under this project. Reportable outcomes are defined as a research result that is or relates to a product, scientific advance, or research tool that makes a meaningful contribution toward the understanding, prevention, diagnosis, prognosis, treatment, and/or rehabilitation of a disease, injury or condition, or to improve the quality of life. Examples include:

- *data or databases;*
- *biospecimen collections;*
- *audio or video products;*
- *software;*
- *models;*
- *educational aids or curricula;*
- *instruments or equipment;*
- *research material (e.g., Germplasm; cell lines, DNA probes, animal models);*
- *clinical interventions;*
- *new business creation; and*
- *other.*

None

7. PARTICIPANTS & OTHER COLLABORATING ORGANIZATIONS

What individuals have worked on the project?

Provide the following information for: (1) PDs/PIs; and (2) each person who has worked at least one person month per year on the project during the reporting period, regardless of the source of compensation (a person month equals approximately 160 hours of effort). If information is unchanged from a previous submission, provide the name only and indicate "no change."

Name:	Dr. David Wilson
Project Role:	Principal Investigator
Researcher Identifier (e.g. ORCID ID):	ORCID ID 0000-0002-1826-7745
Nearest person month worked:	2
Contribution to Project:	unchanged
Name:	Dr. Anniina Färkkilä
Project Role:	Postdoctoral fellow
Researcher Identifier (e.g. ORCID ID):	n/a
Nearest person month worked:	3
Contribution to Project:	unchanged
Name:	Dr. Adetunji T. Toriola
Project Role:	Co-investigator
Researcher Identifier (e.g. ORCID ID):	ORCID ID 0000-0003-1079-2606
Nearest person month worked:	1
Contribution to Project:	unchanged
Name:	Dr. Esther Lu
Project Role:	Co-investigator and biostatistician
Researcher Identifier (e.g. ORCID ID):	ORCID: 0000-0002-9434-7907
Nearest person month worked:	1
Contribution to Project:	unchanged
Name:	Rebecca Cochran
Project Role:	Technician
Researcher Identifier (e.g. ORCID ID):	n/a
Nearest person month worked:	3
Contribution to Project:	unchanged

Has there been a change in the active other support of the PD/PI(s) or senior/key personnel since the last reporting period?
If there is nothing significant to report during this reporting period, state "Nothing to Report."

If the active support has changed for the PD/PI(s) or senior/key personnel, then describe what the change has been. Changes may occur, for example, if a previously active grant has closed and/or if a previously pending grant is now active. Annotate this information so it is clear what has changed from the previous submission. Submission of other support information is not necessary for pending changes or for changes in the level of effort for active support reported previously. The awarding agency may require prior written approval if a change in active other support significantly impacts the effort on the project that is the subject of the project report.

Nothing to report.

What other organizations were involved as partners?
If there is nothing significant to report during this reporting period, state "Nothing to Report."

Describe partner organizations – academic institutions, other nonprofits, industrial or commercial firms, state or local governments, schools or school systems, or other organizations (foreign or domestic) – that were involved with the project. Partner organizations may have provided financial or in-kind support, supplied facilities or equipment, collaborated in the research, exchanged personnel, or otherwise contributed.
Provide the following information for each partnership:
Organization Name:
Location of Organization: (if foreign location list country)
Partner's contribution to the project (identify one or more)
-) *Financial support;*
-) *In-kind support (e.g., partner makes software, computers, equipment, etc., available to project staff);*
-) *Facilities (e.g., project staff use the partner's facilities for project activities);*
-) *Collaboration (e.g., partner's staff work with project staff on the project);*
-) *Personnel exchanges (e.g., project staff and/or partner's staff use each other's facilities, work at each other's site); and*
-) *Other*

Organization Name: University of Helsinki
Location of Organization: (if foreign location list country): Helsinki, Finland
Partner's contribution to the project (identify one or more):
-) Some of the project staff are based at the University of Helsinki
-) Facilities

8. SPECIAL REPORTING REQUIREMENTS

COLLABORATIVE AWARDS: For collaborative awards, independent reports are required from BOTH the Initiating PI and the Collaborating/Partnering PI. A duplicative report is acceptable; however, tasks shall be clearly marked with the responsible PI and research site. A report shall be submitted to **https://ers.amedd.army.mil** for each unique award.

QUAD CHARTS: If applicable, the Quad Chart (available on https://www.usamraa.army.mil) should be updated and submitted with attachments.

9. APPENDICES: Attach all appendices that contain information that supplements, clarifies or supports the text. Examples include original copies of journal articles, reprints of manuscripts and abstracts, a curriculum vitae, patent applications, study questionnaires, and surveys, etc.

Functional profiling of FSH and estradiol in ovarian granulosa cell tumors

Journal:	*Endocrine-Related Cancer*
Manuscript ID	Draft
Manuscript Type:	Research Paper
Date Submitted by the Author:	n/a
Complete List of Authors:	Haltia, Ulla-Maija; University of Helsinki and Helsinki University Hospital, Children's Hospital and Department of Obstetrics and Gynecology Pihlajoki, Marjut; University of Helsinki, Pediatric Research Center, Children's Hospital; Saint Louis Children's Hospital, Washington University School of Medicine, Department of Pediatrics Andersson, Noora; University of Helsinki, Pediatric Research Center, Children's Hospital Mäkinen, Lotta; University of Helsinki, Children's hospital Tapper, Johanna; University of Helsinki and Helsinki University Hospital, Obstetrics and Gynecology Horlings, Hugo; The Netherlands Cancer Institute, Department of Pathology Turpeinen, Ursula; University of Helsinki and HUSLAB, Helsinki University Hospital, Department of Diagnostics and Therapeutics Anttonen, Mikko; University of Helsinki and HUSLAB, Helsinki University Hospital, Clinical Chemistry and Hematology Butzow, Ralf; University of Helsinki and HUSLAB, Helsinki University Hospital, Pathology Unkila-Kallio, Leila; University of Helsinki and Helsinki University Hospital, Obstetrics and Gynecology Carpén, Olli; University of Helsinki and HUSLAB, Department of Pathology, Medicum Wilson, David; Washington University in Saint Louis School of Medicine, Department of Developmental Biology; Saint Louis Children's Hospital, Washington University School of Medicine, Department of Pediatrics Heikinheimo, Markku; University of Helsinki and Helsinki University Hospital, Pediatric Research Center, Children's Hospital; Saint Louis Children's Hospital, Washington University School of Medicine, Department of Pediatrics Färkkilä, Anniina; University of Helsinki and Helsinki University Hospital, Children's Hospital and Department of Obstetrics and Gynecology; Harvard Medical School, Dana-Farber Cancer Institute, Department of Radiation Oncology
Keywords:	granulosa cell tumor, Estrogen receptor, Aromatase, hormonal treatment

Functional profiling of FSH and estradiol in ovarian granulosa cell tumors

Ulla-Maija Haltia[1,2], Marjut Pihlajoki[2], Noora Andersson[2], Lotta Mäkinen[2], Johanna Tapper[1], Hugo M. Horlings[3], Ursula Turpeinen[4], Mikko Anttonen[4], Ralf Bützow[5], Leila Unkila-Kallio[1], Olli Carpén[5], David B Wilson[6], Markku Heikinheimo[2,6]* and Anniina Färkkilä[1,7]

[1] *Department of Obstetrics and Gynecology, University of Helsinki and Helsinki University Hospital, Helsinki, Finland*

[2]*Children's Hospital, University of Helsinki and Helsinki University Hospital, Helsinki, Finland*

[3]*Department of Pathology, the Netherlands Cancer Institute, Amsterdam, the Netherlands*

[4]*HUSLAB, Helsinki University Hospital, Helsinki, Finland*

[5]*Pathology, University of Helsinki and Helsinki University Hospital, Helsinki, Finland*

[6]*Department of Pediatrics, Washington University School of Medicine, Saint Louis, Missouri, USA*

[7]*Radiation Oncology, Dana-Farber Cancer Institute, Boston, USA*

*Corresponding author:

Markku Heikinheimo

Pediatric Research Center, Helsinki University Hospital, PO Box 400, 00290 Helsinki, Finland

markku.heikinheimo@helsinki.fi

Short title: Hormonal profiling of granulosa cell tumors

Keywords: granulosa cell tumor, estrogen receptor, aromatase, hormonal treatment

Word count: 4169

Abstract

Adult-type granulosa cell tumors (AGCTs) are sex-cord derived neoplasms with a propensity for late relapse. AGCTs express hormone receptors and secrete estradiol (E2), therefore aromatase inhibitors and other hormonal modulators have been used empirically in the treatment of recurrent AGCT, albeit with limited success. To provide a more rigorous foundation for hormonal therapy in AGCT, we characterized the expression of key hormone receptors and aromatase in 175 tumor specimens and correlated these results with clinical parameters, including preoperative serum follicle stimulating hormone (FSH), E2, and inhibin B levels. FSH receptor and estrogen receptor beta (ERβ) were expressed in the majority of AGCTs, whereas estrogen receptor alpha (ERα) and G-protein coupled estrogen receptor (GPER1) were detected in only a minority of these tumors. ERβ expression was increased in recurrent tumors. Aromatase immunoreactivity was evident in 48% of AGCTs. None of the markers examined had prognostic significance. Serum FSH and inhibin B levels correlated inversely, suggesting that tumor-derived inhibin B affects pituitary FSH secretion. We assessed the effects of FSH, E2, and the aromatase inhibitor letrozole on AGCT cell viability using two *in vitro* models: KGN cells and primary cultures of AGCT cells. FSH and E2 increased cell viability in some primary AGCTs but not in KGN cells. Letrozole suppressed E2 production in AGCTs, however, it did not impact cell viability. Our demonstration of active FSH and estradiol signaling in AGCT cells affords a scientific rationale for hormonal therapy in this malignancy.

Introduction

Adult-type granulosa cell tumors (AGCTs) are sex cord stromal tumors representing 3-5% of ovarian malignancies. A defining feature of AGCTs is a somatic mutation (c.402C>G; p.C134W) in the *FOXL2* gene, which is thought to play a pivotal role in oncogenesis (Shah, et al. 2009). These tumors are characterized by slow growth and a generally favorable prognosis, with a ten-year survival of 84% (McConechy, et al. 2016). Up to 30% of patients diagnosed with AGCT experience a late relapse. The mainstay of treatment for AGCT is surgical resection, but improved medical therapies are needed for advanced and relapsed disease. Current chemotherapeutic regimens show limited efficacy (van Meurs, et al. 2014a), and no prospectively validated targeted therapies exist for this unique tumor type.

AGCTs secrete estradiol (E2), inhibin B, and anti-Müllerian hormone (AMH), and tumor hormone production accounts for many of the signs and symptoms of the disease (Bryk, et al. 2015; Lappohn, et al. 1989; Rey, et al. 1996). AGCTs are known to express certain hormone receptors (Alexiadis, et al. 2011; Farinola, et al. 2007; Fuller, et al. 1998), but the importance of hormonal signaling in AGCT progression remains uncertain. Hormonal therapies, such as GnRH-analogues and aromatase inhibitors, have been used empirically in AGCT with limited efficacy (van Meurs, et al. 2015; van Meurs, et al. 2014b); however, the biological foundation for these treatments has not been clearly established.

Clinically, AGCTs are often diagnosed at perimenopause when gonadotropin levels rapidly increase, and follicle stimulating hormone (FSH) signaling has been proposed to be one of the main drivers of AGCT growth (Fuller and Chu 2004). In normal granulosa cells, FSH promotes cell proliferation by cAMP-mediated signaling cascades, leading to increased aromatase (CYP19A1)

expression and elevated serum E2 levels, essential for normal ovarian function (Dewailly, et al. 2016; Stocco 2008). The gene expression profile of AGCTs has been shown to mimic that of FSH-stimulated granulosa cells (Chu, et al. 2002), suggesting that this gonadotropin signaling pathway is active in these neoplasms. Regarding *CYP19A1*, FSH is known to increase its mRNA levels via specific transcription factors, and FOXL2 has been shown to act as a direct regulator of this gene (Fleming, et al. 2010). Data concerning the expression and functionality of CYP19A1 in AGCTs are scarce, although the ability of AGCTs to secrete E2 implies its increased activity in tumor tissue.

Estrogens are known to exert strong mitogenic effects in breast and endometrial cancers (Clemons and Goss 2001; Plaza-Parrochia, et al. 2017) and to inhibit apoptosis in normal granulosa cells (Billig, et al. 1993), but their impact on AGCT proliferation/survival is less clear. The effects of E2 are mediated through two distinct nuclear receptors estrogen receptor-α (ERα) and -β (ERβ), both expressed in AGCTs (Chu, et al. 2000; Ciucci, et al. 2018). Additionally, E2 can act through a membrane-bound G-protein linked estrogen receptor (GPER1) that has been observed in AGCTs (Francois, et al. 2015). The expression levels, prognostic implications, and functional roles of FSH, CYP19A1, and E2 in AGCTs have not been reported.

Here, using a combination of quantitative real-time PCR (qPCR), RNA *in situ* hybridization, and immunohistochemistry (IHC), we profile the expression of the FSH receptor (FSHR), estrogen receptors (ERα, ERβ, GPER1), and CYP19A1 in a large cohort of 175 *FOXL2* mutation-positive AGCTs with rich clinical and follow-up data. We augment this expression profiling with measurements of hormone levels in 51 preoperative serum samples. In functional analyses, we show that FSH increases *CYP19A1* expression and E2 production in an established AGCT cell line (KGN) and in primary cultures of AGCT cells. We demonstrate that stimulation with FSH or E2

does not affect cell viability in KGN cells but does increase viability in primary AGCTs. Our results thus indicate a specific pattern of hormonal dependency in AGCTs and support the further clinical exploration of hormonal modulators in the treatment of AGCT.

Materials and methods

Patients and samples

Patient and sample data are shown in Table 1 and 2. All of the AGCTs tested positive for the *FOXL2* (c.402C>G; p.C134W) mutation, and histological diagnoses were verified by an expert pathologist (R.B.). Normal ovaries (n=4) were obtained from women undergoing ovariectomy for benign indications. We constructed a tumor tissue microarray (TMA) containing quadruple cores from 121 primary and 54 recurrent AGCTs from representative formalin-fixed, paraffin embedded (FFPE) samples (Table 1). Serum samples from 47 AGCT patients were collected prior to surgery for either primary or recurrent AGCT (Table 2). Short-term primary tumor cell cultures were established from fresh AGCT samples from six patients (Supplementary Table 1). Informed consent was obtained from patients who donated blood or fresh AGCT tumor samples for the study. The ethics committee of Helsinki University Central Hospital and the National Supervisory Authority for Welfare and Health in Finland approved this study.

Serum analyses

Preoperative samples were obtained from 47 AGCT patients (Table 2) within a month before surgery and prepared and stored at -80° C until the analysis. All the studied serum markers (FSH, E2, and inhibin B) were measured in the HUSLAB hospital clinical laboratory: automated immunoassays for FSH (Abbott Laboratories, IL, USA) and E2 (Siemens Healthcare, Erlangen, Germany) and ELISA for inhibin B (Beckman Coulter, CA, USA). All the samples were classified

as follows according to the patient's menopausal status at sample retrieval: "premenopausal" if the patient had one or two ovaries and menopause was not indicated in the medical records and "postmenopausal" if both ovaries had been removed, independent of age, or if the patient was postmenopausal according to her medical history.

Immunostaining

The ACGT TMA and normal ovary tissue sections were subjected to immunohistochemistry (IHC) as described (Soini, et al. 2018). Staining was performed using mouse monoclonal antibody for CYP19A1 (Novusbio, NBP2-33336, dilution 1:5000), rabbit monoclonal antibody for ERα (Thermo clone SP1, dilution 1:25) and mouse monoclonal antibody for ERβ (Novocastra, NCL-ERβ, dilution 1:200).

Samples were scored by two independent researchers (U-M.H. and N.A.) and disagreements were resolved by a joint review. Staining intensity was classified from 0-3 (0=negative, 1= weak, 2=moderate, 3=strong intensity). Images were generated using 3DHISTECH Pannoramic 250 FLASH II digital slide scanner at Genome Biology Unit (Research Programs Unit, Faculty of Medicine, University of Helsinki, and Biocenter Finland). The scanning was done using 40x objective (Zeiss Plan-Apochromat 40x/NA 0.95) and applying the extended focus option using seven focus levels.

RNA in situ hybridization

RNA *in situ* hybridization was performed on freshly cut 5 µm sections of the TMA using RNAscope 2.5 HD detection kit-BROWN (#322310, ACDBio, Milano, IT) for target mRNA detection. In short, tissue sections were baked for 1 h at 60°C, then deparaffinized and treated with hydrogen peroxide for 10 min at room temperature. Target retrieval was performed for 15 min at 100°C, followed by protease plus treatment for 15 min at 40°C. The probes Hs-*FSHR* (#400501),

147 Hs-*CYP19A1* (#430861), Hs-*GPER* (#553361), positive control probe Hs-*PPIB* (#313901) and
148 negative control probe *DapB* (#310043) were hybridized for 2 h at 40°C followed by signal
149 amplification steps. The samples were incubated for 60 min with AMP 5–reagent. The sections
150 were next treated with DAB for 10 min at room temperature followed by counterstaining with 50%
151 hematoxylin. The sections were dipped in ammonium water and dehydrated in ethanol series and
152 UltraClear before mounting. Two researchers (U-M.H. and N.A.) performed the scoring
153 independently and disagreements were resolved by a joint review. Staining intensity was classified
154 from 0 to 3 (0=negative, 1= weak, 2=moderate, 3=high intensity).
155
156 *Hormone stimulation in KGN cell line and primary cultured AGCT cells*
157 The *FOXL2* c.402C>G mutation-positive KGN cell line (Nishi, et al. 2001), originating from a
158 recurrent AGCT, was obtained from the Riken BioResource Center. KGN cells were passaged <6
159 months following receipt or resuscitation of a frozen cell vial, and tested negative for mycoplasma
160 infection. Short-term primary tumor cell cultures were established as described (Kyronlahti, et al.
161 2010) from fresh primary (n=3) or recurrent (n=3) AGCT samples, all tested positive for the
162 *FOXL2* (c.402C>G; p.C134W) mutation. To increase the cell number, primary AGCT cells were
163 first cultured for 3-4 days in Dulbecco's modified Eagle's medium (DMEM)/Ham's F-12 medium,
164 supplemented with 10% fetal calf serum (FCS), penicillin/streptomycin, and L-glutamine in a
165 humidified environment at 37°C and 5% CO.
166 Both KGN and primary cultured AGCT cells were grown for 10 or 3 days prior to hormone
167 stimulation, respectively, in phenol red free DMEM:F12 medium supplemented with 10% charcoal
168 stripped FCS, L-glutamine and antibiotics to deplete the cells from external hormones. Next, 10 000
169 KGN and primary AGCT cells per well were plated on 96-well plates in hormone-depleted medium
170 for the cell viability assay. For RNA extraction and medium collection, 600 000 cells per well were
171 plated on 6-well plates. After the cells had attached, they were treated with 100 nM of FSH (#HOR-

253, Immuno Diagnostics, Hämeenlinna, Finland), 1000 nM of E2 (#E2758, Sigma-Aldrich, St Louis, USA), 2 µM testosterone (#86500, Sigma-Aldrich), or 5 µM dose of letrozole (#L6545, Sigma-Aldrich). Cell viability was measured after 96 hours using the WST-1 assay (Sigma-Aldrich).

Quantitative real-time PCR (qPCR)

Total RNA was extracted using the NucleoSpin RNA/Protein kit (Macherey-Nagel, Düren, DE). Reverse transcription was performed using the Reverse Transcriptase Core Kit, and qPCR was carried out using the MESA GREEN qPCR MasterMix Plus for SYBR Assay (both from Eurogentec, Seraing, BE). *ACTB* was used as reference gene for mRNA expression. Primer pairs used are listed in Supplementary Table 2.

E2 measurement

Medium was collected from KGN and AGCT primary cells at 96 h time point and analyzed for E2 concentration using a mass spectrophotometer at HUSLAB. Calibrators containing 25-1000 pmol/l of estradiol (Cerilliant) were prepared in 50% methanol. Forty µl of sample extracts and calibrators were analysed on an LC-MS/MS system equipped with an AB Sciex 5500 triple quandrupole mass spectrometer. Data were acquired and processed with the Analyst Software (Ver 1.6.2; AB Sciex).

Statistical analyses

The immunohistochemical data and categorical variables were analyzed with contingency tabling (2x2) and chi-square or Fisher´s exact tests. For cell culture data one-way ANOVA followed by with-control Dunnett´s or Student´s t-test was used. The comparison between primary and recurrent tumors was performed by matched-pair t-test analysis. Serum hormone levels differed from normal distribution even after performing logarithmic transformation and thus Spearman´s rho was

198 reported. Survival curves of different groups were illustrated by Kaplan-Meier plots and compared
199 with the Log-rank test. Two-sided p-value less than 0.05 was considered statistically significant. All
200 data were analyzed using JMP pro13.
201
202 **Results**
203
204 *FSHR is widely expressed in AGCTs*
205 Since gonadotropins are speculated to play a role in AGCT progression, we characterized the
206 expression of FSH receptor (*FSHR*) using RNA *in situ* hybridization on a TMA of 175 AGCTs.
207 *FSHR* mRNA was detected in 90% of AGCTs (Fig 1 A-D), and the signal was strong or moderate
208 in 60% of the tumors (Figure 1 A-D, Table 3). *FSHR* expression was lower in tumors with high
209 mitotic activity (p=0.01), but expression did not correlate with other clinical parameters such as
210 tumor size, stage, or risk of recurrence.
211
212 *Serum inhibin B levels correlate inversely with FSH levels in AGCT patients*
213
214 Next, we analyzed FSH, E2 and inhibin B levels in 51 preoperative serum samples. FSH levels
215 were generally low in AGCT patients, with median levels of 1.55 IU/l (range 0.05-15.3 IU/l) and
216 6.6 IU/l (range 0.1-60.3 IU/l) in premenopausal and postmenopausal patients, respectively. For E2
217 the median level was 0.125 nmol/l (range 0.01-0.48 nmol/l) in premenopausal patients and 0.15
218 nmol/l (range 0.04-1.05 nmol/l) in postmenopausal patients. Serum FSH levels were significantly
219 lower in patients with large (tumors >10 cm in diameter) when compared to patients with smaller
220 tumors (<10 cm in diameter) (p=0.001). FSH and E2 levels did not correlate with each other,
221 however FSH and inhibin B levels showed a strong inverse correlation (Spearman´s rho -0.75,
222 p<0.0001), consistent with the suppressive effect of circulating inhibin B on FSH secretion from the

pituitary (Supplementary Fig. 1). In accordance with previous findings (Farkkila, et al. 2015), inhibin B levels were higher in patients with larger tumors (p=0.01). Next, we assessed the preoperative serum FSH levels from synchronous samples of 36 AGCT patients whose tumors were represented in the TMA. We observed significantly increased tumor ERα expression in patients with low serum inhibin B levels (p=0.04), suggesting diminished inhibin B – FSH feedback in high ERα expressing AGCTs. We found no significant correlations between serum FSH or E2 levels and other estrogen receptors.

FSH increases CYP19A1 expression and E2 production in AGCT cells in vitro

To study the functional role of FSH in AGCTs, KGN and primary AGCT cells were stimulated with FSH for 96 h and then gene expression levels and E2 production were measured by qPCR and mass spectrometry, respectively. In KGN cells, *FSHR* expression was increased by FSH stimulation (Figure 1 E). Also *CYP19A1* mRNA levels (Figure 1F) and the amount of E2 in cell culture supernatants (Figure 2A) were significantly increased by FSH. Additionally, FSH stimulated the expression of *ESR1*, the gene encoding ERα, whereas no statistically significant change in ERβ coding *ESR2* or *GPER1* levels was seen in KGN cells (Fig. 1G-I). FSH stimulation did not have an effect on viability in this cell line (Fig 1J).

In primary patient-derived AGCT cells, consistent with our findings in KGN cells, FSH stimulation significantly increased the expression of *CYP19A1* (Figure 1F) and secretion of E2 into the culture medium (Figure 2B). Interestingly, the level of FSH or E2 in patient´s preoperative serum sample did not correlate with the amount of E2 measured in the culture media (Supplementary Table 1). In contrast to the KGN cell line, FSH stimulation increased the mRNA expression of all the estrogen receptors (*ESR1*, *ESR2,* and *GPER1)* in all six of the patient-derived primary AGCT cells (Fig 1G-

I). Moreover, FSH stimulation increased cell viability in three of six AGCT primary cell cultures by 26 to 43 % (Fig 1J, Supplementary Table 1). The weaker responsiveness of KGN cells to FSH may be due to the low FSHR expression status in these cells, compared to that of primary AGCTs (Supplementary Fig. 2). Importantly, these results indicate active hormonal signaling in AGCT cells.

CYP19A1 is expressed in a subset of AGCTs

Aromatase inhibitors have been used in the treatment of relapsed AGCT (van Meurs et al. 2014a). These drugs inhibit the synthesis of estrogens from androgen precursors by binding to aromatase. To assess the expression *CYP19A1* in AGCTs, we performed RNA *in situ* hybridization and IHC on the TMA. *CYP19A1* mRNA was detected in 15% of the tumor specimens by RNA *in situ* hybridization (Figure 3A-D). CYP19A1 immunoreactivity was detected in 48% of the tumors, and 17% showed moderate or strong staining (Figure 3E-H, Table 3). *CYP19A1* mRNA expression correlated significantly with the moderate/high CYP19A1 protein expression ($p<0.0001$). CYP19A1 protein expression also correlated positively with ERα expression ($p=0.009$). There were no correlations between *CYP19A1* expression and clinical parameters such as tumor size, stage, or recurrence rate. Interestingly, *CYP19A1* expression in the tumor tissue did not correlate with circulating E2, FSH, or inhibin B levels.

Aromatase inhibition with letrozole suppresses E2 production in AGCT cells

Next, we studied the functional effects of CYP19A1 inhibition in KGN and primary AGCT cells. For this purpose, cells were treated with 5 μM dose of the aromatase inhibitor letrozole and 2 μM dose of testosterone as a substrate for CYP19A1. Testosterone significantly stimulated both E2

production and cell viability in both KGN and primary AGCT cells, confirming the presence of functional CYP19A1. FSH consistently enhanced the production of E2 in the presence of testosterone (Figure 2A-B). Interestingly, letrozole treatment completely suppressed E2 production in the cell cultures (with and without FSH stimulation) but had no effect on cell viability in either KGN or primary AGCT cells (Figure 2C-D, p-values shown in Supplementary Table 3).

ERβ is the main estrogen receptor in AGCTs and its expression is higher in recurrent tumors

Next, we characterized estrogen receptor expression in the AGCT TMA using IHC or RNA *in situ* hybridization. ERα immunoreactivity was observed in 33% of the tumors, and ERβ protein was detected in 94% (Figure 4A-H, Table 3). In the ERα-positive tumors, the staining pattern was nuclear in 59% and cytoplasmic in 48% of the tumors. ERβ immunoreactivity was exclusively nuclear and classified as moderate or strong in 67% of the tumors. *GPER1* mRNA expression was detected only in 14 % of the tumors by RNA *in situ* hybridization (Figure 4I-L). Our results thus confirm that ERβ is the predominant estrogen receptor in AGCT.

ERβ expression levels were significantly higher in recurrent AGCTs when compared to primary tumors (p=0.001). Furthermore, paired analysis of primary and recurrent samples from same patients demonstrated a significantly stronger ERβ immunoreactivity in the recurrent AGCTs (p = 0.0013) compared to the primary tumor (Figure 5A). A similar pattern between primary and recurrent samples was noted for *GPER1* mRNA expression, although the levels of expression were low (Figure 5B). There were no significant differences in the expression levels of ERα between primary and recurrent samples. We also found no correlation between any of the estrogen receptor expression patterns and tumor size, stage at primary diagnosis, recurrence rate, or menopause status

297 at the time of sample retrieval. None of the estrogen receptors had prognostic significance in terms
298 of disease-free or overall survival.
299
300 *E2 increases AGCT cell viability*
301
302 Since FSH stimulation increased aromatase expression, E2 production, and AGCT cell viability, we
303 next explored whether E2 alone affects AGCT cell viability. We found that exogenous E2 (0.1 nM-
304 1000 nM) did not affect the viability of KGN cells (Figure 4P). However, in primary AGCT cells
305 E2 (1000 nM) increased the cell number on average by 36 % in four out of the six studied samples
306 (range 23-57%) (Figure 4P, Supplementary Table 1). In one recurrent tumor, E2 had no effect and
307 in one primary tumor E2 decreased cell number by 21%. Interestingly, the tumors that did not
308 respond to E2 also did not respond to FSH stimulation, suggesting heterogeneous hormonal
309 dependencies in individual AGCTs. No correlation between the level of FSH or E2 in patient´s
310 preoperative serum sample and response to E2 stimulation could be seen (Supplementary Table 1).
311 We also found that E2 had no effect on the expression levels of estrogen receptors *ESR1*, *ESR2*, and
312 *GPER1* in KGN cells (Figure 4M-O). However, in primary AGCT cells, E2 treatment increased
313 *ESR2* expression in all of the cultures indicating a positive feedback mechanism of E2 and ESR2
314 expression in AGCTs (Figure 4N).
315
316
317 **Discussion**
318
319 Hormonal activity is one of the hallmarks of AGCTs. Indeed, these tumors are often diagnosed in
320 perimenopause due to signs or symptoms of hormone production, such as vaginal bleeding caused
321 by estrogen-induced endometrial hyperplasia. As the peak incidence of AGCTs is in perimenopause

or early postmenopause, it has been suggested that alterations in circulating hormone levels, such as the rise in serum gonadotropin levels, contributes to tumor formation. Additional knowledge on the possible hormonal modulation of these unique tumors is needed given that anti-hormone therapies are currently used in AGCT patient care.

Here, we characterized the expression of sex hormone receptors in a large set of diagnostically validated AGCTs with an extensive clinical data and follow-up time. The expression of FSHR has not been studied earlier in more than a few individual AGCTs, probably due to lack of specific IHC compatible antibodies. By using RNA *in situ* hybridization, we now demonstrate robust *FSHR* expression in a majority of AGCTs. Following FSH stimulation, an increase in cell number was observed in 3/6 of the tested AGCT samples. This FSH effect in primary AGCT cultures may be mediated by cAMP mediated E2 production or other FSH-induced signaling such as P13K/Akt and MAPK pathways (Jamieson and Fuller 2012). KGN cell viability was not affected by FSH, which may be due to the low FSHR expression status in these cells. Our data is in line with earlier findings regarding low serum FSH levels in AGCT patients (Healy, et al. 1993; Jobling, et al. 1994), and the inverse correlation between serum FSH and inhibin B levels in this study supports the notion that tumor-derived inhibin B regulates pituitary FSH secretion.

The role of FSH in inducing CYP19A1 activity in normal granulosa cells is well established (Erickson and Hsueh 1978). We found a significant increase in expression of *CYP19A1* gene after FSH stimulation in both KGN and primary AGCT cells, supporting the role of FSH in E2 production in tumor cells. An earlier study using primary rat granulosa cells showed that FSH regulates *CYP19A1* via GATA4 (Kwintkiewicz, et al. 2007), a transcription factor known to be overexpressed in AGCTs (Anttonen et al. 2005). Another study reported the direct regulation of aromatase by FOXL2 and proposed that the C134W mutation increases this stimulatory effect

(Fleming et al. 2010). We found that CYP19A1 protein is expressed in 48% of the studied tumors, which is a lower proportion than previously reported (Kato, et al. 2016; Kitamura, et al. 2017). The number of AGCTs expressing *CYP19A1* mRNA (15%) was lower than expected based on protein expression; this discrepancy may be due to the short half-life of *CYP19A1* mRNA (Sahmi 2006). Optimal CYP19A1 may require constitutive FSH stimulation, which is suppressed in AGCT patients through negative feedback of the pituitary by tumor-derived inhibin B. Another factor secreted by AGCTs, AMH, has been shown to attenuate FSH-mediated stimulation of CYP19A1 expression (Dewailly et al. 2016). Thus, AGCTs exhibit self-limiting regulation of *CYP19A1* expression (Farkkila, et al. 2017).

The role of E2 in AGCT growth and survival is controversial. Estrogen promotes tumor growth in various cancers (Thomas and Gustafsson 2011), and the safety of estrogen replacement therapy of AGCT patients remains questionable (Guidozzi 2013). In a previous study with a long follow-up time, postmenopausal estrogen replacement therapy did not negatively impact the prognosis of AGCT patients (Bryk, et al. 2016). Furthermore, earlier studies on KGN cells did not support a growth-stimulating effect of E2 (Chu, et al. 2004; Ciucci et al. 2018; Francois et al. 2015); indeed, it has been shown that E2 may decrease KGN cell migration (Francois et al. 2015). In line with these reports, we did not find any effect on KGN cell viability in response to E2 stimulation. However, an increase in cell number was detected in 4/6 of the primary AGCT cell cultures tested. Low levels of estrogen receptors in KGN cells likely explain the unresponsiveness of this cell line to E2, emphasizing the importance of using complementary cellular models for AGCT studies.

Consistent with earlier studies (Alexiadis et al. 2011; Chu et al. 2000), we found that ERβ was the principal estrogen receptor expressed in AGCTs. ERα expression was markedly lower than ERβ, but its correlation with circulating FSH and tissue CYP19A1 expression and the fact that FSH

stimulation increased ERα expression suggest that ERα may have a functional role in a subset of AGCTs. In other hormone-related malignancies, such as breast and prostate cancer, ERα is considered tumorigenic whereas ERβ mostly functions as a tumor suppressor by blocking the proliferation and inducing apoptosis (Bonkhoff 2018; Lazennec 2006; Thomas and Gustafsson 2011). ERβ effects are also dependent on the ERβ-subtype (Ciucci, et al. 2014; Shaaban, et al. 2008). Increased ERβ expression in recurrent tumors suggests the significance of ERβ in this unique slow growing tumor type, but the specific effect of ERβ in tumor progression awaits further evidence.

Several case studies report variable responses to divergent hormonal treatments in AGCTs, and among these therapies aromatase inhibitors have been the most promising (van Meurs et al. 2014a). Our results regarding stimulatory effect of E2 in AGCT primary cells support the concept of aromatase inhibition in AGCT therapy. We did not, however, observe any changes in cell viability after letrozole treatment, even though the used doses were sufficient to suppress E2 production in AGCT cells. This unresponsiveness to letrozole was also noted in our earlier study when the cell viability of seven primary AGCT samples were studied by high-throughput drug screening (Haltia, et al. 2017). In our patient series a total of 10 patients were treated with letrozole, generally as a last therapeutic option when other medical treatments had proven ineffective. Only one of these patients had stable disease while 9/10 had disease progression during letrozole treatment. Our findings on negligible efficacy of aromatase inhibitors in AGCT *in vitro* are thus in keeping with the clinical practice. An increased cell viability in response to testosterone stimulation raises questions of the role of testosterone in AGCTs. As letrozole did not suppress the testosterone-induced cell viability, it is possible that testosterone exerts its effects through estrogen-independent mechanisms (Gleicher, et al. 2011; Ono, et al. 2014). A recent study reported moderate staining for androgen

receptor in AGCT cells, also implicating further studies on the role of androgens in this unique tumor type (Ciucci et al. 2018).

The present work confirms the wide expression of sex hormone receptors, and active hormonal signaling in AGCTs. Given the robust effects of FSH on CYP19A1 activity, and E2 on AGCT cell growth, our results encourage further exploration of anti-estrogen therapies in AGCTs. Prospective clinical studies are needed to determine the optimal compounds and dosing of hormonal therapies in AGCTs.

Declaration of interest

The authors declare that there is no conflict of interest that could be perceived as prejudicing the impartiality of this research.

Funding

This study was supported by grants from the Academy of Finland, Sigrid Jusélius Foundation, Helsinki University Hospital Research Funds, University of Helsinki Graduate school, Sladjana M. Crosley Foundation for GCT Research, and DoD Award W81XWH-16-1-0188.

References

Alexiadis M, Eriksson N, Jamieson S, Davis M, Drummond AE, Chu S, Clyne CD, Muscat GE & Fuller PJ 2011 Nuclear receptor profiling of ovarian granulosa cell tumors. *Horm Cancer* **2** 157-169.

Anttonen M, Unkila-Kallio L, Leminen A, Butzow R & Heikinheimo M 2005 High GATA-4 expression associates with aggressive behavior, whereas low anti-Mullerian hormone expression associates with growth potential of ovarian granulosa cell tumors. *J Clin Endocrinol Metab* **90** 6529-6535.

Billig H, Furuta I & Hsueh AJ 1993 Estrogens inhibit and androgens enhance ovarian granulosa cell apoptosis. *Endocrinology* **133** 2204-2212.
Bonkhoff H 2018 Estrogen receptor signaling in prostate cancer: Implications for carcinogenesis and tumor progression. *Prostate* **78** 2-10.
Bryk S, Farkkila A, Butzow R, Leminen A, Heikinheimo M, Anttonen M, Riska A & Unkila-Kallio L 2015 Clinical characteristics and survival of patients with an adult-type ovarian granulosa cell tumor: a 56-year single-center experience. *Int J Gynecol Cancer* **25** 33-41.
Bryk S, Farkkila A, Butzow R, Leminen A, Tapper J, Heikinheimo M, Unkila-Kallio L & Riska A 2016 Characteristics and outcome of recurrence in molecularly defined adult-type ovarian granulosa cell tumors. *Gynecol Oncol* **143** 571-577.
Chu S, Mamers P, Burger HG & Fuller PJ 2000 Estrogen receptor isoform gene expression in ovarian stromal and epithelial tumors. *J Clin Endocrinol Metab* **85** 1200-1205.
Chu S, Nishi Y, Yanase T, Nawata H & Fuller PJ 2004 Transrepression of estrogen receptor beta signaling by nuclear factor-kappab in ovarian granulosa cells. *Mol Endocrinol* **18** 1919-1928.
Chu S, Rushdi S, Zumpe ET, Mamers P, Healy DL, Jobling T, Burger HG & Fuller PJ 2002 FSH-regulated gene expression profiles in ovarian tumours and normal ovaries. *Mol Hum Reprod* **8** 426-433.
Ciucci A, Ferrandina G, Mascilini F, Filippetti F, Scambia G, Zannoni GF & Gallo D 2018 Estrogen receptor beta: Potential target for therapy in adult granulosa cell tumors? *Gynecol Oncol*.
Ciucci A, Zannoni GF, Travaglia D, Petrillo M, Scambia G & Gallo D 2014 Prognostic significance of the estrogen receptor beta (ERbeta) isoforms ERbeta1, ERbeta2, and ERbeta5 in advanced serous ovarian cancer. *Gynecol Oncol* **132** 351-359.
Clemons M & Goss P 2001 Estrogen and the risk of breast cancer. *N Engl J Med* **344** 276-285.
Dewailly D, Robin G, Peigne M, Decanter C, Pigny P & Catteau-Jonard S 2016 Interactions between androgens, FSH, anti-Mullerian hormone and estradiol during folliculogenesis in the human normal and polycystic ovary. *Hum Reprod Update* **22** 709-724.
Erickson GF & Hsueh AJ 1978 Stimulation of aromatase activity by follicle stimulating hormone in rat granulosa cells in vivo and in vitro. *Endocrinology* **102** 1275-1282.
Farinola MA, Gown AM, Judson K, Ronnett BM, Barry TS, Movahedi-Lankarani S & Vang R 2007 Estrogen receptor alpha and progesterone receptor expression in ovarian adult granulosa cell tumors and Sertoli-Leydig cell tumors. *Int J Gynecol Pathol* **26** 375-382.
Farkkila A, Haltia UM, Tapper J, McConechy MK, Huntsman DG & Heikinheimo M 2017 Pathogenesis and treatment of adult-type granulosa cell tumor of the ovary. *Ann Med* **49** 435-447.
Farkkila A, Koskela S, Bryk S, Alfthan H, Butzow R, Leminen A, Puistola U, Tapanainen JS, Heikinheimo M, Anttonen M, et al. 2015 The clinical utility of serum anti-Mullerian hormone in the follow-up of ovarian adult-type granulosa cell tumors--A comparative study with inhibin B. *Int J Cancer* **137** 1661-1671.
Fleming NI, Knower KC, Lazarus KA, Fuller PJ, Simpson ER & Clyne CD 2010 Aromatase is a direct target of FOXL2: C134W in granulosa cell tumors via a single highly conserved binding site in the ovarian specific promoter. *PLoS One* **5** e14389.
Francois CM, Wargnier R, Petit F, Goulvent T, Rimokh R, Treilleux I, Ray-Coquard I, Zazzu V, Cohen-Tannoudji J & Guigon CJ 2015 17beta-estradiol inhibits spreading of metastatic cells from granulosa cell tumors through a non-genomic mechanism involving GPER1. *Carcinogenesis* **36** 564-573.
Fuller PJ & Chu S 2004 Signalling pathways in the molecular pathogenesis of ovarian granulosa cell tumours. *Trends Endocrinol Metab* **15** 122-128.
Fuller PJ, Verity K, Shen Y, Mamers P, Jobling T & Burger HG 1998 No evidence of a role for mutations or polymorphisms of the follicle-stimulating hormone receptor in ovarian granulosa cell tumors. *J Clin Endocrinol Metab* **83** 274-279.

Gleicher N, Weghofer A & Barad DH 2011 The role of androgens in follicle maturation and ovulation induction: friend or foe of infertility treatment? *Reprod Biol Endocrinol* **9** 116.
Guidozzi F 2013 Estrogen therapy in gynecological cancer survivors. *Climacteric* **16** 611-617.
Haltia UM, Andersson N, Yadav B, Farkkila A, Kulesskiy E, Kankainen M, Tang J, Butzow R, Riska A, Leminen A, et al. 2017 Systematic drug sensitivity testing reveals synergistic growth inhibition by dasatinib or mTOR inhibitors with paclitaxel in ovarian granulosa cell tumor cells. *Gynecol Oncol* **144** 621-630.
Healy DL, Burger HG, Mamers P, Jobling T, Bangah M, Quinn M, Grant P, Day AJ, Rome R & Campbell JJ 1993 Elevated serum inhibin concentrations in postmenopausal women with ovarian tumors. *N Engl J Med* **329** 1539-1542.
Jamieson S & Fuller PJ 2012 Molecular pathogenesis of granulosa cell tumors of the ovary. *Endocr Rev* **33** 109-144.
Jobling T, Mamers P, Healy DL, MacLachlan V, Burger HG, Quinn M, Rome R & Day AJ 1994 A prospective study of inhibin in granulosa cell tumors of the ovary. *Gynecol Oncol* **55** 285-289.
Kato N, Uchigasaki S, Fukase M & Kurose A 2016 Expression of P450 Aromatase in Granulosa Cell Tumors and Sertoli-Stromal Cell Tumors of the Ovary: Which Cells Are Responsible for Estrogenesis? *Int J Gynecol Pathol* **35** 41-47.
Kitamura S, Abiko K, Matsumura N, Nakai H, Akimoto Y, Tanimoto H & Konishi I 2017 Adult granulosa cell tumors of the ovary: a retrospective study of 30 cases with respect to the expression of steroid synthesis enzymes. *J Gynecol Oncol* **28** e31.
Kwintkiewicz J, Cai Z & Stocco C 2007 Follicle-stimulating hormone-induced activation of Gata4 contributes in the up-regulation of Cyp19 expression in rat granulosa cells. *Mol Endocrinol* **21** 933-947.
Kyronlahti A, Kauppinen M, Lind E, Unkila-Kallio L, Butzow R, Klefstrom J, Wilson DB, Anttonen M & Heikinheimo M 2010 GATA4 protects granulosa cell tumors from TRAIL-induced apoptosis. *Endocr Relat Cancer* **17** 709-717.
Lappohn RE, Burger HG, Bouma J, Bangah M, Krans M & de Bruijn HW 1989 Inhibin as a marker for granulosa-cell tumors. *N Engl J Med* **321** 790-793.
Lazennec G 2006 Estrogen receptor beta, a possible tumor suppressor involved in ovarian carcinogenesis. *Cancer Lett* **231** 151-157.
McConechy MK, Farkkila A, Horlings HM, Talhouk A, Unkila-Kallio L, van Meurs HS, Yang W, Rozenberg N, Andersson N, Zaby K, et al. 2016 Molecularly Defined Adult Granulosa Cell Tumor of the Ovary: The Clinical Phenotype. *J Natl Cancer Inst* **108**.
Nishi Y, Yanase T, Mu Y, Oba K, Ichino I, Saito M, Nomura M, Mukasa C, Okabe T, Goto K, et al. 2001 Establishment and characterization of a steroidogenic human granulosa-like tumor cell line, KGN, that expresses functional follicle-stimulating hormone receptor. *Endocrinology* **142** 437-445.
Ono YJ, Tanabe A, Nakamura Y, Yamamoto H, Hayashi A, Tanaka T, Sasaki H, Hayashi M, Terai Y & Ohmichi M 2014 A low-testosterone state associated with endometrioma leads to the apoptosis of granulosa cells. *PLoS One* **9** e115618.
Plaza-Parrochia F, Romero C, Valladares L & Vega M 2017 Endometrium and steroids, a pathologic overview. *Steroids* **126** 85-91.
Rey RA, Lhomme C, Marcillac I, Lahlou N, Duvillard P, Josso N & Bidart JM 1996 Antimullerian hormone as a serum marker of granulosa cell tumorsof the ovary: comparative study with serum alpha-inhibin and estradiol. *Am J Obstet Gynecol* **174** 958-965.
Shaaban AM, Green AR, Karthik S, Alizadeh Y, Hughes TA, Harkins L, Ellis IO, Robertson JF, Paish EC, Saunders PT, et al. 2008 Nuclear and cytoplasmic expression of ERbeta1, ERbeta2, and ERbeta5 identifies distinct prognostic outcome for breast cancer patients. *Clin Cancer Res* **14** 5228-5235.

Shah SP, Kobel M, Senz J, Morin RD, Clarke BA, Wiegand KC, Leung G, Zayed A, Mehl E, Kalloger SE, et al. 2009 Mutation of FOXL2 in granulosa-cell tumors of the ovary. *N Engl J Med* **360** 2719-2729.

Soini T, Pihlajoki M, Andersson N, Lohi J, Huppert KA, Rudnick DA, Huppert SS, Wilson DB, Pakarinen MP & Heikinheimo M 2018 Transcription Factor GATA6: A Novel Marker and Putative Inducer of Ductal Metaplasia in Biliary Atresia. *Am J Physiol Gastrointest Liver Physiol*.

Stocco C 2008 Aromatase expression in the ovary: hormonal and molecular regulation. *Steroids* **73** 473-487.

Thomas C & Gustafsson JA 2011 The different roles of ER subtypes in cancer biology and therapy. *Nat Rev Cancer* **11** 597-608.

van Meurs HS, Buist MR, Westermann AM, Sonke GS, Kenter GG & van der Velden J 2014a Effectiveness of chemotherapy in measurable granulosa cell tumors: a retrospective study and review of literature. *Int J Gynecol Cancer* **24** 496-505.

van Meurs HS, van der Velden J, Buist MR, van Driel WJ, Kenter GG & van Lonkhuijzen LR 2015 Evaluation of response to hormone therapy in patients with measurable adult granulosa cell tumors of the ovary. *Acta Obstet Gynecol Scand* **94** 1269-1275.

van Meurs HS, van Lonkhuijzen LR, Limpens J, van der Velden J & Buist MR 2014b Hormone therapy in ovarian granulosa cell tumors: a systematic review. *Gynecol Oncol* **134** 196-205.

Figure legends

Figure 1. *FSHR* mRNA expression and the effect of FSH stimulation in AGCTs. A-D: RNA *in situ* hybridization was used to quantify *FSHR* expression in the AGCT TMA. Representative images of low (A,B) and high (C,D) staining patterns. Original magnifications 80 x (scale bar: 20µm) and 160 x (scale bar: 10µm). E-I: Expression of *FSHR* (E), C*YP19A1* (F), *ESR1* (G), *ESR2* (H), and *GPER1* (I) was quantified in KGN cell line and cultured primary AGCT cells by qPCR after stimulation with FSH (0 or 100 ng/ml) for 96 hours. Black columns: KGN cell line; grey columns: primary AGCT cells. J: KGN data represents the average of three independent experiments. Results are shown as mean ±SEM and statistical significance ($p<0.05$) was assessed by one-way ANOVA followed by Dunnett´s test.

Figure 2. Letrozole blocks E2 production but does not affect cell viability in primary AGCT cells. KGN cells and six primary AGCT cultures were stimulated with FSH and letrozole (L) for 96

556 hours. Testosterone (T) was provided as a substrate. A-B: E2 concentrations in cell culture
557 supernatants were measured by mass spectrometry. C-D: After stimulation cell viability was
558 assessed by WST-1 assay. P-values for panels C and D are shown in Supplementary Table 3.
559
560 **Figure 3.** *CYP19A1* is expressed in a subset of AGCTs. *CYP19A1* expression was assessed in the
561 TMA by RNA *in situ* hybridization (A-D) and IHC (E-H). Representative images of low (A-B, E-F)
562 and high (C-D, G-H) staining of AGCTs. Magnifications: 80 x (scale bar: 20µm) and 160 x (scale
563 bar: 10µm) (A-D) and 50 x (scale bar: 50µm) and 100 x (scale bar: 20 µm) (E-H). Arrows indicate
564 positively stained cells.
565
566 **Figure 4.** A-L: Expression of estrogen receptors and effects of E2 stimulation in AGCTs.
567 Expression of ERα and ERβ was assessed by IHC (A-H). Representative images of low and high
568 staining patterns, magnifications 50 x (scale bar: 50µm) and 100 x (scale bar: 20 µm). Expression
569 of *GPER1* mRNA was determined by RNA *in situ* hybridization (I-L). Representative images of
570 low and high staining patterns, magnifications 80 x (scale bars: 20µm) and 160 x (scale bars:
571 10µm). M-O: Expression of *ESR1, ESR2,* and *GPER1* was assessed by qPCR after stimulation with
572 E2 (0-1000 nM) for 96 hours. P: Cell viability was measured after stimulation with E2 (0-1000 nM)
573 for 96 hours. Black columns: KGN cell line; grey columns: primary AGCT cells.
574
575 **Figure 5.** ERβ and *GPER1* expression levels were increased in recurrent AGCTs compared with
576 primary tumors. Paired analysis of the expression of estrogen receptors ERβ (A) and *GPER1* (B) in
577 16 patients with both primary and recurrent tumor samples in the TMA.
578

Table 1. Clinicopathologic data of the patients (A) and samples (B) in the tumor tissue microarray (TMA)

A Patients n=138	n (% of total)
Age at diagnosis, years[a]	53 (26-81)
Tumor stage at diagnosis	
I	126 (93)
II	8 (6)
III	1 (1)
Follow-up time, years[a]	15.0 (0.7-42.3)
Recurrence	
Yes	51 (37)
No	87 (63)
Survival	
Alive	91 (66)
Dead of AGCT	24 (17)
Dead of other	23 (17)
B Tumor characteristics (n=175)	n (% of total)
Primary	121 (69)
Recurrent	54 (31)
Subtype	
Sarcomatose	72 (42)
Differentiated	98 (58)
Tumor size	
<10 cm	103 (60)
≥10 cm	70 (40)
Nuclear atypia	
High	50 (29)
Low	121 (71)
Mitotic index	
High	48 (28)
Low	123 (72)
MP status at sample retrieval	
Premenopausal	46 (33)
Postmenopausal	92 (67)

[a]Median (range)
MP=menopause

Table 2. Clinicopathologic data of the patients (A) and samples (B) in the serum analysis

A Patients n=47	n (%)
Age at diagnosis, years[a]	56 (26-80)
Tumor stage at diagnosis	
I	47
Follow-up time, years[a]	5.3 (0.4-20.9)
Recurrence	
Yes	19
No	24
B Sample characteristics	
Total n=51	
Primary	31
Recurrent	20
Tumor size	
<10 cm	24
≥10 cm	15
MP status at sample retrieval	
Premenopausal	10
Postmenopausal	41

[a] Median (range)
MP=menopause

Table 3. Marker distributions in AGCT tissue microarray

A	Immunohistochemical staining							
Marker	Negative n (%)		Weak n (%)		Intermediate n (%)		High n (%)	
	Prim	Rec	Prim	Rec	Prim	Rec	Prim	Rec
ERα nuclear/cytoplasmic (n=165)	97/96 (59/58)	36/43 (22/26)	15/0 (9/0)	13/0 (8/0)	3/19 (2/12)	1/7 (1/4)	0	0
ERβ (n=152)	7 (5)	2 (1)	34 (22)	6 (4)	29 (39)	11 (7)	38 (25)	25 (16)
Cyp19A1 (n=156)	60 (38)	21 (13)	36 (23)	13 (8)	12 (8)	5 (3)	4 (3)	5 (3)

B	RNA in situ hybridization							
Marker	Negative n (%)		Weak n (%)		Intermediate n(%)		High n (%)	
	Prim	Rec	Prim	Rec	Prim	Rec	Prim	Rec
FSHR (n=165)	11 (7)	6 (4)	31 (19)	18 (11)	60 (36)	21 (13)	15 (9)	3 (2)
Cyp19A1 (n=167)	104 (62)	38 (23)	8 (5)	5 (3)	5 (3)	7 (4)	0	0
GPER (n=161)	106 (66)	33 (20)	5 (3)	17 (11)	0	0	0	0

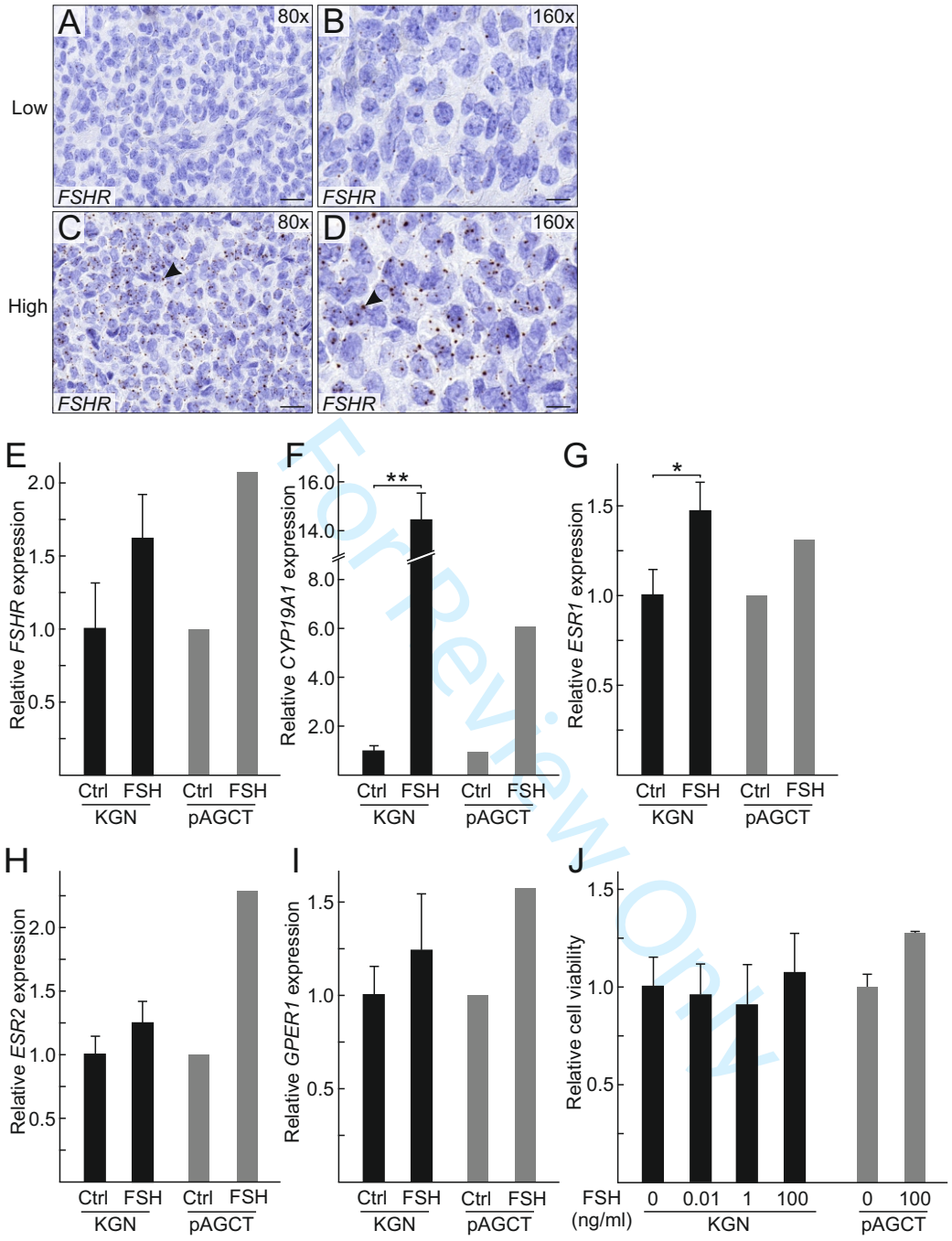

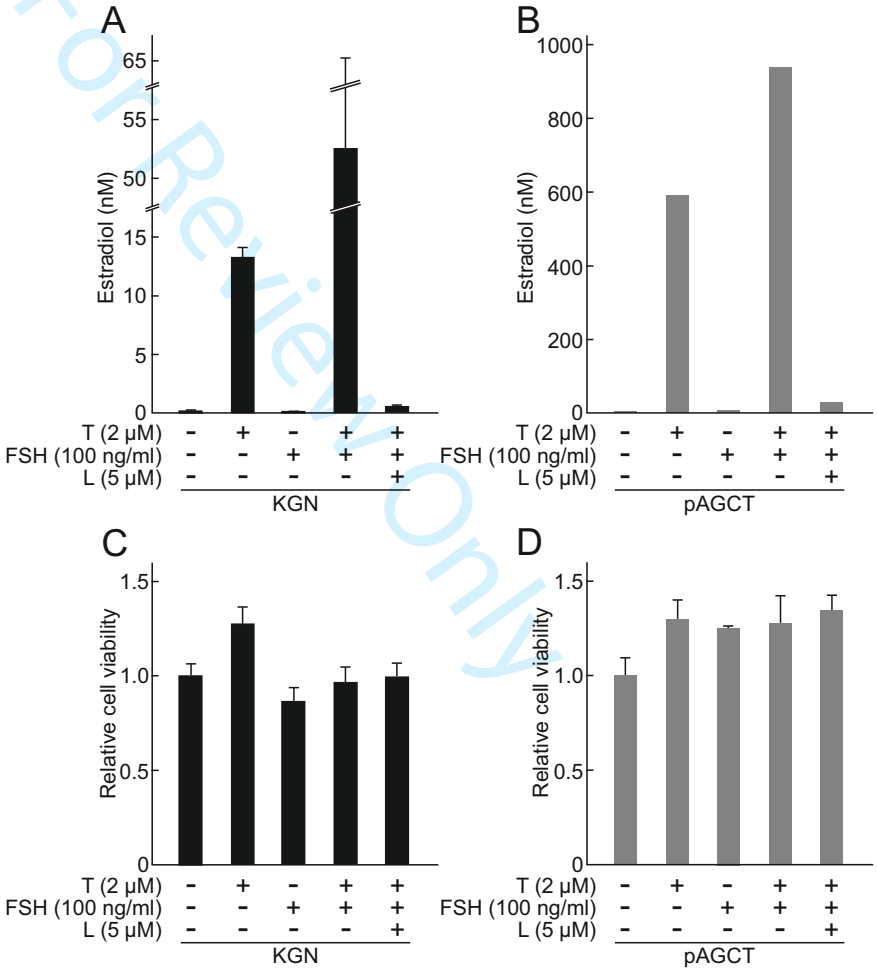

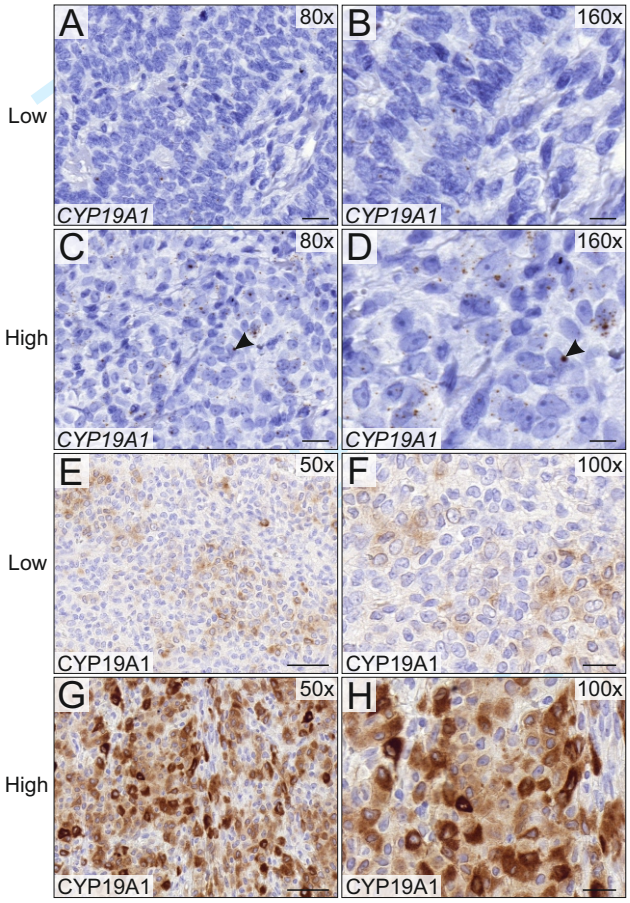
A
80x
B
160x
Low
CYP19A1
CYP19A1
C
80x
D
160x
High
CYP19A1
CYP19A1
E
50x
F
100x
Low
CYP19A1
CYP19A1
G
50x
H
100x
High
CYP19A1
CYP19A1

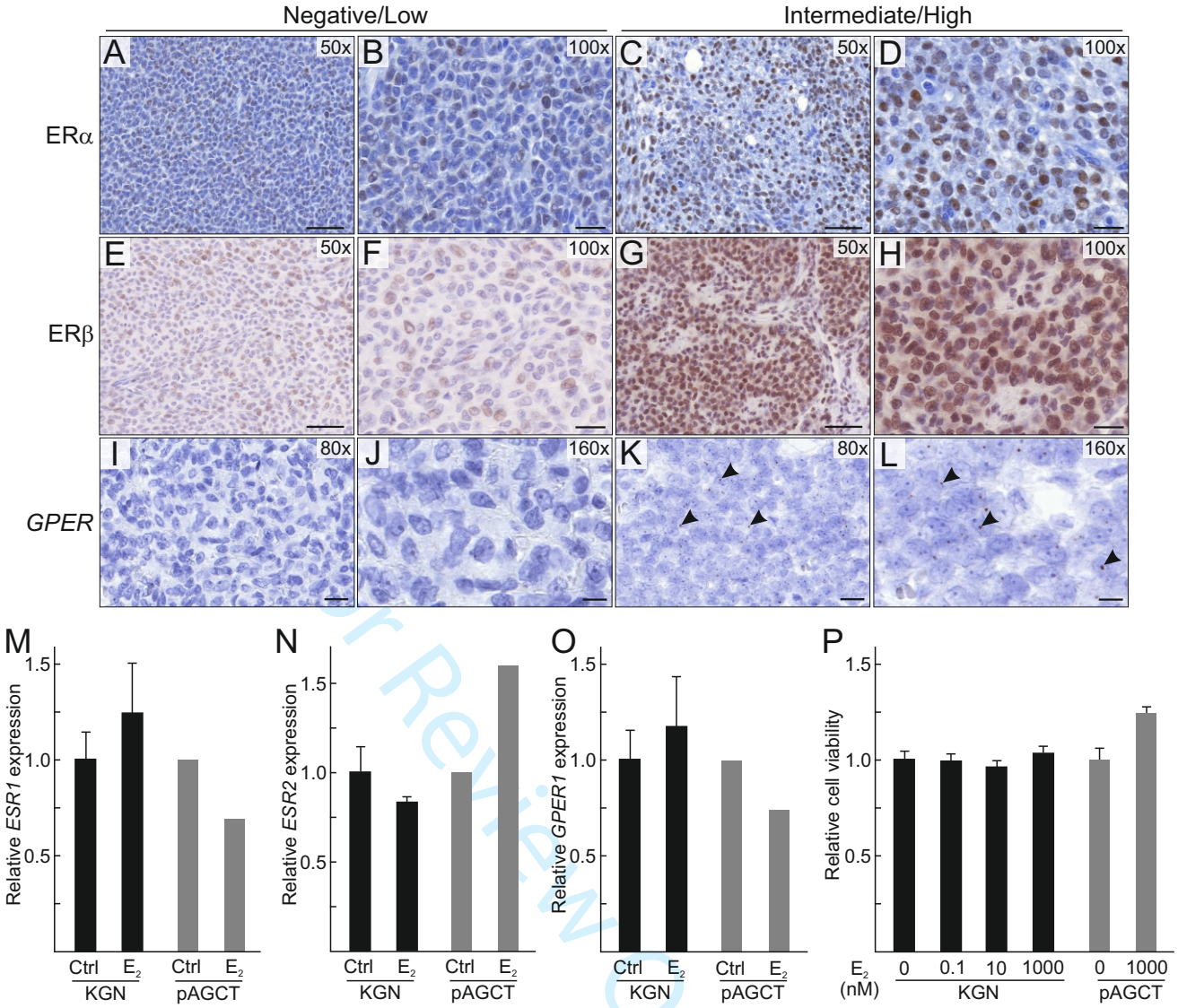

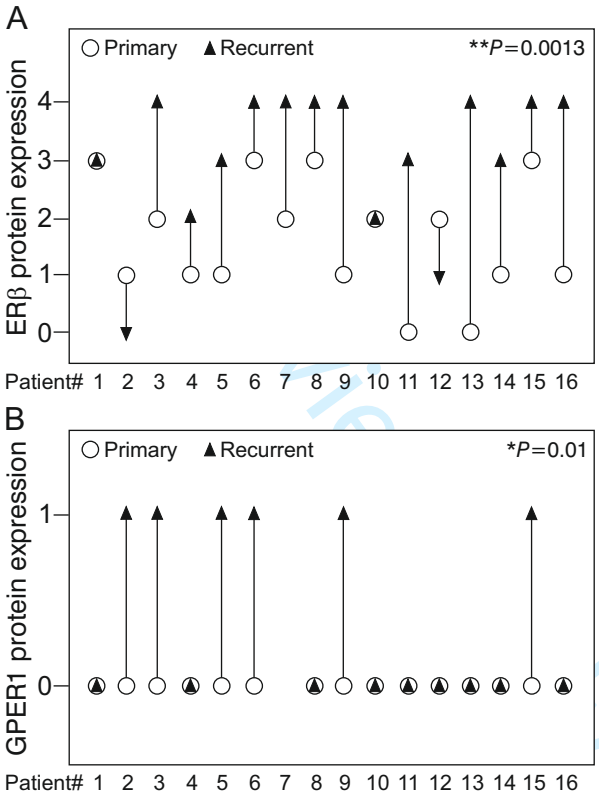
A
Primary
Recurrent
**P=0.0013
ERβ protein expression
4
3
2
1
0
Patient# 1 2 3 4 5 6 7 8 9 10 11 12 13 14 15 16
B
Primary
Recurrent
*P=0.01
GPER1 protein expression
1
0
Patient# 1 2 3 4 5 6 7 8 9 10 11 12 13 14 15 16

Supplementary Table 1. Data on primary cultured AGCT samples

Sample ID	Primary or recurrent tumor	Tumor size (in cm)	Age of the patient at sample retrieval and menopause status (age at primary diagnosis)	Preoperative serum hormone levels	Proportional change in cell number after E2-stimulation	Proportional change in cell number after FSH-stimulation
1	prim	11	53, postMP	E2 0.15 InhB 625 FSH 0.1	0,79	0,87
2	rec	4	49, postMP (45)	E2 0.17 InhB 278 FSH 10.1	1,57	1,05
3	prim	6,5	48, postMP	E2 0.55 InhB >1000 FSH 41	1,40	1,28
4	rec	5	68, postMP (59)	E2 0.17 InhB 61 FSH 42	1,23	1,43
5	prim	4	49, postMP	E2 0.13 InhB 223 FSH 15.4	1,25	1,26
6	rec	2,5	41, postMP (40)	E2 0.14 InhB 221 FSH 44.3	1,03	0,84

MP=menopause

Supplementary Table 2. Quantitative real-time PCR primer sequences

Gene	Reference	Oligonucleotide sequence 5'->3'
ACTB	NM_001101.4	F: CTGACGGCCAGGTCATCA R: CAGACAGCACTGTGTTGGC
CYP19A1	NM_000103.3	F: GGCATGAGTGATGTGATGGGA R: GGCAATTTAGAGTCCTGGTTTGA
ESR1	NM_000125.3	F: TGGAGATCTTCGACATGCTG R: GCCATCAGGTGGATCAAAGT
ESR2	NM_001040275.1	F: AGAGTCCCTGGTGTGAAGCA R: GACAGCGCAGAAGTGAGCATC
FSHR	NM_000145.3	F: TGCCATTCAATGGAACCCAACT R: CGTGGAAAACATCATTAGGCAAT
GPER1	NM_001039966.1	F: ACACACCTGGGTGGACACAA R: GGAGCCAGAAGCCACATCTG

Supplementary Table 3. P values of the hormone stimulations (in Figures 2C and D) using Student's t-test.

A

KGN	Control	Testosterone	FSH	Testosterone + FSH
Testosterone	0.0001	-	-	-
FSH	< 0.0001	< 0.0001	-	-
Testosterone + FSH	0.506	< 0.0001	0.061	-
Testosterone + FSH + Letrozole	0.897	< 0.0001	0.021	0.591

B

pAGCT	Control	Testosterone	FSH	Testosterone + FSH
Testosterone	< 0.0001	-	-	-
FSH	0.0002	0.473	-	-
Testosterone + FSH	< 0.0001	0.771	0.667	-
Testosterone + FSH + Letrozole	< 0.0001	0.447	0.146	0.297

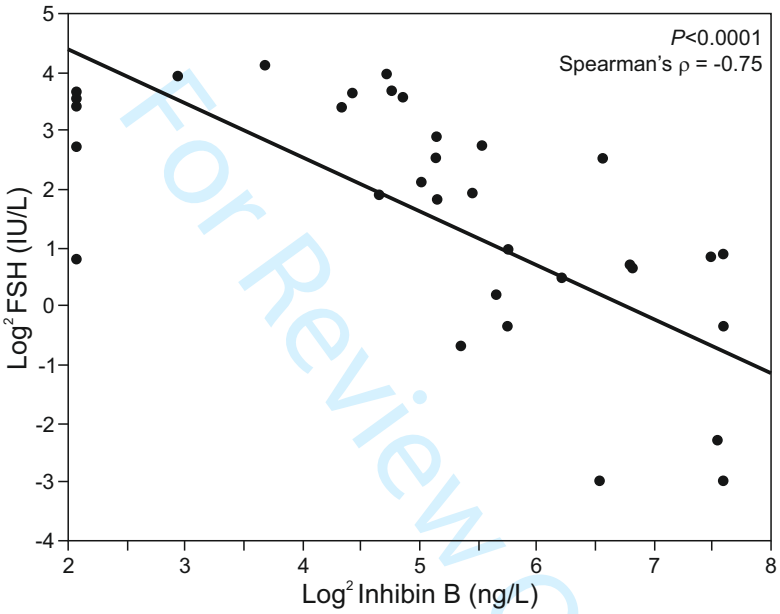

Supplementary Figure 1. Preoperative serum levels of FSH and Inhibin B correlate negatively in AGCT patients.

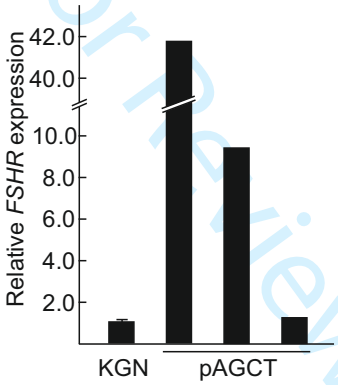

Supplementary Figure 2. Relative expression of *FSHR* mRNA in KGN cells and three primary AGCT cell cultures.

Molecular and Cellular Endocrinology 441 (2017) 164–175

Contents lists available at ScienceDirect

Molecular and Cellular Endocrinology

journal homepage: www.elsevier.com/locate/mce

GLI1$^+$ progenitor cells in the adrenal capsule of the adult mouse give rise to heterotopic gonadal-like tissue

Julia Dörner [a, c], Verena Martinez Rodriguez [a, c], Ricarda Ziegler [a, c], Theresa Röhrig [a, c], Rebecca S. Cochran [a], Ronni M. Götz [a, c], Mark D. Levin [a, 1], Marjut Pihlajoki [d], Markku Heikinheimo [a, d], David B. Wilson [a, b, *]

[a] Department of Pediatrics, Washington University School of Medicine, St. Louis Children's Hospital, St. Louis, MO 63110 USA
[b] Department of Developmental Biology, Washington University School of Medicine, St. Louis, MO 63110 USA
[c] Hochschule Mannheim – University of Applied Sciences, 68163 Mannheim, Germany
[d] University of Helsinki and Helsinki University Central Hospital, Children's Hospital, 00290 Helsinki, Finland

ARTICLE INFO

Article history:
Received 14 April 2016
Received in revised form
26 August 2016
Accepted 28 August 2016
Available online 29 August 2016

Keywords:
Adrenal cortex
Gonadectomy
Gonadotropin
Lineage tracing
Orchiectomy
Ovariectomy

ABSTRACT

As certain strains of mice age, hyperplastic lesions resembling gonadal tissue accumulate beneath the adrenal capsule. Gonadectomy (GDX) accelerates this heterotopic differentiation, resulting in the formation of wedge-shaped adrenocortical neoplasms that produce sex steroids. Stem/progenitor cells that reside in the adrenal capsule and retain properties of the adrenogonadal primordium are thought to be the source of this heterotopic tissue. Here, we demonstrate that GLI1$^+$ progenitors in the adrenal capsule give rise to gonadal-like cells that accumulate in the subcapsular region. A tamoxifen-inducible Cre driver (*Gli1*-creER^{T2}) and two reporters (*R26R*-lacZ, *R26R*-confetti) were used to track the fate of GLI1$^+$ cells in the adrenal glands of B6D2F2 mice, a strain that develops both GDX-induced adrenocortical neoplasms and age-dependent subcapsular cell hyperplasia. In gonadectomized B6D2F2 mice GLI1$^+$ progenitors contributed to long-lived adrenal capsule cells and to adrenocortical neoplasms that expressed *Gata4* and *Foxl2*, two prototypical gonadal markers. *Pdgfra*, a gene expressed in adrenocortical stromal cells, was upregulated in the GDX-induced neoplasms. In aged non-gonadectomized B6D2F2 mice GLI1$^+$ progenitors gave rise to patches of subcapsular cell hyperplasia. Treatment with GANT61, a small-molecule GLI antagonist, attenuated the upregulation of gonadal-like markers (*Gata4*, *Amhr2*, *Foxl2*) in response to GDX. These findings support the premise that GLI1$^+$ progenitor cells in the adrenal capsule of the adult mouse give rise to heterotopic tissue.

1. Introduction

As inbred mice age, patches of tissue resembling gonadal stroma appear beneath the adrenal capsule, a phenomenon known as subcapsular cell hyperplasia (Frith et al., 1983; Ward et al., 2002; Yates et al., 2013; Petterino et al., 2015). This process of ectopic gonadal-like differentiation is strain-dependent and accelerated by prepubertal gonadectomy (GDX) (Bernichtein et al., 2009). The resultant wedge-shaped lesions, termed GDX-induced adrenocortical neoplasms, are composed of two principal cell types: spindle-shaped type A cells that have limited steroidogenic capacity, and sex steroid-producing type B cells that accumulate later within patches of type A cells (Bielinska et al., 2006). The accumulation of type A or B cells is also a hallmark of adrenal neoplasia in several genetically-engineered mouse models (Looyenga and Hammer, 2006; Doghman et al., 2007; Berthon et al., 2010; Lee et al., 2011; Drelon et al., 2012; Hughes et al., 2012; Bandiera et al., 2013; Latre de Late et al., 2014).

Recent studies have shed light on the progenitors that give rise to heterotopic tissue in the adrenal cortex of mice [reviewed in (Bandiera et al., 2015; Röhrig et al., 2015)]. Fate mapping experiments have shown that the adrenal capsule contains long-lived stem/progenitor cells that retain properties of the adrenogonadal primordium (AGP), specialized cells in the genital ridge that are the

* Corresponding author. Box 8208, Washington University School of Medicine, 660 S. Euclid Ave., St. Louis, MO 63110, USA.
E-mail address: wilson_d@wustl.edu (D.B. Wilson).
[1] Current address: Cardiopulmonary Branch, National Heart, Lung, Blood Institute, National Institutes of Health, Bethesda, MD 20892, USA.

http://dx.doi.org/10.1016/j.mce.2016.08.043
0303-7207/

precursors of steroidogenic cells in the adrenal cortex, testis, and ovary (Bandiera et al., 2013). Under basal conditions, these AGP-like cells in the capsule can give rise to normal steroidogenic cells in the adrenal cortex. GDX activates these capsular progenitors and triggers their differentiation into gonadal-like tissue. *Wt1* is expressed in these AGP-like cells, and downregulation of this transcription factor gene is required for their differentiation into adrenocortical cells (Bandiera et al., 2013). WT1 directly activates *Gli1*, a downstream effector of hedgehog signaling, a pathway implicated in steroidogenic cell differentiation in both the adrenal cortex and gonads [reviewed in (Finco et al., 2015)]. Activation of *Gli1* expression by WT1 is thought to inhibit the differentiation of these progenitors into adrenocortical cells and promote their differentiation into gonadal-like cells (Bandiera et al., 2013).

Although *Gli1* has been implicated as a key regulator of heterotopic differentiation in the adrenal cortex of mice, there have been no direct studies tracking the fate of GLI1$^+$ cells during this process. Here, we investigate the fate of GLI1$^+$ progenitors in B6D2F2 mice, a strain that develops both GDX-induced adrenocortical neoplasia and aged-related subcapsular cell hyperplasia (Bernichtein et al., 2007). We demonstrate that GLI1$^+$ capsule cells give rise to GDX-induced neoplasms and to patches of spontaneous subcapsular cell hyperplasia. Additionally, we show that treatment with a small-molecule GLI inhibitor [GLI antagonist 61 (GANT61)] impairs the accumulation of gonadal-like markers in the adrenal glands of gonadectomized mice.

2. Materials and methods

2.1. Experimental animals

Procedures involving mice were approved by an institutional committee for laboratory animal care and were conducted in accordance with NIH guidelines for the care and use of experimental animals. C57Bl/6J mice harboring *Gli1*-creER^{T2} [*Gli1*$^{tm3(cre/ESR1)Alj}$/J] (Ahn and Joyner, 2004), *Rosa26* loxP-stop-loxP lacZ [*R26R*-lacZ; *Gt(ROSA)26Sor*^{tm1Sor}/J] (Pangas et al., 2007), or *R26R*-confetti [B6.Cg-*Gt(ROSA)26Sor*$^{tm1(CAG-Brainbow2.1)Cle}$/J] (Snippert et al., 2010) transgenes were obtained from the Jackson Laboratory (Bar Harbor, ME). These strains were crossed with DBA/2J mice (Jackson Laboratory) to generate B6D2F1 mice carrying the transgenes. B6D2F1 *Gli1*-creER^{T2} mice were crossed with B6D2F1 *R26R*-lacZ or B6D2F1 *R26R*-confetti mice to generate B6D2F2 offspring for analysis. Mice were anesthetized and gonadectomized at 3 weeks of age (Bielinska et al., 2005). Mice carrying the *Gli1*-creER^{T2} transgene were injected subcutaneously with tamoxifen (Sigma; St. Louis, MO; 200 mg/kg in corn oil) at varying times (see figure legends), and adrenal tissue was harvested for analysis 2–5 mo later. *Sf1-cre* mice [FVB-Tg(Nr5a1-cre)2Lowl/J] were obtained from the Jackson Laboratory and genotyped as described (Dhillon et al., 2006; Sodhi et al., 2006). *Sf1-cre* mice were crossed with B6D2F1 *R26R*-confetti mice to assess reporter expression in adrenocortical and gonadal steroidogenic cells. Dopachrome tautomerase-cre (*Dct*-cre) mice were generated as described previously (Guyonneau et al., 2002).

2.2. X-gal staining

Gli1-creER^{T2};*R26R*-lacZ mice were anesthetized and perfusion-fixed with 4% paraformaldehyde in PBS (Pihlajoki et al., 2013). Adrenal glands were harvested, incubated in 4% paraformaldehyde in PBS for an additional 30 min, permeabilized with 100 mM potassium phosphate pH 7.4, 0.02% NP-40 and 0.01% sodium deoxycholate for 5 min, and then stained with X-gal at 37 °C overnight (Narita et al., 1997). After staining, the glands were post-fixed in 4% paraformaldehyde in PBS for 1 h, frozen in OCT cyropreservation media (Tissue-Tek, Torrance, CA), sectioned (10 μm), counterstained with eosin, and examined by light microscopy. Alternatively, the X-gal stained tissue was post-fixed with Karnovsky solution, treated with 2% OsO_4, and embedded in epon (Bielinska et al., 2007). Sections were stained with uranyl acetate and lead citrate and examined by transmission electron microscopy (Bielinska et al., 2007).

2.3. Direct and indirect fluorescence microscopy

Sf1-cre;*R26R*-confetti and *Gli1*-creER^{T2};*R26R*-confetti mice were anesthetized and perfusion-fixed with 4% paraformaldehyde in PBS. Adrenal glands or gonads were harvested and fixed an additional 2 h in 4% paraformaldehyde in PBS. Following fixation, the glands were incubated overnight in 30% sucrose. Tissues then were embedded in OCT and cryosectioned (10 μm). Indirect immunofluorescence was performed (Bielinska et al., 2007) using the primary and secondary antibodies listed in Table 1. The analyses included negative control studies in which the primary or secondary antibodies were omitted. FITC-streptavidin staining of endogenous biotin in zG and zF cells was performed as described (Paul and Laufer, 2011).

2.4. Real time RT-PCR (RT-qPCR)

Total RNA was isolated and subjected to RT-qPCR analysis as described (Pihlajoki et al., 2013). Expression was normalized to the housekeeping genes *Actb* and *Gapdh*. Primer pairs are listed in Supplementary Table 1.

2.5. Pharmacological inhibition of GLI1/2 with GANT61

GANT61 (Cayman Chemical, Ann Arbor, MI) was dissolved in ethanol (50 mg/mL), sonicated on ice, and stored in aliquots at −80 °C. The ethanol stock was warmed and diluted in corn oil (1:4) before injection (50 mg/kg sc daily x 14 days) into gonadectomized weanling female DBA/2J mice (Lauth and Toftgard, 2007;

Table 1
Antibodies used for immunostaining.

Antibody	Primary antibody	Secondary antibody
GATA4	Goat anti-mouse GATA4 (sc-1237, Santa Cruz Biotech, 1:200 dilution)	Donkey anti-goat biotinylated IgG (Jackson Immunoresearch, West Grove, PA) at a 1:1000 dilution) followed by FITC-streptavidin (AlexaFluor-488, S11223, Invitrogen, 1:1000 dilution). Alternatively, the avidin-biotin immunoperoxidase system (Vectastain Elite ABC Kit, Vector Laboratories, Inc., Burlingame, CA) and diaminobenzidine were used to visualize the bound antibody.
PDGFRα	Rabbit anti-mouse PDGFRα (sc-338, Santa Cruz Biotech, 1:100 dilution)	FITC-goat anti-rabbit IgG (111-095-003, Jackson Immunoresearch, 1:1000 dilution)
FOXL2	Goat anti-FOXL2 (IMG-3228; Imgenex, San Diego, CA; 1:400 dilution).	Donkey anti-goat biotinylated IgG (Jackson Immunoresearch) at a 1:1000 dilution) followed by FITC-streptavidin (AlexaFluor-488, S11223, Invitrogen, 1:1000 dilution). Alternatively, the avidin-biotin immunoperoxidase system (Vectastain Elite ABC Kit, Vector Laboratories, Inc.) and diaminobenzidine were used to visualize the bound antibody.

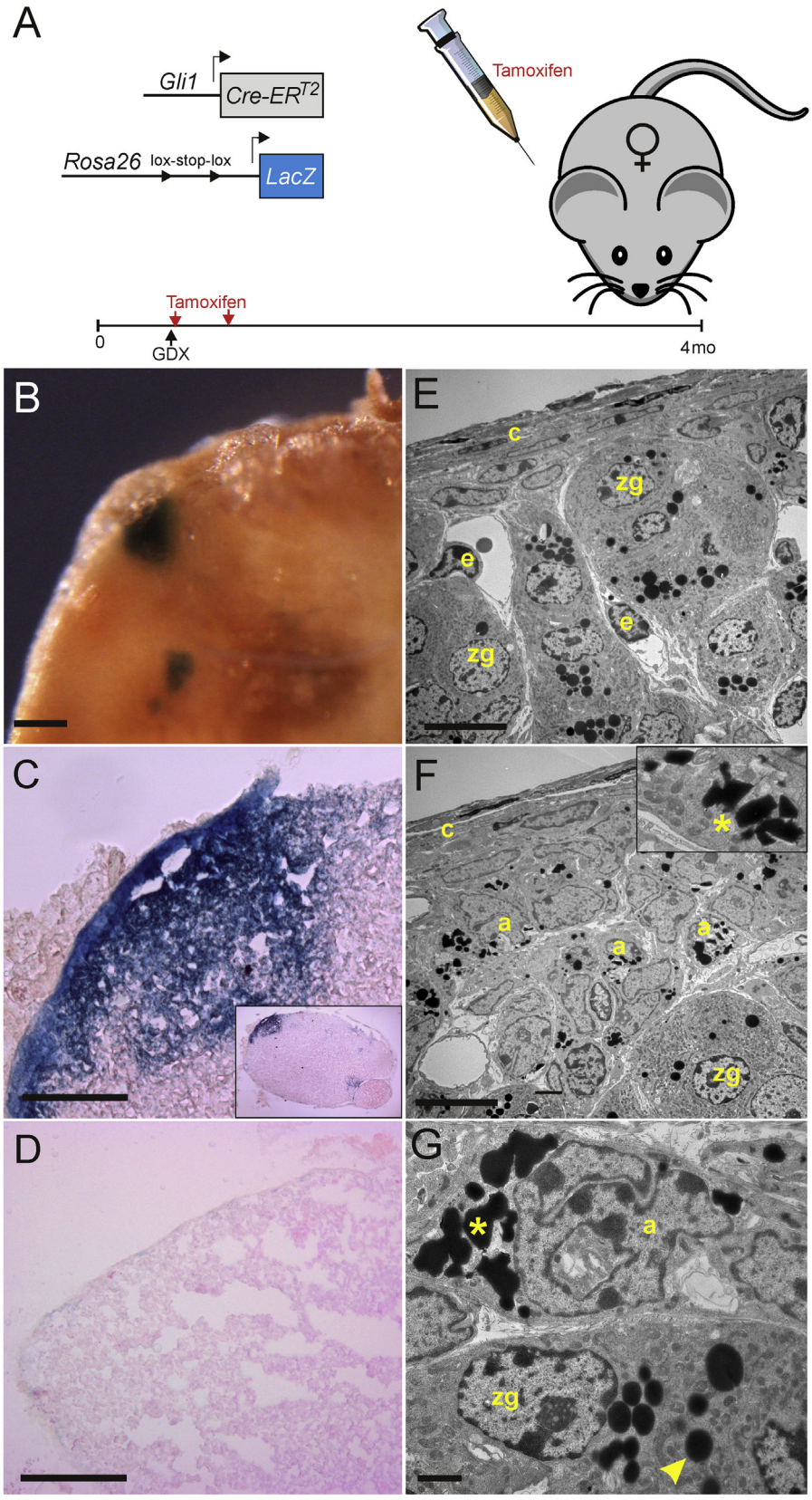

Fig. 1. GLI1^{+} progenitor cells contribute to GDX-induced neoplasms in the adrenal glands of *Gli1*-CreER^{T2};*R26R*-lacZ mice. **A)** Female B6D2F2 *Gli1*-CreER^{T2};*R26R*-lacZ mice were gonadectomized or subjected to sham surgery and then injected with tamoxifen at the indicated times. Adrenal glands were harvested at 4 mo of age. **B)** Whole-mount X-gal staining highlights patches of neoplastic cells. **C)** A wedge-shaped, β-gal^{+} neoplasm in a cryosection of an X-gal stained adrenal. The inset shows a lower magnification view of the same tissue section. **D**) Cryosection of an X-gal stained adrenal gland from a non-gonadectomized, tamoxifen-treated *Gli1*-CreER^{T2};*R26R*-lacZ mouse. Rare, small patches of β-gal^{+} cells are seen in the capsule but not the underlying cortex. **E,F)** Electron photomicrographs of normal and neoplastic adrenal cortex, respectively, from a *Gli1*-CreER^{T2};*R26R*-lacZ mouse. Note the accumulation of ovoid type A cells in the neoplastic cortex. The inset in panel F shows irregularly shaped X-gal crystalloids (*) in a type A cell. **G**) Ultrastructural comparison of a type A cell and zG cell. Type A cells have a polymorphic nucleus, scant smooth endoplasmic reticulum, few mitochondria, and other characteristic features (see the accompanying text). The asterisk indicates irregularly-shaped X-gal crystalloids. The arrowhead highlights a round lipid droplet. Abbreviations: a, type A cell; c, capsule cell; e, endothelial cell; zg, zona glomerulosa cell. Bars: (B) 150 μm, (C,D) 100 μm, (E,F) 10 μm, (G) 1 μm.

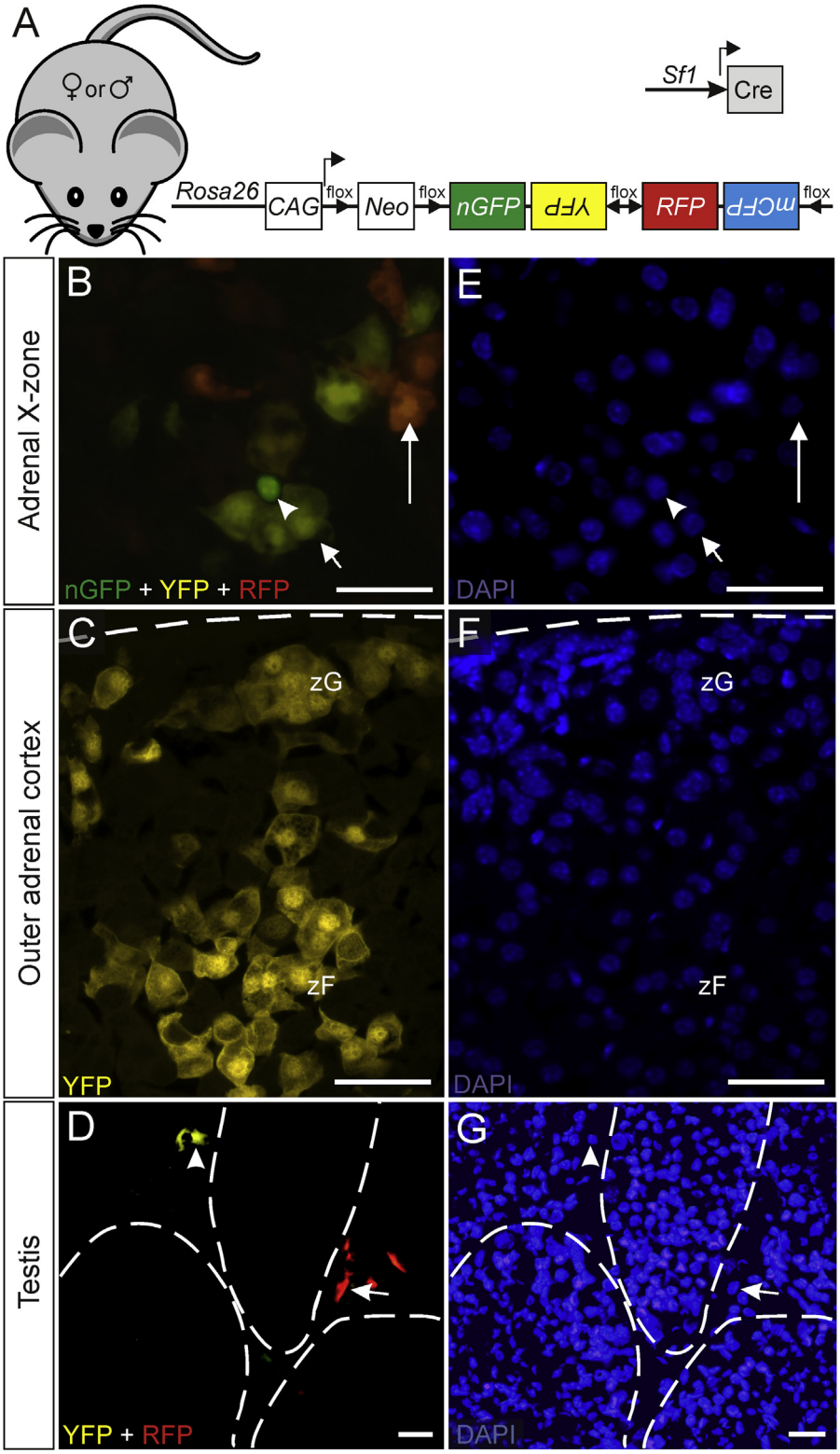

Fig. 2. Labeling of steroidogenic cells in the adrenal cortex and testis of *Sf1*-Cre;*R26R*-confetti mice. A) Adrenal glands or testis were harvested from 2-mo-old *Sf1*-Cre;*R26R*-confetti mice. Tissues were cryosectioned and examined by fluorescence microscopy. **B)** Clusters of nGFP$^+$ (arrowhead), YFP$^+$ (small arrow), and RFP$^+$ (large arrow) cells in the adrenal X-zone of a virgin female. In this image, green in the nGFP signal was selectively enhanced using software, so as to distinguish nGFP$^+$ from YPF$^+$ cells. **C)** A clone of YFP$^+$ zG and zF cells of the outer adrenal cortex of a female. Dashed lines denote the capsule surface. **D)** YFP$^+$ (arrowhead) and RFP$^+$ (arrow) testicular interstitial cells, presumed to be Leydig cells. Dashed lines denote seminiferous tubules. **E-G)** Corresponding DAPI stains. Bars: 30 μm. (For interpretation of the references to colour in this figure legend, the reader is referred to the web version of this article.)

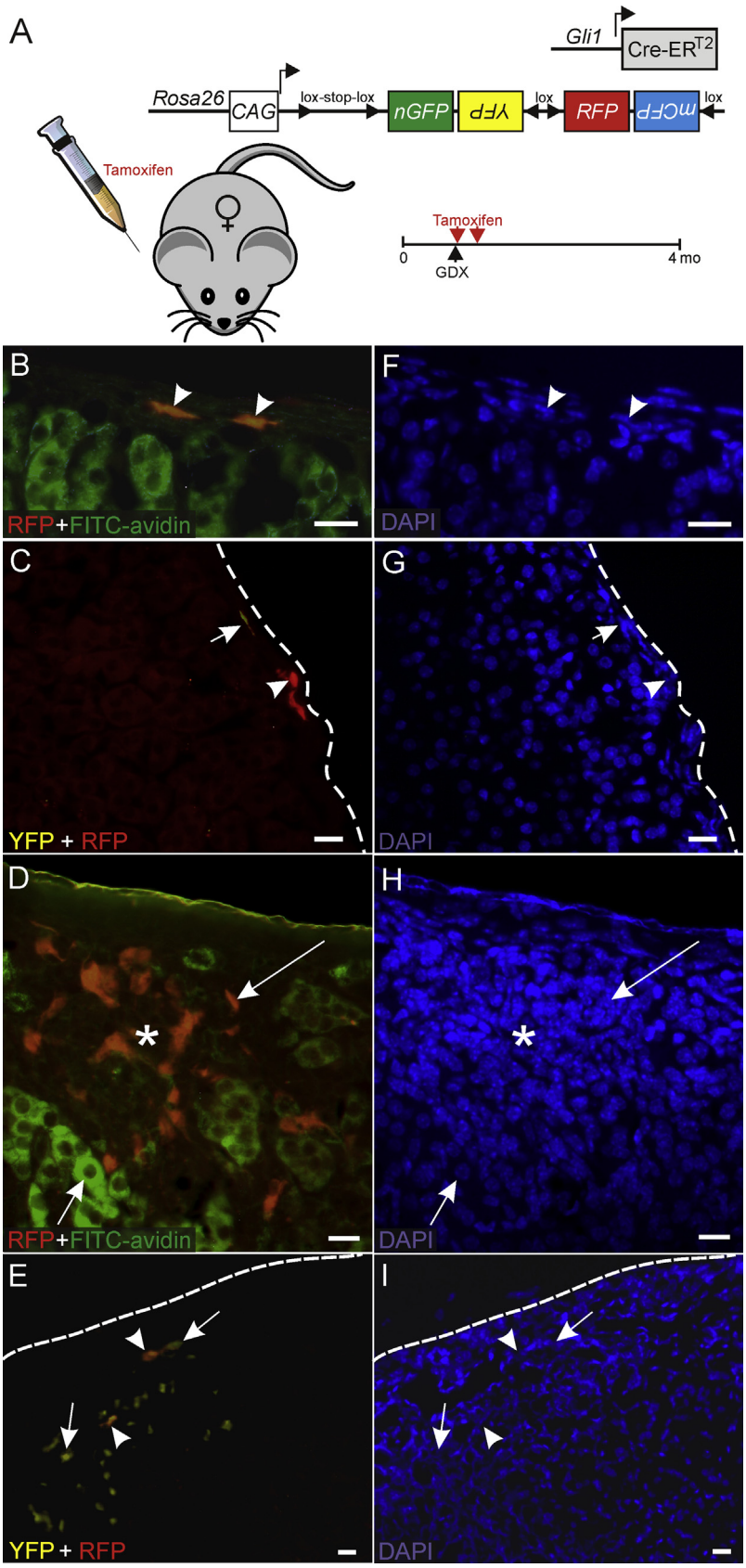

Fig. 3. GLI1^{+} progenitor cells contribute to long-lived capsule cells and to GDX-induced neoplasms in the adrenal glands of *Gli1*-CreER^{T2};*R26R*-confetti mice. A) Female B6D2F2 *Gli1*-CreER^{T2};*R26R*-confetti mice were gonadectomized and injected with tamoxifen at the indicated times. Adrenal glands were harvested, cryosectioned, and examined by fluorescence microscopy. Some of the sections were stained with FITC-streptavidin to detect endogenous biotin in normal steroidogenic cells. **B)** Arrowheads highlight two RFP^{+} capsule cells, presumably derived from a common GLI1^{+} progenitor. Biotin-rich steroidogenic cells are evident in the subjacent cortex. **C)** The arrowhead highlights a clone of RFP^{+}

Kramann et al., 2015). Control GDX DBA/2J mice were injected with vehicle alone (ethanol/corn oil, 1:4). At the indicated timepoints, adrenal tissue was harvested for RT-qPCR analysis or overnight fixation in 4% paraformaldehyde in PBS. The fixed tissue was embedded in paraffin, sectioned (4 μm), and subjected to immunoperoxidase staining (Anttonen et al., 2003; Bielinska et al., 2005; Schillebeeckx et al., 2015) using the primary and secondary antibodies listed in Table 1.

2.6. Isolation of neoplastic and normal tissue using laser capture microdissection (LCM)

Cryosections (10 μm) of mouse adrenal glands were collected on membrane slides (PEN-Membrane 2.0 μm; Leica), fixed in ethanol at −20° C, stained with crystal violet, and then dehydrated by passage through successively higher concentrations of ethanol followed by xylene (Pihlajoki et al., 2013; Schillebeeckx et al., 2013). LCM with a Leica LMD6000 microscope was used to isolate samples from neoplastic or normal tissue. Microdissectates were collected in RNA extraction buffer (RNeasy Mini Kit, Qiagen, Valencia, CA) or Arcturus Picopure RNA isolation kit (Applied Biosystems, Foster City, CA).

3. Results

3.1. Fate mapping in B6D2F2 Gli1-creER^{T2};R26R-lacZ mice

GLI1$^+$ progenitors in the adrenal capsule have been shown to contribute to steroidogenic cells during fetal and early postnatal development (King et al., 2009; Huang et al., 2010; Wood et al., 2013; Bandiera et al., 2015), but the contribution of GLI1$^+$ cells to adrenal homeostasis in adults has not been investigated in detail. We hypothesized that GLI1$^+$ cells are the precursors of GDX-induced adrenocortical neoplasms. To follow the fate of GLI1$^+$ progenitor cells in adult B6D2F2 mice, we used a tamoxifen-inducible cre-driver (*Gli1*-creER^{T2}) and a *Rosa26* flox-stop-flox-lacZ (*R26R*-lacZ) reporter allele. In the presence of tamoxifen, creER^{T2} excises the flox-stop-flox cassette, thereby indelibly activating reporter gene expression in a cell and its descendants (Ahn and Joyner, 2004; King et al., 2009). Whole mount X-gal staining of adrenal glands from gonadectomized, tamoxifen-treated *Gli1*-creER^{T2};*R26R*-lacZ mice demonstrated β-gal activity in discrete patches of cells (Fig. 1B). Sectioning of these adrenal glands showed that the patches of β-gal$^+$ cells corresponded to wedge-shaped subcapsular neoplasms (Fig. 1C). To optimize X-gal labeling of neoplastic cells, we varied the timing and frequency of tamoxifen administration in *Gli1*-creER^{T2};*R26R*-lacZ mice. Two doses of tamoxifen administered in the days following GDX (Fig. 1A) were sufficient to label adrenal capsular progenitors that subsequently gave rise to neoplasms in the mice. In contrast, administration of two doses of tamoxifen to non-gonadectomized *Gli1*-creER^{T2};*R26R*-lacZ mice resulted in only sparse labeling of cells in the adrenal capsule (Fig. 1D).

Transmission electron microscopy was used to further characterize the β-gal$^+$ cells in the adrenal glands of gonadectomized *Gli1*-creER^{T2};*R26R*-lacZ mice. Hydrolysis of X-gal by β-gal generates electron-dense, cytoplasmic crystalloids (Merchant-Larios and Moreno-Mendoza, 1998). Such crystalloids have irregular shapes that distinguish them from electron-dense lipid droplets (Fig. 1G, * *vs*. arrowhead). Crystalloid-laden neoplastic cells accumulated in the subcapsular region of gonadectomized *Gli1*-creER^{T2};*R26R*-lacZ mice and distorted the zonal architecture, displacing zG cells centripetally (Fig. 1F). The crystalloid-laden cells had the ultrastructural hallmarks of type A cells (Middlebrook et al., 2009), such as a polymorphic nucleus, thin cytoplasm, autophagocytic vacuoles, scant smooth endoplasmic reticulum, few mitochondria, and abnormal collagen deposits between cells (Fig. 1G). No crystalloids were observed in zG cells, endothelial cells, or other normal cell types adjacent to the neoplastic cells (Fig. 1E); nor did we detect β-gal$^+$ type B cells in our electron microscopic analysis. It is unclear whether the absence of type B cell labeling reflects a low efficiency of contribution of GLI1$^+$ progenitors to this cell population or inadequate sampling.

On the basis of fate mapping studies with *R26R*-lacZ reporter, we conclude that GDX-induced adrenocortical neoplastic cells, specifically type A cells, are derived from GLI1$^+$ progenitors.

3.2. Fate mapping in B6D2F2 Gli1-creER^{T2};R26R-confetti mice

To refine the lineage tracing analysis, we turned to a fluorescent reporter, *Rosa26* flox-stop-flox-confetti (*R26R*-confetti) (Snippert et al., 2010). The *R26R*-confetti allele comprises two reporting cassettes flanked by LoxP sites; each cassette contains a pair of fluorescent reporters of differing colors in opposite reading frames (Fig. 2A). Cre recombination of this allele randomly labels a cell and its descendants with one of 4 markers: nuclear-localized green fluorescent protein (nGFP), cytoplasmic yellow fluorescent protein (YFP), cytoplasmic red fluorescent protein (RFP), or membrane-tethered cyan fluorescent protein (mCFP). An advantage of this multicolor reporter is that it can be used to sparsely label progenitor cells, facilitating the tracking of individual clones via direct fluorescence.

The sensitivity of a given reporter allele to Cre-mediated recombination may vary among tissue types (Alcolea and Jones, 2013). To ensure that the *R26R*-confetti reporter could label adrenocortical and gonadal(-like) cells, we examined adrenal and gonadal tissue from *Sf1*-cre;*R26R*-confetti mice, which express Cre constitutively in steroidogenic cells. Clusters of cells expressing a single color marker, presumed to reflect clonal populations, were evident in adrenal X-zone cells (Fig. 2B,E), the outer adrenal cortex (Fig. 2C,F), and testicular interstitial cells (Fig. 2D,G). Reporter-expressing cells were more abundant in the X-zone than in the outer cortex, consistent with the observation that *Sf1* is highly expressed in the fetal adrenal, the precursor of the X-zone (Zubair et al., 2008). In agreement with a prior study demonstrating direct lineage conversion of zG to zF cells (Freedman et al., 2013), we observed clonal columns of zG + zF cells expressing a single color marker (Fig. 2C,F), presumably derived from a common stem/progenitor cell.

Of note, we did not detect expression of the mCFP reporter in the adrenal cortex of *Sf1*-cre;*R26R*-confetti mice. This lack of detectable mCFP signal appears to be an idiosyncrasy of the *R26R*-confetti reporter in adrenocortical tissue, because mCFP was seen in heart tissue from a *Dct*-cre;*R26R*-confetti mouse that had been fixed and processed in the same manner (Supplementary Fig. 1).

Next, we examined cryosections of adrenal glands from tamoxifen-treated, gonadectomized *Gli1*-creER^{T2};*R26R*-confetti mice. To distinguish neoplastic from normal adrenocortical tissue in these sections, we relied on a combination of darkfield microscopy, DAPI staining, and FITC-streptavidin labeling. Unlike normal

capsule cells, while the arrow indicates a neighboring YFP$^+$ capsule cell. **D**) GLI1$^+$ derivatives marked with RFP contribute to neoplastic subcapsular cells (large arrow) but not to normal steroidogenic cells (small arrow). The asterisk highlights a region where neoplastic cells are crowded together. **E)** A neoplasm containing 2 distinct clones [YFP$^+$ (arrow) and RFP$^+$ (arrowhead)]. **F-G)** Corresponding DAPI stains. Dashed lines denote the capsule surface. Bars: 25 μm.

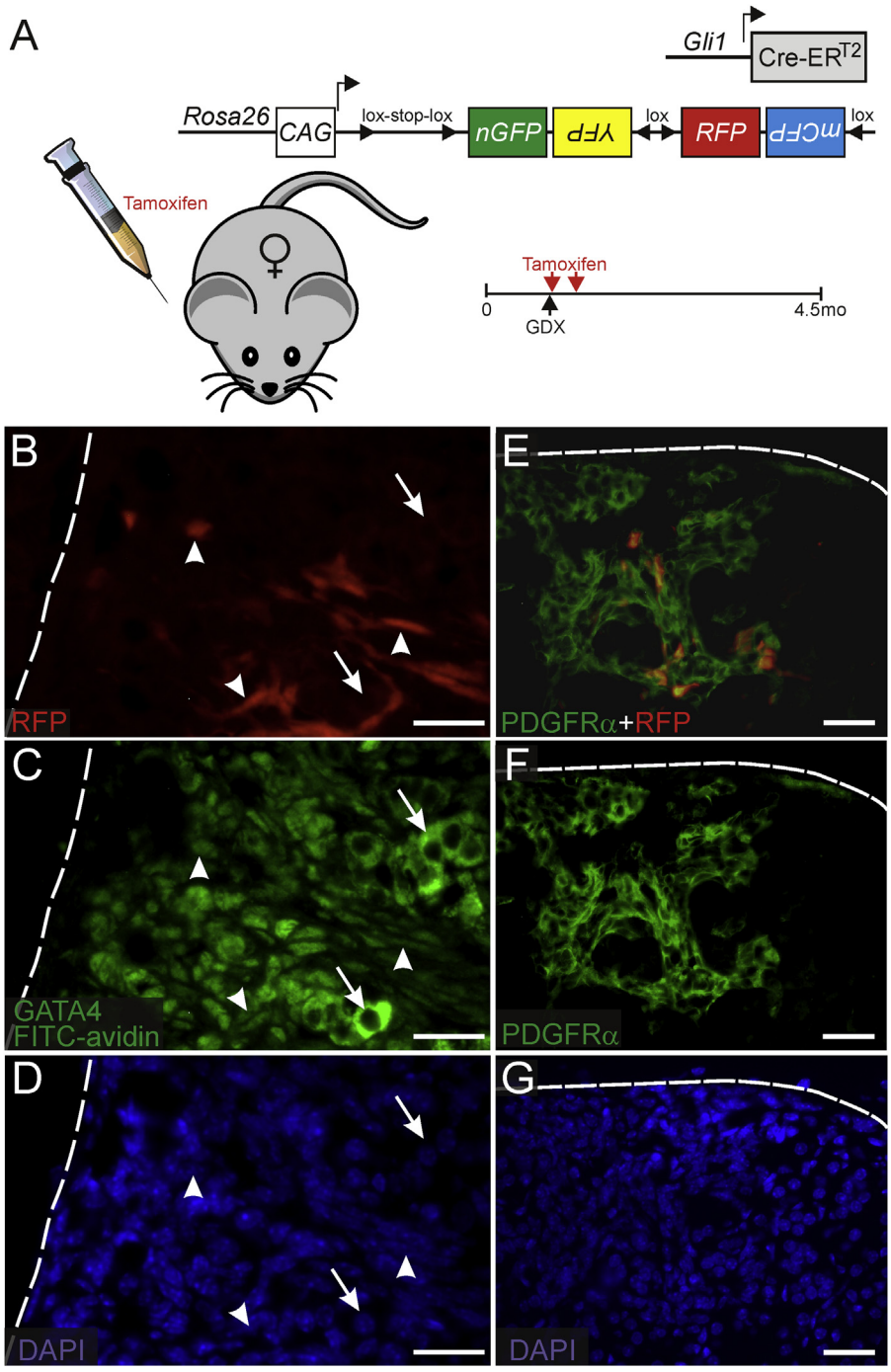

Fig. 4. GLI1^{+} progenitors contribute to GDX-induced adrenocortical neoplasms that express *Gata4* and *Pdgfra*. A) A B6D2F2 *Gli1*-CreER^{T2};*R26R*-confetti female mouse was gonadectomized and injected with tamoxifen at the indicated times. Adrenal glands were harvested, cryosectioned, and immunostained. **B-D)** GLI1^{+} derivatives marked with the RFP reporter contribute to ovoid- and spindle-shaped neoplastic cells exhibiting nuclear GATA4 immunoreactivity (arrowheads) but not to normal steroidogenic cells exhibiting cytoplasmic staining with FITC-streptavidin (arrows). **E-G)** GLI1^{+} derivatives marked with the RFP reporter contribute to cells that stain with PDGFRα antibody. Bars: 25 μm.

zG and zF cells, GDX-induced adrenocortical neoplasms contain scant lipid (Schillebeeckx et al., 2013) and therefore exhibit decreased birefringence when viewed under darkfield optics. When visualized by DAPI staining, the nuclei of normal steroidogenic cells are large, round, and well separated from one another, whereas the nuclei of neoplastic cells are small, oblong, and closely packed (*, Fig. 3D,H). Due to high endogenous biotin content, the cytoplasm of steroidogenic cells in the normal cortex stains directly with FITC-streptavidin (Paul and Laufer, 2011) (Fig. 3B,D,F,H). In contrast, non-steroidogenic (type A) cells in GDX-induced neoplasms do not stain directly with FITC-streptavidin (Fig. 3D,H).

In tamoxifen-treated, gonadectomized *Gli1*-creER^{T2};*R26R*-confetti mice, we observed clusters of capsule cells that expressed a single color reporter, presumed to be descendants of a common GLI1^{+} progenitor (Fig. 3B,C,F,G). These labeled cells persisted in the adrenal capsule for more than 6 mo after tamoxifen treatment, suggesting that they are long-lived. In the subcapsular region of adrenal glands from tamoxifen-treated, gonadectomized *Gli1*-

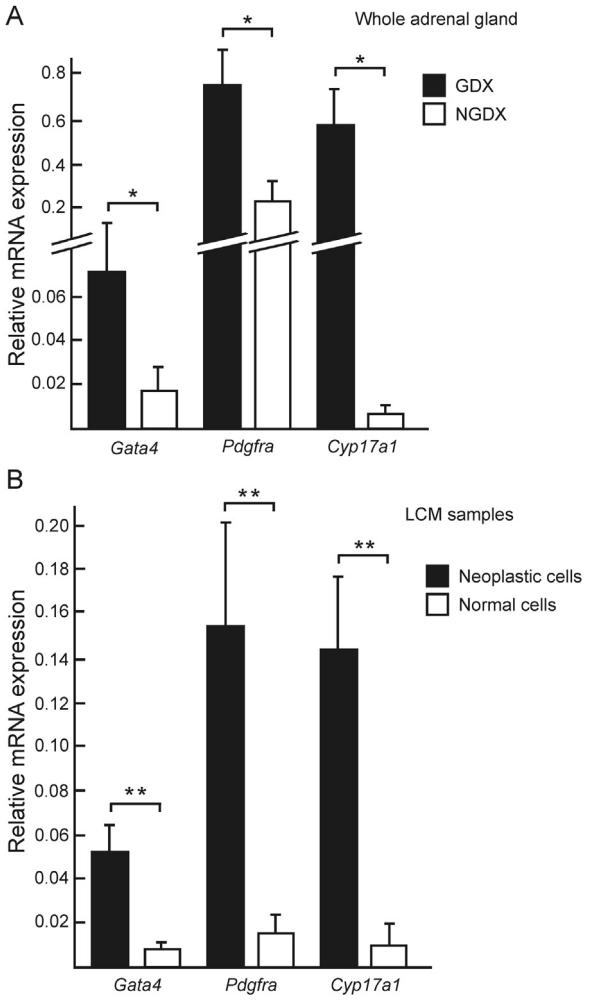

Fig. 5. Expression of gonadal-like differentiation markers in the adrenal glands of 4-mo-old gonadectomized *vs.* intact female DBA/2J mice. A) RNA was isolated from whole adrenal glands of gonadectomized (GDX) or non-gonadectomized (NGDX) mice and subjected to RT-qPCR (n = 3 per group). **B**) RNA was isolated from neoplastic tissue or normal cortical tissue (zG + zF) using laser capture microdissection (LCM) and subjected to RT-qPCR (n = 3 per group). Results were normalized to *Actb* expression. Comparable results were obtained when results were normalized to *Gapdh* expression. *$P < 0.05$, **, $P < 0.01$.

creER^{T2};*R26R*-confetti mice, we observed clones of marked neoplastic cells (Fig. 3D,E,H,I). These reporter-expressing neoplastic cells displaced zF and zG cells centripetally, distorting the cortical architecture. Neoplastic cells expressing the confetti reporter contained scant lipid, and only a small percentage of these cells were classified as steroidogenic on the basis of FITC-streptavidin staining [7 of 365 RFP$^+$ cells (2%) stained directly with FITC-streptavidin at 4 mo post-GDX, n = 6 adrenals]. Importantly, some wedge-shaped tumors in tamoxifen-treated, gonadectomized *Gli1*-creER^{T2};*R26R*-confetti mice contained separate clones of neoplastic cells derived from independent recombination events involving different reporter cassettes (e.g., YFP and RFP; Fig. 3E,I). This suggests that individual tumors can arise from patches of neoplasia-ready GLI1$^+$ progenitor cells in the capsule.

Immunofluorescence microscopy was used to characterize the marked cells in the adrenal glands of tamoxifen-treated, gonadectomized *Gli1*-creER^{T2};*R26R*-confetti mice. We focused our analysis on neoplasms expressing a single color reporter (RFP) and performed indirect immunofluorescence using FITC-conjugated secondary antibodies or biotin-labeled secondary antibody followed by FITC-streptavidin. We observed ovoid- or spindle-shaped neoplastic cells that expressed both RFP and nuclear GATA4, a marker of type A cells (Fig. 4B–D). In contrast to normal steroidogenic cells (arrows, Fig. 4B–D), the RFP$^+$/GATA4$^+$ neoplastic cells did not stain directly with FITC-streptavidin (arrowheads, Fig. 4B–D). Another marker known to be expressed in type A cells, FOXL2 (Schillebeeckx et al., 2015), was detected in RFP$^+$ neoplastic cells (Sup Fig. 2B–D). We also saw neoplastic cells that co-expressed RFP and the platelet derived growth factor receptor PDGFRα (Fig. 4E–G), a marker previously shown to be present in fibroblastic stromal cells of normal adrenal cortex (Wood et al., 2013).

To independently verify that *Pdgfra* was expressed in GDX-induced adrenocortical neoplasms, we performed RT-qPCR analysis on RNA from whole adrenal extracts from gonadectomized *vs.* intact mice (Fig. 5A) and on RNA from laser capture microdissectates of neoplastic *vs.* non-neoplastic adrenocortical tissue (Fig. 5B). For these RT-qPCR experiments, we used DBA/2J mice, a strain that is highly susceptible to GDX-induced adrenocortical neoplasia (Bielinska et al., 2003). Like *Gata4* and *Cyp17a1*, two well-established markers of GDX-induced adrenocortical neoplasia [reviewed in (Röhrig et al., 2015)], expression of *Pdgfra* mRNA was significantly increased in whole adrenal extracts and microdissected neoplastic tissue from gonadectomized mice.

In non-gonadectomized *Gli1*-creER^{T2};*R26R*-confetti mice, we observed long-lived confetti$^+$ cells in the capsule, but these labeled capsule cells did not contribute efficiently to steroidogenic cells in the subjacent cortex (data not shown). In 6-mo-old tamoxifen-treated, non-gonadectomized *Gli1*-creER^{T2};*R26R*-confetti mice, we saw patches of subcapsular cell hyperplasia expressing the confetti reporter (Fig. 6B,C), implying that these spindle-cell lesions, like GDX-induced adrenocortical neoplasms, are derived from GLI1$^+$ progenitors.

We conclude that: 1) the *R26R*-confetti reporter is useful for tracking cell fate in the adrenal cortex, 2) separate clones of GLI1$^+$ progenitor cells contribute individual GDX-induced neoplasms, 3) PDGFRα is a novel marker of GDX-induced adrenocortical neoplasia, and 4) long-lived GLI1$^+$ capsular progenitors give rise to patches of subcapsular cell hyperplasia in older, non-gonadectomized mice.

3.3. GANT61 treatment impairs the expression of gonadal-like markers in the adrenal glands of gonadectomized DBA/2J mice

Studies of mutant mice have shown that GLI1 is not required for hedgehog signaling, because GLI2 can rescue most GLI1 functions (Park et al., 2000; Bai et al., 2002). To garner evidence that GLI factors are crucial for GDX-induced adrenocortical neoplasia, we administered GANT61, an inhibitor of GLI1 and GLI2 (Lauth and Toftgard, 2007; Kramann et al., 2015), to gonadectomized mice (Fig. 7A). For these experiments we used the highly susceptible strain DBA/2J, because previous studies have shown that type A cells accumulate in the adrenal glands of these mice within 2 weeks of GDX (Bielinska et al., 2003). RT-qPCR analysis showed that GANT61 treatment reduced adrenal expression of *Gli1*, a downstream indicator of hedgehog signaling (Fig. 7B). GANT61 treatment also attenuated adrenal expression of 3 gonadal-like markers (*Gata4*, *Amhr2*, *Foxl2*) known to be expressed in type A cells (Röhrig et al., 2015). Immunohistochemical analysis confirmed reduced numbers of GATA4- and FOXL2-immunoreactive cells in the GANT61-treated specimens (Fig. 7C). These pharmacological inhibition studies suggest that GLI factors influence GDX-induced adrenocortical neoplasia.

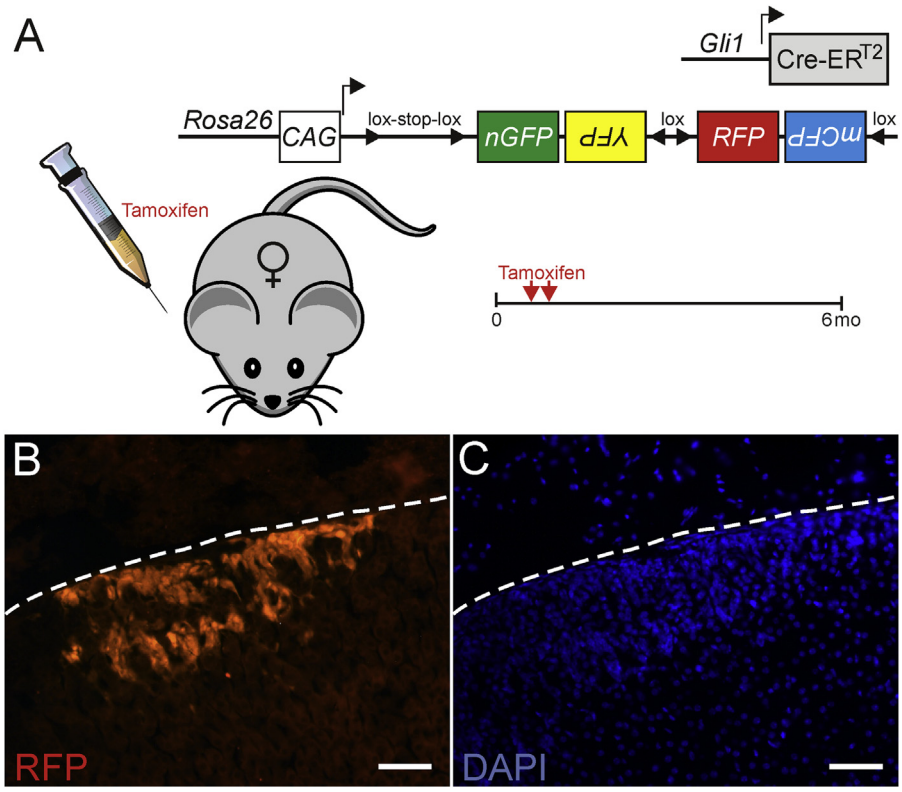

Fig. 6. GLI1^{+} progenitors contribute to subcapsular cell hyperplasia in an older, non-gonadectomized *Gli1*-CreER^{T2};*R26R*-confetti mouse. A) A female B6D2F2 *Gli1*-CreER^{T2};*R26R*-confetti mouse was injected with tamoxifen at the indicated times. Adrenal glands were harvested and cryosectioned. **B)** A clonal patch of subcapsular spindle-cell hyperplasia expressing RFP. **C)** Corresponding DAPI stain. The capsule surface is shown by the dashed lines. Bars: 100 μm.

4. Discussion

Lineage tracing is a powerful approach for understanding tissue development and homeostasis, particularly when it is combined with experimental manipulation of signals that regulate cell-fate decisions (Kretzschmar and Watt, 2012). Here, we have applied lineage tracing techniques to a classic model of altered cell fate: the GDX-induced accumulation of heterotopic tissue in the adrenal glands of mice (Röhrig et al., 2015). Our fate mapping studies with B6D2F2 mice support the premise that GLI1 is a key player in gonadal-like differentiation in the adrenal cortex. Long-lived GLI1^{+} capsular progenitor cells give rise to adrenocortical neoplasms in gonadectomized B6D2F2 mice and to patches of subcapsular cell hyperplasia in older, non-gonadectomized B6D2F2 mice. GANT61 treatment reduces the expression of gonadal-like markers (*Gata4*, *Amhr2*, *Foxl2*) in the adrenal glands of gonadectomized DBA/2J mice, supporting a role for GLI factors in GDX-induced adrenocortical neoplasia.

Our findings complement prior studies showing that distinct pools of stem/progenitor cells exist within the adrenal capsule and subjacent cortex [reviewed in (Pihlajoki et al., 2015; Walczak and Hammer, 2015)]. Progenitor cell populations characterized thus far include those expressing *Wt1*, *Gli1*, *Tcf21*, and *Shh* (Table 2). These progenitor populations may overlap to some degree. For example, WT1^{+} progenitors have been shown to co-express *Gli1* and *Tcf21*. Some of these progenitors give rise to differentiated cells only during specific developmental windows or in response to experimental manipulation. Prior lineage tracing studies with the *Gli1*-creER^{T2} driver have shown that GLI1^{+} progenitors in the adrenal capsule contribute to steroidogenic cells, particularly when tamoxifen induction is performed during fetal development; when tamoxifen is administered postnatally, the labeling of cortical steroidogenic cells appears less robust (King et al., 2009; Huang et al., 2010; Wood et al., 2013). Under the experimental conditions we used (2 doses of tamoxifen administered to weanling B6D2F2 mice) there was negligible contribution of GLI1^{+} cells to steroidogenic cells in the cortex. We surmise that mouse age, the timing of tamoxifen treatment, and other facets of experimental design impact lineage tracing results with the *Gli1*-creERT2 driver. Our findings, coupled with those of other investigators, suggest that the fate of GLI1^{+} cells in the adrenal capsule may differ in the fetus and adult.

In the course of our fate mapping experiments we identified *Pdgfra* as a marker of GDX-induced adrenocortical neoplasia. A previous transcriptome-wide search (Schillebeeckx et al., 2015) designed to detect novel markers of GDX-induced adrenocortical neoplasia overlooked *Pdgfra*, because this gene was not represented on the microarray used in the analysis. Platelet derived growth factor (PDGF) signaling is known to control the differentiation of gonadal steroidogenic cells in both sexes (Schmahl et al., 2008), and PDGFRα is a marker of putative Leydig stem cells in rodents and humans (Landreh et al., 2013, 2014; Odeh et al., 2014). PDGFRα has been shown to be a marker of fibroblastic stromal cells in the non-neoplastic adrenal cortex (Wood et al., 2013). GLI1 has been shown to enhance expression of *Pdgfra* in C3H10T½ mouse mesenchymal cells (Xie et al., 2001).

To our knowledge, this is the first article describing the use of the *R26R*-confetti reporter in adrenocortical tissue. This reporter offers certain advantages compared to other widely used reporters. In particular, sparse multicolor labeling by the confetti reporter permits tracing of individual clones or subclones of cells. Our studies establish that GDX-induced adrenocortical neoplasms

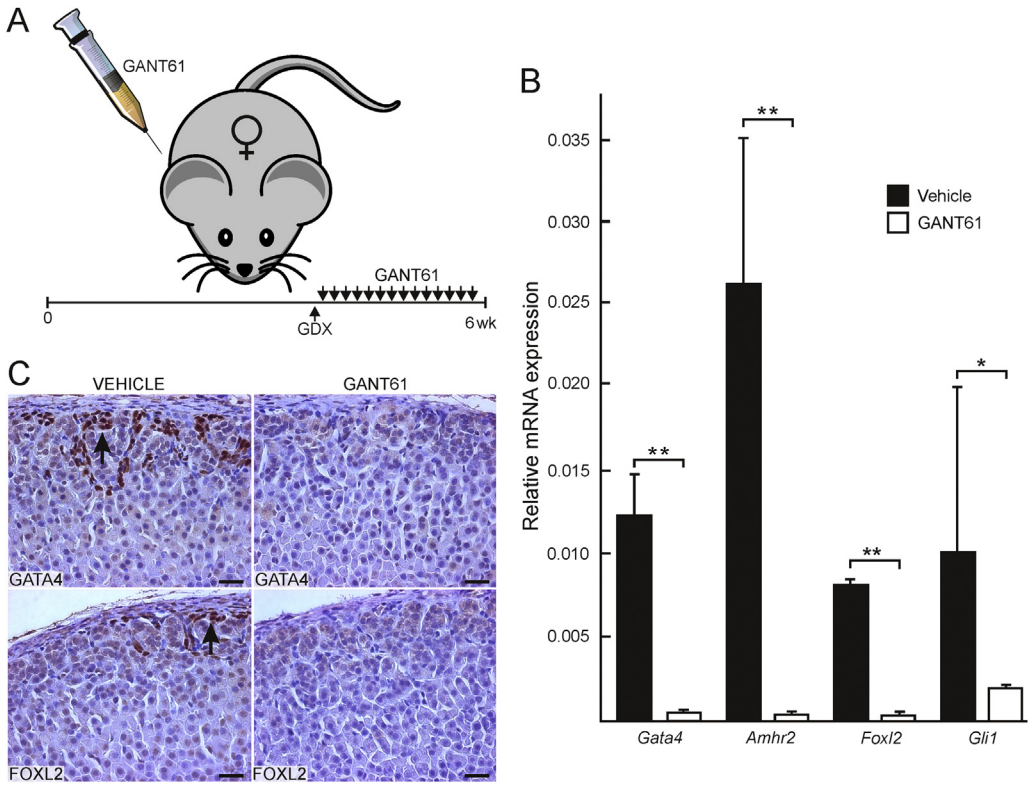

Fig. 7. Expression of gonadal-like differentiation markers in the adrenal glands of gonadectomized female DBA/2J mice treated with GANT61 or vehicle. A) Weanling female mice were gonadectomized and then injected daily with GANT61 (50 mg/kg) or vehicle control. **B)** After 14 days, RNA was isolated from whole adrenal glands and subjected to RT-qPCR (n = 4 per group). Results were normalized to *Actb* expression. Comparable results were obtained when results were normalized to *Gapdh* expression. $^{*}P < 0.05$, $^{**}P < 0.01$. **C)** Adrenal glands from vehicle- or GANT61-treated mice were subjected to immunoperoxidase staining for GATA4 or FOXL2. Nuclear immunoreactivity is evident in type A cells in the subcapsular region of the vehicle-treated adrenals (arrows). Bars: 50 μm.

Table 2
Stem/progenitor cell populations in the periphery of the adrenal gland as defined by fate mapping studies.

Stem/Progenitor population	Location	Comments	References
WT1^{+} progenitors	Capsule	Under basal conditions WT1^{+} capsule cells give rise to adrenocortical cells, but GDX triggers their differentiation into gonadal-like tissue.	(Bandiera et al., 2013)
GLI1^{+} progenitors	Capsule	These cells are descendants of *Sf1*-expressing fetal adrenocortical cells. GLI1^{+} progenitors differentiate into steroidogenic cells, particularly during fetal development. GDX triggers their differentiation into gonadal-like tissue.	(King et al., 2009; Huang et al., 2010; Wood et al., 2013) and this study
TCF21^{+} progenitors	Capsule	TCF21^{+} cells, which are descendants of the AGP rather than SF1^{+} fetal adrenocortical cells, give rise to non-steroidogenic stromal cells in the adrenal cortex.	(Wood et al., 2013)
SHH^{+} Progenitors	Subcapsular region	These cells give rise to steroidogenic cells in the zF and zG but not capsule cells.	(King et al., 2009; Huang et al., 2010)

are polyclonal in nature. Individual wedge-shaped tumors in *Gli1*-creER^{T2};*R26R*-confetti mice are composed of multiple marked clones, each derived from a separate GLI1^{+} capsular progenitor. This suggests that GDX-induced adrenocortical tumors arise from patches of "neoplasia-ready" progenitors in the capsule. Such neoplasia-ready cells may be defined in part by epigenetic modifications that impact the phenotypic plasticity of adrenocortical stem/progenitor cells, allowing some to respond to the hormonal changes associated with GDX (Bielinska et al., 2009; Schillebeeckx et al., 2013, 2015). Epigenetic variability among stem/progenitor cells may explain why GDX of susceptible mouse strains leads to discrete wedges of proliferating neoplastic cells in the adrenal cortex rather than uniform tumor formation along the periphery of the cortex. Interestingly, the level of *Wt1* expression has been shown to vary stochastically among AGP-like stem/progenitor cells in the adrenal capsule, and this variability in *Wt1* expression correlates with differentiation potential (Bandiera et al., 2013). WT1^{low} cells differentiate into cells that express *Sf1*, whereas WT1^{high} express *Gata4*, *Gli1*, and *Tcf21*, have low levels of SF1, and fail to differentiate into normal adrenocortical cells. Since WT1 can directly enhance *Gli1* expression in capsular progenitors (Bandiera et al., 2013) and GLI1^{+} capsular progenitors can give rise to other capsule cells (this study), one can envision a scenario wherein high *Wt1* expression in one stem/progenitor, owing to epigenetic effects, leads to formation of a patch of neoplasia-ready progenitors.

Grant support

NIH grants DK52574, DK075618, and HL094748; American Heart Association grant 13GRNT16850031, DOD grants PC141008 and OC150105, the Sigrid Jusélius Foundation, and the Academy of Finland.

Disclosure summary

The authors have nothing to disclose.

Acknowledgments

We thank members of the histology and laser microscopy cores at Washington University for technical assistance and the laboratory of Ben Humphreys for advice on the GANT61 experiments.

Appendix A. Supplementary data

Supplementary data related to this article can be found at http://dx.doi.org/10.1016/j.mce.2016.08.043.

References

Ahn, S., Joyner, A.L., 2004. Dynamic changes in the response of cells to positive hedgehog signaling during mouse limb patterning. Cell 118, 505–516.
Alcolea, M.P., Jones, P.H., 2013. Tracking cells in their native habitat: lineage tracing in epithelial neoplasia. Nat. Rev. Cancer 13, 161–171.
Anttonen, M., Ketola, I., Parviainen, H., Pusa, A.K., Heikinheimo, M., 2003. FOG-2 and GATA-4 are coexpressed in the mouse ovary and can modulate Müllerian-inhibiting substance expression. Biol. Reprod. 68, 1333–1340.
Bai, C.B., Auerbach, W., Lee, J.S., Stephen, D., Joyner, A.L., 2002. Gli2, but not Gli1, is required for initial Shh signaling and ectopic activation of the Shh pathway. Development 129, 4753–4761.
Bandiera, R., Sacco, S., Vidal, V.P., Chaboissier, M.C., Schedl, A., 2015. Steroidogenic organ development and homeostasis: a WT1-centric view. Mol. Cell Endocrinol. 408, 145–155.
Bandiera, R., Vidal, V.P., Motamedi, F.J., Clarkson, M., Sahut-Barnola, I., von Gise, A., Pu, W.T., Hohenstein, P., Martinez, A., Schedl, A., 2013. WT1 maintains adrenal-gonadal primordium identity and marks a population of AGP-like progenitors within the adrenal gland. Dev. Cell 27, 5–18.
Bernichtein, S., Peltoketo, H., Huhtaniemi, I., 2009. Adrenal hyperplasia and tumours in mice in connection with aberrant pituitary-gonadal function. Mol. Cell Endocrinol. 300, 164–168.
Bernichtein, S., Petretto, E., Jamieson, S., Goel, A., Aitman, T.J., Mangion, J.M., Huhtaniemi, I.T., 2007. Adrenal gland tumorigenesis after gonadectomy in mice is a complex genetic trait driven by epistatic loci. Endocrinology 149, 651–661.
Berthon, A., Sahut-Barnola, I., Lambert-Langlais, S., de Joussineau, C., Damon-Soubeyrand, C., Louiset, E., Taketo, M.M., Tissier, F., Bertherat, J., Lefrancois-Martinez, A.M., et al., 2010. Constitutive beta-catenin activation induces adrenal hyperplasia and promotes adrenal cancer development. Hum. Mol. Genet. 19, 1561–1576.
Bielinska, M., Genova, E., Boime, I., Parviainen, H., Kiiveri, S., Leppaluoto, J., Rahman, N., Heikinheimo, M., Wilson, D.B., 2005. Gonadotropin-induced adrenocortical neoplasia in NU/J nude mice. Endocrinology 146, 3975–3984.
Bielinska, M., Kiiveri, S., Parviainen, H., Mannisto, S., Heikinheimo, M., Wilson, D.B., 2006. Gonadectomy-induced adrenocortical neoplasia in the domestic ferret (*Mustela putorius furo*) and laboratory mouse. Vet. Pathol. 43, 97–117.
Bielinska, M., Parviainen, H., Kiiveri, S., Heikinheimo, M., Wilson, D.B., 2009. Review paper: origin and molecular pathology of adrenocortical neoplasms. Vet. Pathol. 46, 194–210.
Bielinska, M., Parviainen, H., Porter-Tinge, S.B., Kiiveri, S., Genova, E., Rahman, N., Huhtaniemi, I.T., Muglia, L.J., Heikinheimo, M., Wilson, D.B., 2003. Mouse strain susceptibility to gonadectomy-induced adrenocortical tumor formation correlates with the expression of GATA-4 and luteinizing hormone receptor. Endocrinology 144, 4123–4133.
Bielinska, M., Seehra, A., Toppari, J., Heikinheimo, M., Wilson, D.B., 2007. GATA-4 is required for sex steroidogenic cell development in the fetal mouse. Dev. Dyn. 236, 203–213.
Dhillon, H., Zigman, J.M., Ye, C., Lee, C.E., McGovern, R.A., Tang, V., Kenny, C.D., Christiansen, L.M., White, R.D., Edelstein, E.A., et al., 2006. Leptin directly activates SF1 neurons in the VMH, and this action by leptin is required for normal body-weight homeostasis. Neuron 49, 191–203.
Doghman, M., Karpova, T., Rodrigues, G.A., Arhatte, M., De, M.J., Cavalli, L.R., Virolle, V., Barbry, P., Zambetti, G.P., Figueiredo, B.C., et al., 2007. Increased steroidogenic factor-1 dosage triggers adrenocortical cell proliferation and cancer. Mol. Endocrinol. 21, 2968–2987.
Drelon, C., Berthon, A., Ragazzon, B., Tissier, F., Bandiera, R., Sahut-Barnola, I., de Joussineau, C., Batisse-Lignier, M., Lefrancois-Martinez, A.M., Bertherat, J., et al., 2012. Analysis of the role of Igf2 in adrenal tumour development in transgenic mouse models. PLoS One 7, e44171.
Finco, I., LaPensee, C.R., Krill, K.T., Hammer, G.D., 2015. Hedgehog signaling and steroidogenesis. Annu. Rev. Physiol. 77, 105–129.
Freedman, B.D., Kempna, P.B., Carlone, D.L., Shah, M.S., Guagliardo, N.A., Barrett, P.Q., Gomez-Sanchez, C.E., Majzoub, J.A., Breault, D.T., 2013. Adrenocortical zonation results from lineage conversion of differentiated zona glomerulosa cells. Dev. Cell 26, 666–673.
Frith, C.H., Highman, B., Burger, G., Sheldon, W.D., 1983. Spontaneous lesions in virgin and retired breeder BALB/c and C57BL/6 mice. Lab. Anim. Sci. 33, 273–286.
Guyonneau, L., Rossier, A., Richard, C., Hummler, E., Beermann, F., 2002. Expression of Cre recombinase in pigment cells. Pigment. Cell Res. 15, 305–309.
Huang, C.C., Miyagawa, S., Matsumaru, D., Parker, K.L., Yao, H.H., 2010. Progenitor cell expansion and organ size of mouse adrenal is regulated by sonic hedgehog. Endocrinology 151, 1119–1128.
Hughes, C.R., Guasti, L., Meimaridou, E., Chuang, C.H., Schimenti, J.C., King, P.J., Costigan, C., Clark, A.J., Metherell, L.A., 2012. MCM4 mutation causes adrenal failure, short stature, and natural killer cell deficiency in humans. J. Clin. Invest. 122, 814–820.
King, P., Paul, A., Laufer, E., 2009. Shh signaling regulates adrenocortical development and identifies progenitors of steroidogenic lineages. Proc. Natl. Acad. Sci. U. S. A. 106, 21185–21190.
Kramann, R., Fleig, S.V., Schneider, R.K., Fabian, S.L., DiRocco, D.P., Maarouf, O., Wongboonsin, J., Ikeda, Y., Heckl, D., Chang, S.L., et al., 2015. Pharmacological GLI2 inhibition prevents myofibroblast cell-cycle progression and reduces kidney fibrosis. J. Clin. Invest. 125, 2935–2951.
Kretzschmar, K., Watt, F.M., 2012. Lineage tracing. Cell 148, 33–45.
Landreh, L., Spinnler, K., Schubert, K., Hakkinen, M.R., Auriola, S., Poutanen, M., Soder, O., Svechnikov, K., Mayerhofer, A., 2014. Human testicular peritubular cells host putative stem leydig cells with steroidogenic capacity. J. Clin. Endocrinol. Metab. 99, E1227–E1235.
Landreh, L., Stukenborg, J.B., Soder, O., Svechnikov, K., 2013. Phenotype and steroidogenic potential of PDGFRalpha-positive rat neonatal peritubular cells. Mol. Cell Endocrinol. 372, 96–104.
Latre de Late, P., Wakil, A.E., Jarjat, M., de Krijger, R.R., Heckert, L.L., Naquet, P., Lalli, E., 2014. Vanin-1 inactivation antagonizes the development of adrenocortical neoplasia in Sf-1 transgenic mice. Endocrinology 155, 16.
Lauth, M., Toftgard, R., 2007. Non-canonical activation of GLI transcription factors: implications for targeted anti-cancer therapy. Cell Cycle 6, 2458–2463.
Lee, F.Y., Faivre, E.J., Suzawa, M., Lontok, E., Ebert, D., Cai, F., Belsham, D.D., Ingraham, H.A., 2011. Eliminating SF-1 (NR5A1) sumoylation in vivo results in ectopic hedgehog signaling and disruption of endocrine development. Dev. Cell 21, 315–327.
Looyenga, B.D., Hammer, G.D., 2006. Origin and identity of adrenocortical tumors in inhibin knockout mice: implications for cellular plasticity in the adrenal cortex. Mol. Endocrinol. 20, 2848–2863.
Merchant-Larios, H., Moreno-Mendoza, N., 1998. Mesonephric stromal cells differentiate into Leydig cells in the mouse fetal testis. Exp. Cell Res. 244, 230–238.
Middlebrook, B.S., Eldin, K., Li, X., Shivasankaran, S., Pangas, S.A., 2009. Smad1-Smad5 ovarian conditional knockout mice develop a disease profile similar to the juvenile form of human granulosa cell tumors. Endocrinology 150, 5208–5217.
Narita, N., Bielinska, M., Wilson, D., 1997. Cardiomyocyte differentiation by GATA-4 deficient embryonic stem cells. Development 122, 3755–3764.
Odeh, H.M., Kleinguetl, C., Ge, R., Zirkin, B.R., Chen, H., 2014. Regulation of the proliferation and differentiation of leydig stem cells in the adult testis. Biol. Reprod. 90, 123.
Pangas, S.A., Jorgez, C.J., Tran, M., Agno, J., Li, X., Brown, C.W., Kumar, T.R., Matzuk, M.M., 2007. Intraovarian activins are required for female fertility. Mol. Endocrinol. 21, 2458–2471.
Park, H.L., Bai, C., Platt, K.A., Matise, M.P., Beeghly, A., Hui, C.C., Nakashima, M., Joyner, A.L., 2000. Mouse Gli1 mutants are viable but have defects in SHH signaling in combination with a Gli2 mutation. Development 127, 1593–1605.
Paul, A., Laufer, E., 2011. Endogenous biotin as a marker of adrenocortical cells with steroidogenic potential. Mol. Cell Endocrinol. 336, 133–140.
Petterino, C., Naylor, S., Mukaratirwa, S., Bradley, A., 2015. Adrenal gland background findings in CD-1 (Crl:CD-1(ICR)BR) mice from 104-week carcinogenicity studies. Toxicol. Pathol. 43, 816–824.
Pihlajoki, M., Dorner, J., Cochran, R.S., Heikinheimo, M., Wilson, D.B., 2015. Adrenocortical zonation, renewal, and remodeling. Front. Endocrinol. 6, 27.
Pihlajoki, M., Gretzinger, E., Cochran, R., Kyrönlahti, A., Schrade, A., Hiller, T., Sullivan, L., Shoykhet, M., Schoeller, E.L., Brooks, M.D., et al., 2013. Conditional mutagenesis of *Gata6* in SF1-positive cells causes gonadal-like differentiation in the adrenal cortex of mice. Endocrinology 154, 1754–1767.
Röhrig, T., Pihlajoki, M., Ziegler, R., Cochran, R.S., Schrade, A., Schillebeeckx, M., Mitra, R.D., Heikinheimo, M., Wilson, D.B., 2015. Toying with fate: redirecting the differentiation of adrenocortical progenitor cells into gonadal-like tissue. Mol. Cell Endocrinol. 408, 165–177.
Schillebeeckx, M., Pihlajoki, M., Gretzinger, E., Yang, W., Thol, F., Hiller, T., Löbs, A.-K., Röhrig, T., Schrade, A., Cochran, R., et al., 2015. Novel markers of gonadectomy-induced adrenocortical neoplasia. Mol. Cell Endocrinol. 399, 122–130.
Schillebeeckx, M., Schrade, A., Lobs, A.K., Pihlajoki, M., Wilson, D.B., Mitra, R.D.,

2013. Laser capture microdissection-reduced representation bisulfite sequencing (LCM-RRBS) maps changes in DNA methylation associated with gonadectomy-induced adrenocortical neoplasia in the mouse. Nucleic Acids Res. 41, e116.
Schmahl, J., Rizzolo, K., Soriano, P., 2008. The PDGF signaling pathway controls multiple steroid-producing lineages. Genes Dev. 22, 3255–3267.
Snippert, H.J., van der Flier, L.G., Sato, T., van Es, J.H., van den Born, M., Kroon-Veenboer, C., Barker, N., Klein, A.M., van Rheenen, J., Simons, B.D., et al., 2010. Intestinal crypt homeostasis results from neutral competition between symmetrically dividing Lgr5 stem cells. Cell 143, 134–144.
Sodhi, C.P., Li, J., Duncan, S.A., 2006. Generation of mice harbouring a conditional loss-of-function allele of Gata6. BMC Dev. Biol. 6, 19.
Walczak, E.M., Hammer, G.D., 2015. Regulation of the adrenocortical stem cell niche: implications for disease. Nat. Rev. Endocrinol. 11, 14–28.
Ward, J.M., Anver, M.R., Mahler, J.F., Devor-Henneman, D.E., Maronpot, R.R., Sundberg, J.P., Frederickson, R.M., 2002. Pathology of mice commonly used in genetic engineering (C57BL/6; B6,129; and FVB/n). In: Pathology of Genetically Engineered Mice. Ames, Iowa State University Press, pp. 161–179.
Wood, M.A., Acharya, A., Finco, I., Swonger, J.M., Elston, M.J., Tallquist, M.D., Hammer, G.D., 2013. Fetal adrenal capsular cells serve as progenitor cells for steroidogenic and stromal adrenocortical cell lineages in M. musculus. Development 140, 4522–4532.
Xie, J., Aszterbaum, M., Zhang, X., Bonifas, J.M., Zachary, C., Epstein, E., McCormick, F., 2001. A role of PDGFRalpha in basal cell carcinoma proliferation. Proc. Natl. Acad. Sci. U. S. A. 98, 9255–9259.
Yates, R., Katugampola, H., Cavlan, D., Cogger, K., Meimaridou, E., Hughes, C., Metherell, L., Guasti, L., King, P., 2013. Adrenocortical development, maintenance, and disease. Curr. Top. Dev. Biol. 106, 239–312.
Zubair, M., Parker, K.L., Morohashi, K., 2008. Developmental links between the fetal and adult zones of the adrenal cortex revealed by lineage tracing. Mol. Cell Biol. 28, 7030–7040.

REPRODUCTION
RESEARCH

Probing GATA factor function in mouse Leydig cells via testicular injection of adenoviral vectors

Gervette M Penny[1], Rebecca B Cochran[1], Marjut Pihlajoki[2], Antti Kyrönlahti[2], Anja Schrade[2], Merja Häkkinen[3], Jorma Toppari[4], Markku Heikinheimo[1,2] and David B Wilson[1,5]

[1]*Department of Pediatrics, Washington University School of Medicine, St. Louis Children's Hospital, St. Louis, Missouri, USA,* [2]*Children's Hospital, University of Helsinki and Helsinki University Hospital, Helsinki, Finland,* [3]*University of Eastern Finland, School of Pharmacy, Kuopio, Finland,* [4]*Department of Physiology, Institute of Biomedicine, University of Turku and Department of Pediatrics, Turku University Hospital, Turku, Finland and* [5]*Department of Developmental Biology, Washington University School of Medicine, St. Louis Children's Hospital, St. Louis, Missouri, USA*

Correspondence should be addressed to D B Wilson; Email: wilson_d@wustl.edu

Abstract

Testicular Leydig cells produce androgens essential for proper male reproductive development and fertility. Here, we describe a new Leydig cell ablation model based on Cre/Lox recombination of mouse *Gata4* and *Gata6*, two genes implicated in the transcriptional regulation of steroidogenesis. The testicular interstitium of adult *Gata4*$^{flox/flox}$; *Gata6*$^{flox/flox}$ mice was injected with adenoviral vectors encoding Cre + GFP (Ad-Cre-IRES-GFP) or GFP alone (Ad-GFP). The vectors efficiently and selectively transduced Leydig cells, as evidenced by GFP reporter expression. Three days after Ad-Cre-IRES-GFP injection, expression of androgen biosynthetic genes (*Hsd3b1*, *Cyp17a1* and *Hsd17b3*) was reduced, whereas expression of another Leydig cell marker, *Insl3*, was unchanged. Six days after Ad-Cre-IRES-GFP treatment, the testicular interstitium was devoid of Leydig cells, and there was a concomitant loss of all Leydig cell markers. Chromatin condensation, nuclear fragmentation, mitochondrial swelling, and other ultrastructural changes were evident in the degenerating Leydig cells. Liquid chromatography-tandem mass spectrometry demonstrated reduced levels of androstenedione and testosterone in testes from mice injected with Ad-Cre-IRES-GFP. Late effects of treatment included testicular atrophy, infertility and the accumulation of lymphoid cells in the testicular interstitium. We conclude that adenoviral-mediated gene delivery is an expeditious way to probe Leydig cell function *in vivo*. Our findings reinforce the notion that GATA factors are key regulators of steroidogenesis and testicular somatic cell survival.

Free Finnish abstract: A Finnish translation of this abstract is freely available at http://www.reproduction-online.org/content/154/4/455/suppl/DC2.

Reproduction (2017) **154** 455–467

Introduction

Testicular Leydig cells are essential for proper male phenotypic differentiation and fertility (Teerds & Huhtaniemi 2015). Two distinct populations of Leydig cells arise sequentially during mammalian development (Virtanen & Toppari 2014). Fetal Leydig cells, which appear soon after testicular organogenesis (E12.5 in the mouse), produce androgens required for masculinization of the fetus (O'Shaughnessy & Fowler 2011, Wen *et al.* 2016, Shima & Morohashi 2017). Adult Leydig cells, which arise in the pre-pubertal period, secrete androgens essential for sexual maturation and spermatogenesis (Teerds & Huhtaniemi 2015). Both populations of Leydig cells possess the enzymes required for conversion of cholesterol into androstenedione (cholesterol side chain cleavage enzyme (CYP11A1), 3β-hydroxysteroid dehydrogenase (HSD3B1) and cytochrome P450 17α-hydroxylase/17,20-lyase (CYP17A1)) (O'Shaughnessy *et al.* 2002). Adult Leydig cells, but not their fetal counterparts, possess HSD17B3, an enzyme that metabolizes androstenedione into testosterone (O'Shaughnessy *et al.* 2000, Shima *et al.* 2013).

Cell-specific ablation models have provided insight into the development and function of Leydig cells (Smith *et al.* 2015). The most widely used of these models entails administration of ethane dimethane sulfonate (EDS) to adult rats, which triggers the rapid destruction of Leydig cells via apoptosis (Teerds *et al.* 1989). Three to six weeks after EDS treatment, the adult Leydig cell population regenerates (Kerr *et al.* 1985, Molenaar *et al.* 1986). This model has allowed investigators to identify factors that regulate Leydig cell differentiation

ISSN 1470–1626 (paper) 1741–7899 (online)
DOI: 10.1530/REP-17-0311
Online version via www.reproduction-online.org

(Molenaar *et al.* 1986, Yan *et al.* 2000, Sriraman *et al.* 2003, Salva *et al.* 2004, O'Shaughnessy *et al.* 2008, Zhang *et al.* 2013, O'Shaughnessy *et al.* 2014, Lobo *et al.* 2015, Zhang *et al.* 2015). Additionally, the EDS model has shed light on stem Leydig cells present in peritubular and perivascular locations within the testicular interstitium (Kilcoyne *et al.* 2014, Chen *et al.* 2017). One limitation of EDS is that it does not cause Leydig cell destruction in mice except at high doses that may be associated with additional off-target effects (Smith *et al.* 2015).

Here, we describe a new Leydig cell ablation model based on delivery of Cre recombinase into the testes of mice harboring floxed alleles of *Gata4* and *Gata6*, two key regulators of steroidogenic cell differentiation and function (Tevosian 2014, Röhrig *et al.* 2015, Tremblay 2015). *Gata4* and *Gata6* are expressed in fetal/adult Leydig cells (Ketola *et al.* 1999, 2002, Mazaud-Guittot *et al.* 2014) and have been shown to activate the promoters of several steroidogenic genes, including *Cyp11a1* and *Cyp17a1* (Tremblay & Viger 2001, Jimenez *et al.* 2003, Rahman *et al.* 2004, Sher *et al.* 2007). Conditional targeting of *Gata4* in the adrenogonadal primordium and fetal/adult Leydig cells using *Sf1-Cre* produces undervirilized mice with small testes that lack mature sperm (Manuylov *et al.* 2011). Simultaneous deletion of both *Gata4* and *Gata6* using *Sf1-cre* results in a more severe testicular phenotype marked by a paucity of Leydig cells, reduced testosterone production and the accumulation of adrenal-like cells in the interstitium (Padua *et al.* 2015). To focus on the function of GATA factors in Leydig cells of the adult mouse, we devised a conditional gene deletion strategy that relies on intratesticular injection of an adenoviral vector encoding Cre. We show that deletion of *Gata4*+*Gata6* in this manner leads to attenuated steroidogenesis followed by destruction of adult Leydig cells. More broadly, our results show that adenoviral-mediated gene delivery is an expeditious and selective means of probing Leydig cell function *in vivo*.

Materials and methods

Experimental animals

Procedures involving mice were approved by the institutional committee for laboratory animal care and were conducted in accordance with the National Research Council's (NRC) publication *Guide for Care and Use of Laboratory Animals*. *Gata4*$^{flox/flox}$ mice (also termed *Gata4*$^{tm1.1Sad}$/J), *Gata6*$^{flox/flox}$ mice (also termed *Gata6*$^{tm2.1Sad}$/J) and *Sf1-Cre* mice (also termed FVB-Tg(Nr5a1-cre)2Lowl/J) were obtained from the Jackson Laboratory (Bar Harbor, ME, USA) and genotyped as described (Watt *et al.* 2004, Dhillon *et al.* 2006, Oka *et al.* 2006, Sodhi *et al.* 2006). *Gata4*$^{flox/flox}$ mice were crossed with *Gata6*$^{flox/flox}$ mice to produce *Gata4*$^{flox/flox}$; *Gata6*$^{flox/flox}$ mice. Male *Sf1-Crel; Gata4*$^{flox/flox}$; *Gata6*$^{flox/flox}$ mice were generated using an established breeding scheme (Padua *et al.* 2015, Tevosian *et al.* 2015). All mice had free access to water and standard rodent chow and were exposed to 12-h light/12-h darkness photoperiods. At specified times, mice were killed by CO_2 asphyxiation.

Intratesticular injection

We obtained recombinant human adenovirus (serotype 5, dE1/E3) expressing green fluorescent protein (GFP) alone (Ad-GFP) or in combination with Cre (Ad-Cre-IRES-GFP) from Vector Biolabs (Philadelphia, PA, USA). Male *Gata4*$^{flox/flox}$; *Gata6*$^{flox/flox}$ mice (2 months old) were anesthetized with a cocktail of ketamine (100 mg/kg) and xylazine (10 mg/kg) ip. The intra- and post-operative analgesic regimen included buprenorphine (0.05 mg/kg *sc*) and carprofen (5 mg/kg *sc*). We employed two different surgical techniques to inject adenovirus. In initial experiments, an abdominal incision (Qamar *et al.* 2015) was made to expose the testes for injection. To avoid the potentially confounding variable of surgically induced cryptorchidism, a scrotal incision (Kojima *et al.* 2003) was made in the subsequent experiments. These alternative methods yielded comparable results, particularly at early time points (<7 days) post injection, indicating that surgical approach was not a major determinant of experimental outcome. Adenovirus (20 µL, 1×10^7 plaque formation units (pfu) per µL in Dulbecco's Modified Eagle's medium (DMEM) containing 2% BSA and 2.5% glycerol (v/v)) was injected slowly into the interstitial space of each testes using a 30-gauge needle. Sham-operated mice underwent skin incision and testes visualization without intratesticular injection.

Histological analyses

Whole testes or other organs were fixed by overnight immersion in Bouin's solution (Sigma) or 4% paraformaldehyde (PFA) in PBS. Paraffin-embedded tissue sections (5 µm) were stained with hematoxylin and eosin (H&E) or subjected to immunostaining (Anttonen *et al.* 2003, Krachulec *et al.* 2012). The type of fixation and the primary/secondary antibodies used for each antigen are listed in Table 1. Bound antibody was visualized using the avidin-biotin immunoperoxidase system (Vectastain Elite ABC Kit, Vector Laboratories, Inc., Burlingame, CA, USA) and diaminobenzidine. Terminal deoxynucleotidyl transferase dUTP nick end labeling (TUNEL) staining was performed on paraffin-embedded tissue sections using the ApopTag Peroxidase *In Situ* Apoptosis kit (EMD Millipore). For direct visualization of GFP, cryosections (10 µm) were prepared after embedding unfixed testes in O.C.T. compound (Thomas Scientific, Swedesboro, NJ, USA). These sections were mounted in Immu-Mount containing DAPI (ThermoFisher Scientific) and photographed using an Olympus BX60 fluorescence microscope.

Quantitative RT-PCR (RT-qPCR)

RNA was isolated from whole testes (Kyrönlahti *et al.* 2011) and subjected to RT-qPCR analysis as described (Dörner *et al.* 2017),

Table 1 Tissue fixation methods and antibodies used for immunohistochemistry.

Antigen	Marker of	Fixative	Primary antibody	Secondary antibody
GFP	Adenoviral infection	Bouin's	ab290, rabbit polyclonal, Abcam, Cambridge, MA; 1:500	Goat anti-rabbit biotinylated IgG, NEF-813, NEN Life Science, Boston, MA; 1:2000
GATA4	Leydig cells, Sertoli cells, perivascular cells, some peritubular cells	4% PFA in PBS	sc-1237, goat polyclonal, Santa Cruz Biotechnology, Santa Cruz, CA; 1:200	Donkey anti-goat biotinylated IgG, Jackson Immunoresearch, West Grove, PA; 1:1000
GATA6	Leydig cells, Sertoli cells	4% PFA in PBS	AF1700, goat polyclonal, R&D Systems; 1:100)	Goat anti-rabbit biotinylated IgG, NEF-813, NEN Life Science, Boston, MA; 1:2000
Cleaved caspase-3	Apoptosis	4% PFA in PBS	sc-1225, goat polyclonal, Santa Cruz Biotechnology, Santa Cruz, CA; 1:200	Donkey anti-goat biotinylated IgG, Jackson Immunoresearch, West Grove, PA; 1:1000
CD3ε	T-lymphocytes	4% PFA in PBS	145-2C11, hamster monoclonal, Abcam, Cambridge, MA; 1:500	Goat anti-hamster biotinylated IgG, BA-9100, Vector Labs, Burlingame, CA; 1:800
CYP17A1	Leydig cells	Bouin's	sc-66850, rabbit polyclonal, Santa Cruz Biotechnology, Santa Cruz, CA; 1:200	Goat anti-rabbit biotinylated IgG, NEF-813, NEN Life Science, Boston, MA; 1:2000
F4/80	Macrophages	4% PFA in PBS	ab16911, rat monoclonal, Abcam, Cambridge, MA; 1:500	Goat anti-rat biotinylated IgG, JGR066003, Accurate Chemical and Scientific Corp., Westbury, NY; 1:800
HSD17B3	Leydig cells	Bouin's	sc-135044, rabbit polyclonal, Santa Cruz Biotechnology, Santa Cruz, CA; 1:200	Goat anti-rabbit biotinylated IgG, NEF-813, NEN Life Science, Boston, MA; 1:2000
HSD3B1	Leydig cells	Bouin's	sc-30820, goat polyclonal, Santa Cruz Biotechnology, Santa Cruz, CA; 1:200	Donkey anti-goat biotinylated IgG, Jackson Immunoresearch, West Grove, PA; 1:1000

using the primers listed in Table 2. Expression was normalized to the housekeeping genes *Gapdh* and *Actb*.

Electron microscopy

Mice were anesthetized and perfused for 20 min with modified Karnovsky fixative (2.5% glutaraldehyde and 2% paraformaldehyde in 0.1 M cacodylate buffer) via a needle inserted into the left ventricle (Pihlajoki *et al.* 2013). Testes were harvested, incubated overnight at 4°C in the same fixative, rinsed and then postfixed in 2% OsO_4 for 1 h. The samples were dehydrated and embedded in epoxy resin. Thick sections (1 µm) were stained with toluidine blue and examined by light microscopy to determine which blocks were to be thin-sectioned. Thin sections were stained with uranyl acetate and lead citrate and photographed using a JEOL 1400 transmission electron microscope.

Liquid chromatography-tandem mass spectrometry (LC-MS/MS)

Testicular biopsies (~30 mg each; $n=4$ per group) were harvested and frozen at −80°C. Testis tissue was homogenized in 200 µL of 0.9% saline using Precellys beads (KT 03961-1-003.2, Bertin Technologies, France). Tissue homogenates were spiked with isotope-labeled steroids as internal standards. Samples were then extracted with 1 mL of toluene (Chromasolv plus for HPLC, Sigma), dried and reconstituted in 30% acetonitrile. Steroids were measured using an Agilent 1290 Series HPLC system connected to an Agilent 6495

Table 2 Primers for RT-qPCR.

Gene	Oligonucleotide sequence (5′→3′)	Reference
Actb	F: GCGTGACATCAAAGAGAAGC R: AGGATTCCATACCCAAGAAGG	NM_007393.3
Gapdh	F: GCTCACTGGCATGGCCTTCCGTG R: TGGAAGAGTGGGAGTTGCTGTTGA	NM_008084.2
Cyp11a1	F: AGGGGTGGACACGACCTCCA R: TGCTGGCTTTGAGGAGTGGAACC	NM_019779.3
Cyp11b1	F: GCTTCACCATGTGCTGAAATCC R: AGAAGAGAGGGCAATGTGTCA	NM_001033229.3
Cyp17a1	F: CCAGATGGTGACTCTAGGCCTCTTGTC R: GGTCTGTATGGTAGTCAGTATCG	NM_007809.3
Insl3	F: CACGCAGCCTGTGGAGACCC R: CGCTGGCGCTGAGAAGCCT	NM_013564.7
Hsd3b1	F: TGGACAAAGTATTCCGACCAG R: GGCACACTTGCTTGAACACAG	NM_008293.3
Hsd17b3	F: GAGTTGGCCAGACAYGGACT R: AGCTTCCAGTGGTCCTCTCA	NM_008291.3
Sox9	F: AGGAAGTCGGTGAAGAACGG R: GGACCCTGAGATTGCCCAGA	NM_011448.4

Triple Quadrupole mass spectrometer. Standard compounds were obtained from Sigma, Steraloids (Newport, RI, USA), Fluka (Bucharest, Romania) and Riedel-de Haën (Seelze, Germany). A publication detailing the analytical method is in preparation.

Assessment of reproductive function

To assess fertility, male mice that had undergone intratesticular injection with Ad-GFP or Ad-Cre-IRES-GFP were housed continuously with fertility-proven female *Gata4*$^{flox/flox}$; *Gata6*$^{flox/flox}$ mice and the number of offspring documented. Serum luteinizing hormone (LH) levels were measured by ELISA (ERK R7017, Endocrine Technologies; Newark, CA, USA).

Statistical methods

Steroid, mRNA and LH levels in different groups of mice were compared using the Student's *t* test. Fertility was compared via two population proportions testing. Statistical significance was set at the following: $*P<0.05$ and $**P<0.01$.

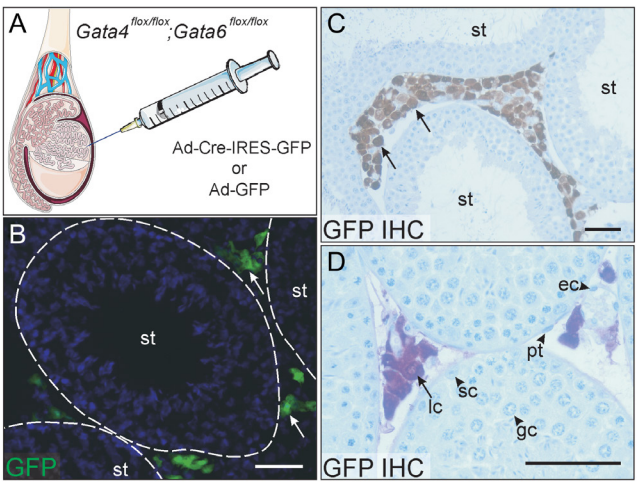

Figure 1 Intratesticular injection of adenovirus results in the selective and efficient transduction of Leydig cells. (A) Adenoviral injection strategy. (B) Two days after injection of Ad-Cre-IRES-GFP, testes were cryosectioned, counterstained with DAPI and examined by fluorescence microscopy. Seminferous tubules are outlined by dashed lines. White arrows highlight GFP$^+$ cells in the testicular interstitium. (C and D) Three days after injection of Ad-Cre-IRES-GFP, testes were harvested, fixed in Bouin's solution and subjected to immunoperoxidase staining for GFP. Black arrows in panels C & D highlight GFP$^+$ Leydig cells. Note that Leydig cells were transduced efficiently, whereas other cell types (endothelial, peritubular, Sertoli and germ cells) were not. Prepared using image vectors from Servier Medical Art (http://smart.servier.com/), licensed under the Creative Commons Attribution 3.0 Unported License (http://creativecommons.org/license/by/3.0/). Ad, adenovirus; ec, endothelial cell; gc, germ cell; GFP, green fluorescent protein; IHC, immunohistochemistry; IRES, internal ribosomal entry site; pt, peritubular cell; sc, Sertoli cell; st, seminiferous tubule. Scale bars = 50 µm.

Results

Overview of the adenoviral injection strategy

The testes of adult *Gata4*$^{flox/flox}$; *Gata6*$^{flox/flox}$ mice were injected with replication incompetent adenoviral vectors encoding Cre + GFP (Ad-Cre-IRES-GFP) or GFP alone (Ad-GFP) (Fig. 1A). We opted to delete *Gata4* and *Gata6* simultaneously to decrease the chance of a compensatory response and increase the likelihood of a robust phenotype. The dose of virus introduced into each testis was 2×10^8 pfu. Based on an estimate of 3×10^6 Leydig cells per testis (Hu *et al.* 2010), this dose corresponded to a multiplicity of infection (MOI) of ~70 virions per target cell, similar to the MOI of 100 used previously to transduce primary cultures of mouse Leydig cells (Schrade *et al.* 2015).

Leydig cells were efficiently transduced by the adenoviral vectors, as evidenced by GFP reporter expression 2–3 days post injection (dpi) (Fig. 1B and C). Moreover, there was uniform expression of the GFP reporter throughout the interstitial compartment, implying adequate dispersion of the small volume (20 µL) of injected virus. Other interstitial cell types, such as peritubular cells and vascular cells, were not efficiently transduced (Fig. 1D). There was no GFP expression within the seminiferous tubules, indicating that neither Sertoli cells nor germ cells were infected (Fig. 1B, C and D). Immunostaining of extragonadal organs showed scattered GFP expression in hepatocytes but no appreciable expression of GFP in submaxillary glands, lungs, heart or adrenal glands (data not shown).

Leydig cell ablation in the testes of mice injected with Ad-Cre-IRES-GFP

The testes of *Gata4*$^{flox/flox}$; *Gata6*$^{flox/flox}$ mice were injected with Ad-GFP or Ad-Cre-IRES-GFP and then harvested at varying times for light microscopic analysis. At 3 dpi, Leydig cells were evident in both the Ad-GFP- and Ad-Cre-IRES-GFP-treated mice (Fig. 2A and B). Six days after Ad-Cre-IRES-GFP injection, however, the testicular interstitium was depleted of Leydig cells (Fig. 2C and D). Cells remaining in the interstitial compartment of these mice were mainly vascular cells (endothelial cells, smooth muscle cells and pericytes) and resident macrophages (Supplementary Fig. 1A and B, see section on supplementary data given at the end of this article). Leydig cell depletion persisted in the Ad-Cre-IRES-GFP-treated mice at 12 dpi (Fig. 2E and F) and at later time points (see below).

Delayed inflammatory response in the testes of mice injected with adenovirus

By 12 dpi, there was a lymphocytic infiltrate in the testicular interstitium of both the Ad-GFP- and

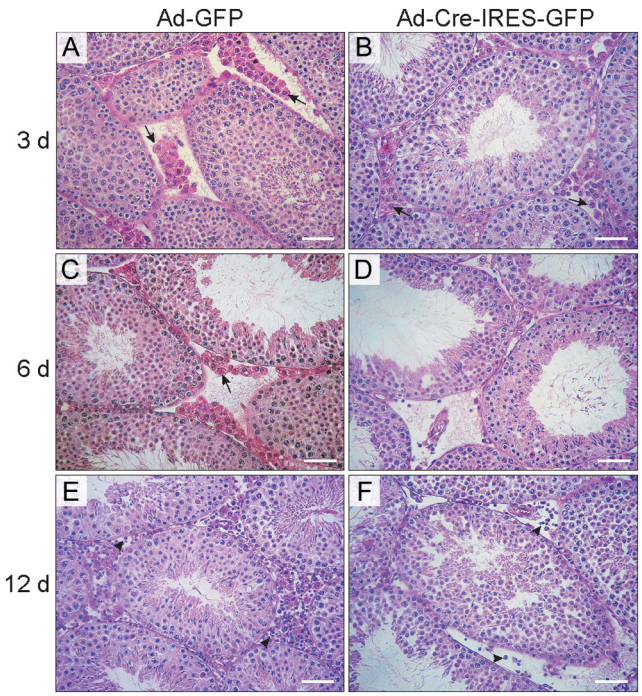

Figure 2 Morphological changes in the testes of *Gata4*$^{flox/flox}$; *Gata6*$^{flox/flox}$ mice injected with adenoviral vectors. Mouse testes were injected with Ad-GFP (A, C and E) or Ad-Cre-IRES-GFP (B, D and F). Tissue was harvested at the indicated times, fixed in Bouin's solution and stained with H&E. (A and B) After 3 days, Leydig cells were visible in the testes of mice injected with either Ad-GFP or Ad-Cre-IRES-GFP (arrows). (C and D) By 6 days, however, the Ad-Cre-IRES-GFP-treated testes were devoid of Leydig cells. (E and F) After 12 days, lymphocytes (arrowheads) were evident in the interstitium of both the Ad-GFP- and Ad-Cre-IRES-GFP-injected testes. Scale bars = 50 µm.

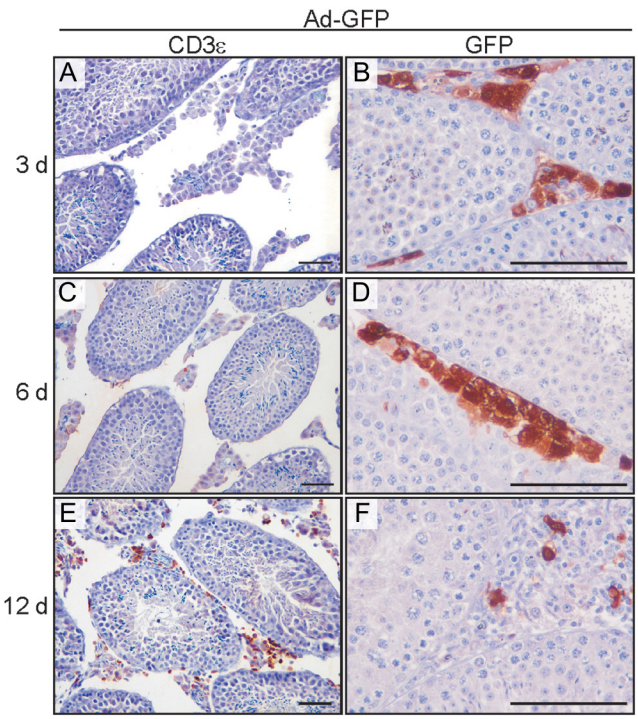

Figure 3 Adenoviral injection triggers the delayed appearance of a T-lymphocytic infiltrate in the testicular interstitium and a concomitant loss of reporter gene expression. The testes of 2-month-old mice were injected with Ad-GFP. Tissue was harvested at the indicated times, fixed in PFA (A, C and E) or Bouin's solution (B, D and F) and immunostained for CD3ε (A, C and E) or GFP (B, D and F). Note the loss of reporter gene expression at day 12, coinciding with T-cell infiltration. Scale bars = 50 µm.

Ad-Cre-IRES-GFP-injected mice (Fig. 2E and F). Immunostaining with CD3ε (Fig. 3A, C and E) confirmed that the infiltrating cells were T-lymphocytes. In the testes of mice subjected to sham surgery, there was no evidence of an inflammatory response (data not shown). In mice injected with Ad-GFP, there was a loss of reporter gene expression at 12 dpi that coincided with T-cell infiltration into the testicular interstitium (Fig. 3B, D and F). In addition to curtailing the survival of infected cells, immune cell infiltration may obfuscate the physiological impact of transgene expression (Yang *et al.* 1994, Blanchard & Boekelheide 1997). To circumvent the technical limitations imposed by lymphocyte infiltration, we focused the subsequent histological, ultrastructural and biochemical analyses on early time points post infection (days 3–7), when the effects of Cre-Lox recombination on Leydig cell function/survival could be assessed in the absence of overt T-cell infiltration.

Expeditious Cre-mediated recombination in Leydig cells

To confirm Cre-mediated recombination, testes sections were immunostained for GATA4 and GATA6. Ordinarily, nuclear GATA4 immunoreactivity is evident in Leydig cells, Sertoli cells and some peritubular cells of the adult mouse (Supplementary Fig. 2A) (Viger *et al.* 1998, Ketola *et al.* 1999, Bielinska *et al.* 2007). At 3 dpi, GATA4 was present in Leydig cells of *Gata4*$^{flox/flox}$; *Gata6*$^{flox/flox}$ mice treated with Ad-GFP but was absent from Leydig cells of mice treated with Ad-Cre-IRES-GFP (Fig. 4A and B), verifying efficient Cre-mediated gene recombination in this cell type. GATA4 staining was preserved in Sertoli cells of mice treated with Ad-Cre-IRES-GFP, underscoring the notion that adenovirus injected into the testicular interstitium selectively infects Leydig cells. At 6 dpi, GATA4$^+$ Leydig cells were evident in Ad-GFP treated testes but not in Ad-Cre-IRES-GFP-treated testes (Fig. 4C and D). Scattered GATA4$^+$ pericytes were observed in the interstitium of the Ad-Cre-IRES-GFP-treated testes (Fig. 4D and Supplementary Fig. 2B). Quantitative analysis of random microscopic fields confirmed a marked reduction in GATA4-immunoreactive interstitial cells in the Ad-Cre-IRES-GFP-treated animals at 3 and 6 dpi ($P < 0.01$) (Supplementary Fig. 3). As with GATA4, staining for GATA6 demonstrated a loss of Leydig cell immunoreactivity in mice injected with Ad-Cre-IRES-GFP (Supplementary Fig. 4).

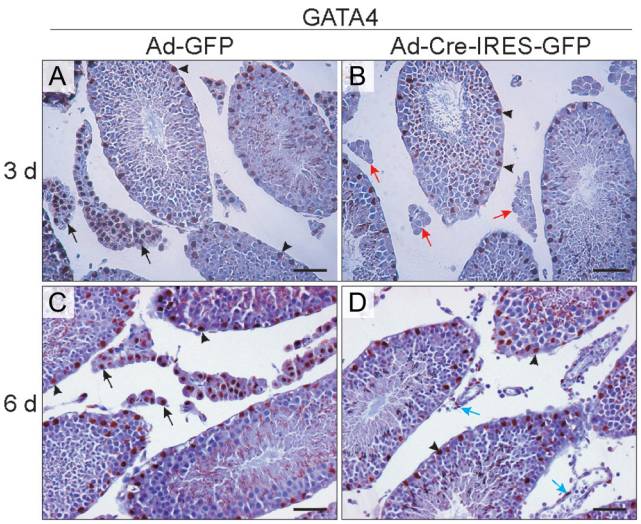

Figure 4 GATA4 immunostaining in the testes of *Gata4*$^{flox/flox}$; *Gata6*$^{flox/flox}$ mice injected with Ad-GFP or Ad-Cre-IRES-GFP. The testes of 2-month-old mice were injected with Ad-GFP (A and C) or Ad-Cre-IRES-GFP (B and D). Tissue was harvested at the indicated times, fixed in PFA and subjected to GATA4 immunoperoxidase staining. (A and B) At 3 days post injection, GATA4 immunoreactivity was evident in Leydig cells of mice injected with Ad-GFP (black arrows) but absent from Leydig cells of mice injected with Ad-Cre-IRES-GFP (red arrows), confirming efficient Cre-mediated recombination in this cell type. In contrast, GATA4 immunoreactivity was preserved in Sertoli cells (arrowheads). (C and D) At 6 days post injection, GATA4$^+$ Leydig cells were evident in Ad-GFP-treated testes (black arrows) but not in Ad-Cre-IRES-GFP-treated testes. GATA4$^+$ pericytes were observed in the interstitium of the Ad-Cre-IRES-GFP-treated testes (blue arrows). Scale bars = 50 µm.

Changes in gene expression following Cre-mediated recombination

We used RT-qPCR to compare the expression of Leydig and Sertoli cell markers in the testes of *Gata4*$^{flox/flox}$; *Gata6*$^{flox/flox}$ mice injected with Ad-GFP or Ad-Cre-IRES-GFP (Fig. 5A and B). At 3 dpi, expression of the Leydig cell marker *Insl3* (Anand-Ivell *et al.* 2009) was comparable in the two groups, confirming the presence of intact Leydig cells. In contrast, at this time point, there was an acute downregulation of androgen biosynthetic genes (*Hsd3b1*, *Cyp17a1*, *Hsd17b3*) in mice treated with Ad-Cre-IRES-GFP ($P < 0.01$). By 7 dpi, all Leydig cell markers examined (*Insl3*, *Cyp11a1*, *Hsd3b1*, *Cyp17a1*, *Hsd17b3*) were markedly attenuated ($P < 0.01$) in the mice injected with Ad-Cre-IRES-GFP, consistent with ablation of this cell type. Expression of *Sox9*, a Sertoli cell marker, was unchanged at 3 and 7 dpi, reinforcing the premise that Ad-Cre-IRES-GFP injection selectively affects the interstitial compartment.

To validate the RT-qPCR findings, we performed immunohistochemistry for HSD3B1, CYP17A1 and HSD17B3 (Fig. 6). Six days after injection of Ad-Cre-IRES-GFP, immunoreactivity for these steroidogenic enzymes was reduced, consistent with a loss of Leydig cells.

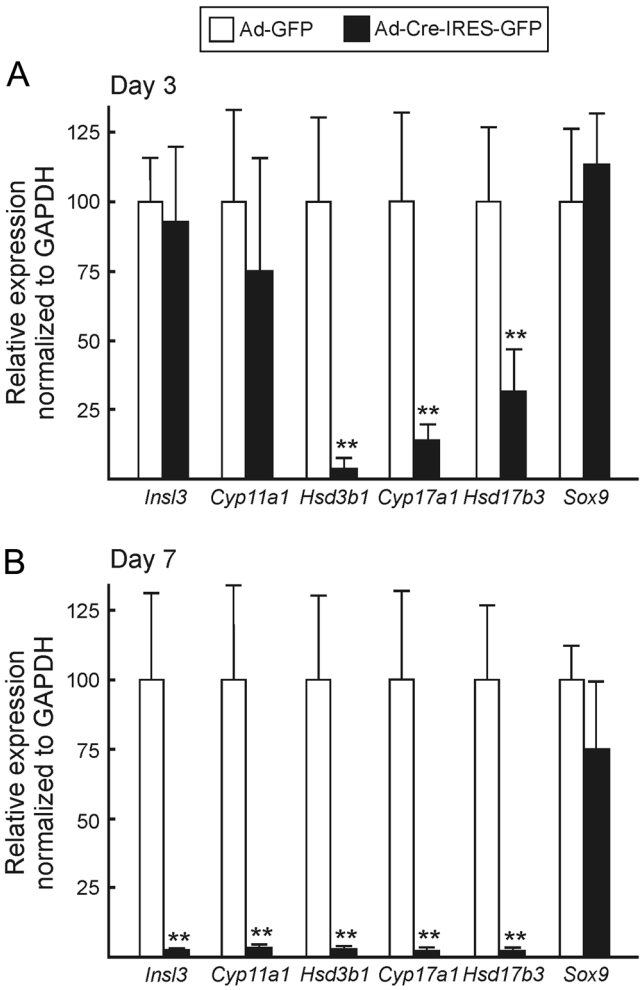

Figure 5 RT-qPCR analysis of testes from *Gata4*$^{flox/flox}$; *Gata6*$^{flox/flox}$ mice injected with Ad-GFP or Ad-Cre-IRES-GFP. The testes of 2-month-old mice were injected with Ad-GFP or Ad-Cre-IRES-GFP. At 3 days (A) or 7 days (B) post-infection, RNA was extracted from whole testis and subjected to RT-qPCR. Results were normalized to expression of the housekeeping gene *Gapdh*. Normalization to *Actb* expression yielded similar results. Values are expressed as the mean ± S.D. ($n = 4$ per group; $^{**}P < 0.01$).

Ultrastructural and biochemical analysis of cell death in mice injected with Ad-Cre-IRES-GFP

To gain insights into the process of Leydig cell death in the adenovirus injection model, resin-embedded tissue was processed for light microscopy (Supplementary Fig. 5) and transmission electron microscopy (Fig. 7A, B, C and D and Supplementary Fig. 6). Vacuole-laden activated macrophages, harbingers of Leydig cell death, were prominent in the testicular interstitium of mice treated 4 days earlier with Ad-Cre-IRES-GFP. Leydig cells exposed to Ad-Cre-IRES-GFP, but not Ad-GFP, contained clumps of condensed chromatin beneath the nuclear membrane. Nuclear fragmentation was evident in some of these Leydig cells. Cytoplasmic organelles in Ad-Cre-IRES-GFP-treated Leydig cells had changes not seen in their Ad-GFP-treated counterparts,

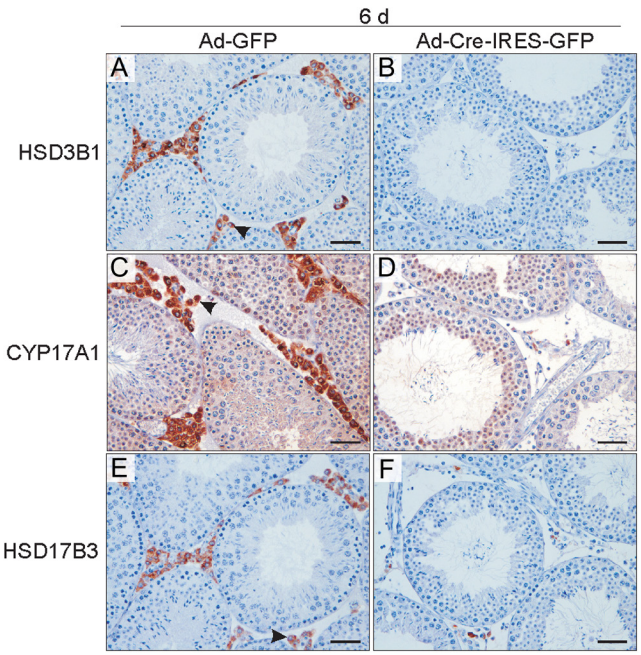

Figure 6 Immunostaining for steroidogenic enzymes in the testes of *Gata4*$^{flox/flox}$; *Gata6*$^{flox/flox}$ mice injected with Ad-GFP or Ad-Cre-IRES-GFP. The testes of 2-month-old mice were injected with Ad-GFP (A, C and E) or Ad-Cre-IRES-GFP (B, D and F). Tissue was harvested 6 days later, fixed in Bouin's solution and subjected to immunostaining for HSD3B1 (A and B), CYP17A1 (C and D) or HSD17B3 (E and F). Bars = 50 µm.

such as mitochondrial swelling, loss of definition of mitochondrial cristae and enlargement of lipid droplets. Some of these degenerative changes were suggestive of apoptosis (Jackson *et al.* 1986, Gao *et al.* 2002), but other forms of cell death (e.g., necroptosis, ferroptosis) could not be excluded based on ultrastructural analysis alone.

Looking for biochemical evidence of Leydig cell apoptosis, we performed immunostaining for cleaved (activated) caspase-3 and TUNEL staining. Compared to sham-operated mice, there was no increase in cleaved caspase-3 immunoreactivity in the Ad-GFP or Ad-Cre-IRES-GFP mice 3 dpi (data not shown). Similarly, there was no evidence of increased TUNEL staining in either the Ad-GFP or the Ad-Cre-IRES-GFP mice 3 or 6 dpi (data not shown). Thus, the mechanistic basis of Leydig cell death in the Ad-Cre-IRES-GFP mice remains uncertain.

Reduced androgen levels in the testes of mice injected with Ad-Cre-IRES-GFP

We used LC-MS/MS to quantify steroids in testis homogenates from *Gata4*$^{flox/flox}$; *Gata6*$^{flox/flox}$ mice treated 7 days earlier with Ad-GFP or Ad-Cre-IRES-GFP (Fig. 8). Testes from mice injected with Ad-Cre-IRES-GFP had reduced levels of androstenedione ($P < 0.01$) and testosterone ($P < 0.05$). On the other hand, there was no difference in the levels of intratesticular corticosterone in mice injected with Ad-GFP vs Ad-Cre-IRES-GFP (41 ± 14 pmol/g vs 31 ± 17 pmol/g, $P = 0.4$).

Late effects of adenovirus-mediated gene targeting

In contrast to EDS-induced ablation/regeneration in the rat, there was slow and variable Leydig cell regeneration in the testes of *Gata4*$^{flox/flox}$; *Gata6*$^{flox/flox}$ mice treated with Ad-Cre-IRES-GFP. By ~30 dpi, much of the testicular interstitium remained devoid of Leydig cells (Fig. 9A). Residual Leydig cells clustered in small patches, and

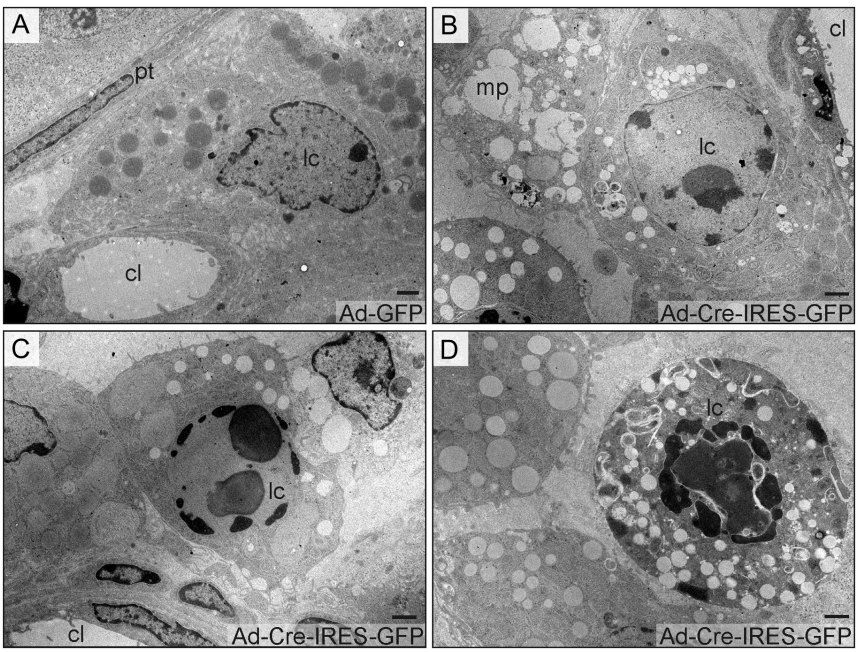

Figure 7 Degenerative changes in Leydig cells of *Gata4*$^{flox/flox}$; *Gata6*$^{flox/flox}$ mice injected with Ad-Cre-IRES-GFP. The testes of 2-month-old mice were injected with Ad-GFP (A) or Ad-Cre-IRES-GFP (B-D). Tissue was harvested 4 days later and analyzed by transmission electron microscopy. (A) Normal Leydig cell with a thin rim of heterochromatin beneath the nuclear membrane. (B) Leydig cell with patches of condensed chromatin; adjacent is an activated macrophage with filopodia and large vacuoles containing cellular debris. (C) Leydig cell with prominent chromatin condensation. (D) Leydig cell exhibiting nuclear fragmentation. cl, capillary lumen; lc, Leydig cell; mp, macrophage; pt, peritubular cell. Scale bars = 1 µm.

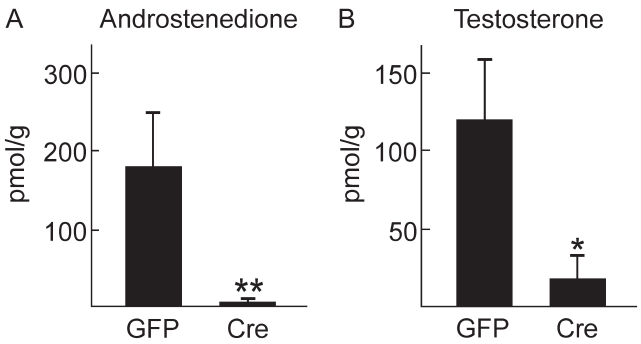

Figure 8 Steroid hormone levels in testis homogenates from *Gata4*$^{flox/flox}$*; Gata6*$^{flox/flox}$ mice injected with Ad-GFP or Ad-Cre-IRES-GFP. Ad-GFP ('GFP') or Ad-Cre-IRES-GFP ('Cre') was injected into the testes of 2-month-old *Gata4*$^{flox/flox}$*; Gata6*$^{flox/flox}$ mice. Tissue was harvested 7 days later. Testis homogenates were extracted and subjected to LC-MS/MS to determine the concentrations of (A) androstenedione and (B) testosterone. Values are expressed as pmol steroid per g of testis (mean ± S.D.; *$P < 0.05$; **$P < 0.01$; $n = 4$ per group).

all were GATA4$^+$ suggesting that these cells or their stem cell progenitors escaped adenovirus-mediated Cre inactivation (Fig. 9B). Some of these Leydig cells appeared cytomegalic (Fig. 9B), perhaps reflecting a compensatory response to impaired regeneration. Between ~30 and ~120 dpi, the number of Leydig cells (all of which were GATA4$^+$) increased (Fig. 9C, D, E and F), although there was mouse-to-mouse variability in the extent of Leydig cell regeneration. Underscoring the inconsistency in Leydig cell recovery, serum LH values at 90–92 dpi ranged from 0.6 to 32 ng/mL (mean = 11 ng/mL, $n = 4$), whereas serum LH values for age-matched sham controls were consistently low (mean = 0.5 ± 0.2 ng/mL, $n = 5$). By ~90 dpi, patches of lymphoid cells were evident in the testicular interstitium of mice treated with Ad-Cre-IRES-GFP (Fig. 9C, D, E and F). The void created by Leydig cell ablation may have permitted the accumulation of these lymphoid patches, which were as large as 1 mm in diameter. Neither the variable Leydig cell regeneration nor the accumulation of lymphoid aggregates was attributable to impaired clearance of virus, as there was no evidence of persistent GFP immunoreactivity between ~30 and ~90 dpi (data not shown). In the months following Ad-Cre-IRES-GFP injection, changes were seen in the seminiferous epithelium (e.g., thinning, vacuolization, absence of mature sperm), consistent with inadequate androgen production (Fig. 9C, D, E and F and data not shown). Testicular atrophy was evident in some of the older Ad-Cre-IRES-GFP-injected mice, likely reflecting impaired spermatogenesis (Fig. 9G). When *Gata4*$^{flox/flox}$*; Gata6*$^{flox/flox}$ mice treated with Ad-Cre-IRES-GFP ($n = 5$) were housed for 3 months with fertility-proven wild-type females, no progeny were observed. By comparison, 3 of 4 *Gata4*$^{flox/flox}$*; Gata6*$^{flox/flox}$ mice injected with Ad-GFP-sired pups in the months following injection ($P < 0.05$).

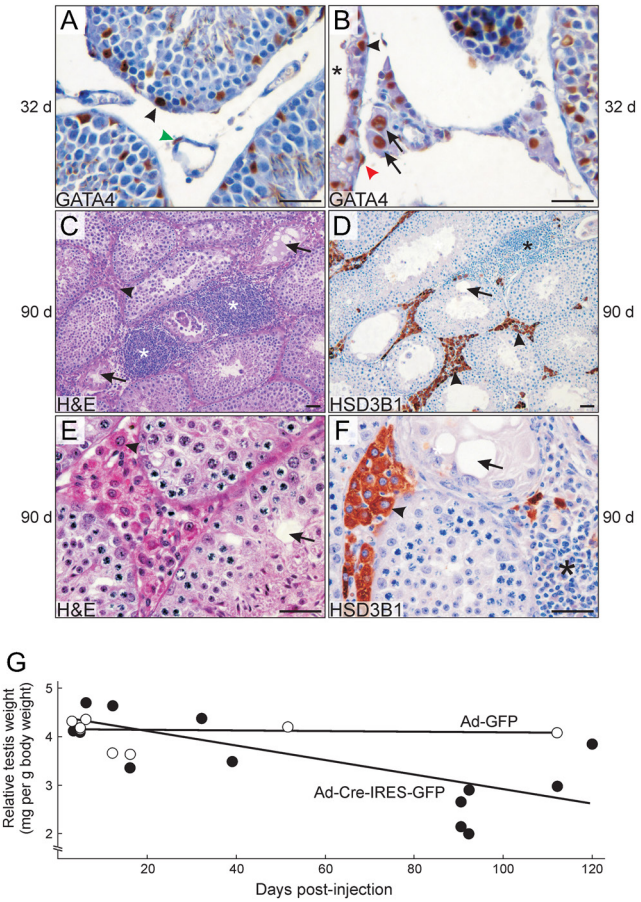

Figure 9 Late changes in testicular histology and weight following injection of Ad-Cre-IRES-GFP into *Gata4*$^{flox/flox}$*; Gata6*$^{flox/flox}$ mice. (A and B) GATA4 immunostaining of PFA-fixed testis from a mouse injected 1 month earlier with Ad-Cre-IRES-GFP. As shown in panel A, most of the testicular interstitial space lacked Leydig cells. Panel B shows a rare patch of Leydig cells that are GATA4 immunoreactive, suggesting that they or their progenitors escaped Cre inactivation. Some of these Leydig cells exhibited cytomegaly (black arrows). Other GATA4$^+$ cell types seen are Sertoli cells (black arrowheads), pericytes (green arrowhead) and peritubular cells (red arrowhead). The asterisk indicates a seminferous tubule with thin epithelium. (C, D, E and F) H&E staining and HSD3B1 immunostaining of Bouin's-fixed testis from mice injected 3 months earlier with Ad-Cre-IRES-GFP. Arrowheads highlight Leydig cells. Arrows indicate seminiferous tubule degeneration. Asterisks highlight lymphoid aggregates. (G) The testes of 2-month-old mice were injected with Ad-GFP (open circle) or Ad-Cre-IRES-GFP (closed circle). At the indicated times, testes were harvested and weighed. Data points represent the average of two testes per mouse. There was no statistical difference between the slopes of the curves ($P = 0.4$). Scale bars = 25 µm.

Tevosian and coworkers have shown that male *Sf1*-cre; *Gata4*$^{flox/flox}$*; Gata6*$^{flox/flox}$ mice survive congenital adrenocortical aplasia due to production of corticoids by adrenal-like cells that accumulate in the testes postnatally (Padua *et al.* 2015, Tevosian *et al.* 2015). These heterotopic cells express adrenocortical markers (*Cyp21a1*, *Cyp11b1*, *Cyp11b2* and *Mc2r*). To test whether adrenal-like cells arise in the testes of

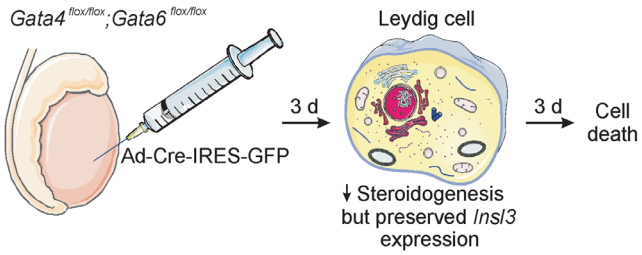

Advantages	Disadvantages
Leydig cell-specific	Lymphocytic infiltrate limits analysis at later time points
Efficient and temporally controllable	Incomplete Leydig cell regeneration

Figure 10 Salient features of the adult Leydig cell ablation model. Injection of Ad-Cre-IRES-GFP into the testicular interstitium of adult mice resulted in the selective transduction of Leydig cells. At 3 days post infection, there was decreased transcription of steroidogenic enzyme genes, but expression of *Insl3*, another Leydig cell marker, was unchanged. By 6 days post infection, there was Leydig cell destruction. Prepared using image vectors from Servier Medical Art (http://smart.servier.com/), licensed under the Creative Commons Attribution 3.0 Unported License (http://creativecommons.org/license/by/3.0/).

Gata4$^{flox/flox}$; *Gata6*$^{flox/flox}$ mice injected with Ad-Cre-IRES-GFP, we performed RT-qPCR analysis for adrenal markers. In contrast to the testes of *Sf1*-cre; *Gata4*$^{flox/flox}$; *Gata6*$^{flox/flox}$ mice (which were included in the analysis as positive controls), there was no upregulation of adrenal markers in the testes of *Gata4*$^{flox/flox}$; *Gata6*$^{flox/flox}$ mice that had been injected 90 days earlier with Ad-Cre-IRES-GFP vs Ad-GFP (data not shown).

Discussion

Cell-specific ablation models have proven invaluable for the analysis of Leydig cell differentiation and function (Smith *et al.* 2015). We have developed a new Leydig cell ablation model, the features of which are summarized in Fig. 10. Our approach relies on adenoviral-mediated delivery of Cre recombinase into the testicular interstitium of mice harboring floxed alleles of *Gata4* and *Gata6*. This method of gene delivery has inherent advantages for the study of Leydig cells. As shown here and elsewhere (Blanchard & Boekelheide 1997, Hall *et al.* 2000, Kojima *et al.* 2003, LeCouter *et al.* 2003, Shiraishi & Ascoli 2007, Qamar *et al.* 2009, Qamar *et al.* 2015, Schrade *et al.* 2015), adenovirus efficiently transduces Leydig cells *in vitro* and *in vivo*. Moreover, adenovirus injected into the testicular interstitium selectively infects Leydig cells, thereby minimizing off-target effects. Adenoviral vectors rarely integrate into host chromosomes (0.001–1% of infected cells), so Leydig cell gene expression is not subject to viral DNA integration effects (Mitani & Kubo 2002). Recombinant adenovirus has been used to drive the expression of not only Cre but also small hairpin RNAs (shRNAs) (Machitani *et al.* 2013). Such adenoviral shRNA constructs could be used to silence genes in the Leydig cells of mice lacking floxed alleles. Thus, our adenoviral delivery method could be adapted to study the roles of other genes implicated in Leydig cell function.

The principal shortcoming of adenoviral gene delivery is that it triggers an immune response in the testis and other organs (Blanchard & Boekelheide 1997, Hendrickx *et al.* 2014, Tsuzuki *et al.* 2016). In the liver, where this response has been characterized in detail, adenoviral transduction stimulates a lymphocytic infiltrate that leads to destruction of genetically modified cells and repopulation with hepatocytes lacking the transgene (Yang *et al.* 1994). This immune response is directed against *de novo*-synthesized viral components and is independent of MOI (Yang *et al.* 1994). In the liver and other cell types, the lymphocytic infiltrate typically appears ~10 days post infection and resolves ~30 days post infection, coinciding with a loss of transgene expression (Yang *et al.* 1994, Blanchard & Boekelheide 1997). We circumvented this limitation of the adenoviral delivery system by focusing on changes in Leydig cell gene expression, function and survival at early time points (<7 days) post infection, before the appearance of a pronounced T-lymphocytic infiltrate. Another limitation of the adenoviral injection method is its relative irreversibility. The method apparently kills a significant fraction of Leydig cell precursors, although some escape Cre-mediated recombination and partially repopulate the interstitium after several weeks. Inflammation may accentuate the adverse effects of adenoviral-mediated gene targeting.

The interstitial injection technique described here complements other methods for delivering transgenes or inhibitory RNAs to specific testicular cell populations in rodents. Retrograde instillation of adenoviral vectors into efferent ductules can transduce cells within the seminiferous tubules (Blanchard & Boekelheide 1997, Kanatsu-Shinohara *et al.* 2002, Kojima *et al.* 2003, Hooley *et al.* 2009). Injection of retrovirus (Kanatsu-Shinohara *et al.* 2004) or lentivirus (Ikawa *et al.* 2002, Kim *et al.* 2010) into the testis results in infection of multiple cell types including germ cells, Sertoli cells and/or Leydig cells. Direct testicular injection of a buffered salt solution can be used to introduce shRNA into germ cells, albeit with low transfection efficiency (<5%) (Ho *et al.* 2017). Early gonadal development can be disrupted by cultivating organs in hanging droplets of media supplemented with *vivo*-morpholinos (Rudigier *et al.* 2017). Cre can be targeted to mouse Leydig cells by germline transmission of transgenes, such as *Sf1*-Cre (Bingham *et al.* 2006), *CYP11A1*-iCre (Wu *et al.* 2007) and *Cyp17a1*-iCre (Bridges *et al.* 2008). Although germline Cre transgenes avoid the problem of virus-induced host immunity, generation

of such mouse mutants is time consuming, and interpretation of the resultant testicular phenotypes may be challenging because of context-dependent effects, variable degrees of Cre-mediated recombination, compensatory responses, alternative pathways of differentiation and functional redundancy (Smith 2011, Tevosian 2014). Adenoviral delivery of Cre or shRNA affords a means of probing the *in vivo* function of a gene in Leydig cells before committing to germline transmission of a Leydig cell-specific Cre transgene. Intratesticular injection of adenovirus also can be used to study the short-term impact of overexpression of a gene in Leydig cells. For instance, LeCouter *et al*. (2003) used interstitial injection of adenoviral vectors to drive the expression of angiogenic peptides in mouse testis; histological changes characteristic of angiogenesis were evident 7 dpi.

In vitro studies have provided genetic evidence that GATA factors regulate steroidogenesis in Leydig cells. For example, silencing of *Gata4* in Leydig tumor cell lines (MA-10, mLTC-1) and primary adult Leydig cells has been shown to impair the expression of androgen biosynthetic genes (*Cyp11a1*, *Hsd3b1*, *Cyp17a1*) (Bergeron *et al*. 2015, Schrade *et al*. 2015). In keeping with these prior reports, we found that adenovirus-mediated deletion of *Gata4/6* in adult Leydig cells caused the acute downregulation of genes involved in sex steroid production, whereas expression of another Leydig cell marker, *Insl3*, was preserved at early time points. An advantage of our *in vivo* model over cell culture-based systems is that the functional changes observed in response to conditional gene targeting occur in a more physiologic milieu of endocrine and paracrine factors (e.g., LH).

In our model of adenoviral-mediated targeting of *Gata4/6*, we found that the acute decline in testicular steroidogenesis was followed days later by Leydig cell death. This finding is reminiscent of a study in which treatment of MA-10 cells with an apoptosis-inducing agent caused a decrease in steroid production in advance to cell death (King *et al*. 1998). GATA4 has been shown to enhance cell survival and/or decrease apoptosis in Leydig cell lines and other steroidogenic cell types (Bennett *et al*. 2013, Anttonen *et al*. 2014, Schrade *et al*. 2015, Pihlajoki *et al*. 2016). The precise mechanism of cell death in our model remains unclear. Ultrastructural analysis of Ad-Cre-IRES-GFP-treated Leydig cells demonstrated organelle changes compatible with apoptosis and other forms of cell death. In the rat EDS model, Leydig cells undergo apoptosis. This process is mediated by caspase-3 activation (Kim *et al*. 2000) but does not involve Bcl-2 family members (Taylor *et al*. 1998); instead, EDS appears to act through activation of Fas (Taylor *et al*. 1999) and other pro-apoptotic factors (Li *et al*. 2012). We found no immunohistological evidence of caspase-3 activation in our model, and TUNEL staining was negative. In cultured gonadal somatic cell lines, silencing of *Gata4* impairs glycolysis and causes other metabolic derangements (Schrade *et al*. 2015, Schrade *et al*. 2016). Thus, it is conceivable that altered metabolism contributes to Leydig cell death in our adenoviral injection model.

Gata4 is expressed in not only fetal/adult Leydig cells but also in putative stem Leydig cells (Kilcoyne *et al*. 2014). Circumstantial evidence supports a role for GATA4 in the differentiation of Leydig stem/progenitor cells. For example, enforced expression of *Gata4* plus two other transcription factors (*Sf1* and *Dmrt1*) can reprogram mouse fibroblasts into Leydig-like cells (Yang *et al*. 2017). GATA6, like GATA4, has been implicated in mesenchymal stem cell function (Almalki & Agrawal 2016). The incomplete regeneration of Leydig cells that typifies our adenoviral injection model could reflect, at least partly, impaired Leydig stem cell function, and future experiments will explore this possibility.

Supplementary data

This is linked to the online version of the paper at http://dx.doi.org/10.1530/REP-17-0311.

Declaration of interest

The authors declare that there is no conflict of interest that could be perceived as prejudicing the impartiality of the research reported.

Funding

This work was supported by DOD grants PC141008 and OC150105, the Prostate Cancer Foundation, NIH grant DK52574, the Sigrid Jusélius Foundation and the Academy of Finland.

Acknowledgments

The authors thank members of the histology and electron microscopy cores for technical assistance, Celeste Morley and Betsy Todd for providing reagents, Ronni M Götz for assistance with pilot studies and Ida Qin for statistical analysis.

References

Almalki SG & Agrawal DK 2016 Key transcription factors in the differentiation of mesenchymal stem cells. *Differentiation* **92** 41–51. (doi:10.1016/j.diff.2016.02.005)

Anand-Ivell R, Heng K, Hafen B, Setchell B & Ivell R 2009 Dynamics of INSL3 peptide expression in the rodent testis. *Biology of Reproduction* **81** 480–487. (doi:10.1095/biolreprod.109.077552)

Anttonen M, Ketola I, Parviainen H, Pusa AK & Heikinheimo M 2003 FOG-2 and GATA-4 are coexpressed in the mouse ovary and can modulate Müllerian-inhibiting substance expression. *Biology of Reproduction* **68** 1333–1340. (doi:10.1095/biolreprod.102.008599)

Anttonen M, Pihlajoki M, Andersson N, Georges A, L'Hote D, Vattulainen S, Färkkilä A, Unkila-Kallio L, Veitia RA & Heikinheimo M 2014 FOXL2,

GATA4, and SMAD3 co-operatively modulate gene expression, cell viability and apoptosis in ovarian granulosa cell tumor cells. *PLoS ONE* **9** e85545. (doi:10.1371/journal.pone.0085545)

Bennett J, Baumgarten SC & Stocco C 2013 GATA4 and GATA6 silencing in ovarian granulosa cells affects levels of mRNAs involved in steroidogenesis, extracellular structure organization, IGF-I activity, and apoptosis. *Endocrinology* **154** 4845–4858. (doi:10.1210/en.2013-1410)

Bergeron F, Nadeau G & Viger RS 2015 GATA4 knockdown in MA-10 Leydig cells identifies multiple target genes in the steroidogenic pathway. *Reproduction* **149** 245–257. (doi:10.1530/REP-14-0369)

Bielinska M, Seehra A, Toppari J, Heikinheimo M & Wilson DB 2007 GATA-4 is required for sex steroidogenic cell development in the fetal mouse. *Developmental Dynamics* **236** 203–213. (doi:10.1002/dvdy.21004)

Bingham NC, Verma-Kurvari S, Parada LF & Parker KL 2006 Development of a steroidogenic factor 1/Cre transgenic mouse line. *Genesis* **44** 419–424. (doi:10.1002/dvg.20231)

Blanchard KT & Boekelheide K 1997 Adenovirus-mediated gene transfer to rat testis in vivo. *Biology of Reproduction* **56** 495–500. (doi:10.1095/biolreprod56.2.495)

Bridges PJ, Koo Y, Kang DW, Hudgins-Spivey S, Lan ZJ, Xu X, DeMayo F, Cooney A & Ko C 2008 Generation of Cyp17iCre transgenic mice and their application to conditionally delete estrogen receptor alpha (Esr1) from the ovary and testis. *Genesis* **46** 499–505. (doi:10.1002/dvg.20428)

Chen H, Wang Y, Ge R & Zirkin BR 2017 Leydig cell stem cells: identification, proliferation and differentiation. *Molecular and Cellular Endocrinology* **445** 65–73. (doi:10.1016/j.mce.2016.10.010)

Dhillon H, Zigman JM, Ye C, Lee CE, McGovern RA, Tang V, Kenny CD, Christiansen LM, White RD, Edelstein EA *et al*. 2006 Leptin directly activates SF1 neurons in the VMH, and this action by leptin is required for normal body-weight homeostasis. *Neuron* **49** 191–203. (doi:10.1016/j.neuron.2005.12.021)

Dörner J, Martinez Rodriguez V, Ziegler R, Rohrig T, Cochran RS, Götz RM, Levin MD, Pihlajoki M, Heikinheimo M & Wilson DB 2017 GLI1$^+$ progenitor cells in the adrenal capsule of the adult mouse give rise to heterotopic gonadal-like tissue. *Molecular and Cellular Endocrinology* **441** 164–175. (doi:10.1016/j.mce.2016.08.043)

Gao HB, Tong MH, Hu YQ, Guo QS, Ge R & Hardy MP 2002 Glucocorticoid induces apoptosis in rat leydig cells. *Endocrinology* **143** 130–138. (doi:10.1210/endo.143.1.8604)

Hall SJ, Bar-Chama N, Ta S & Gordon JW 2000 Direct exposure of mouse spermatogenic cells to high doses of adenovirus gene therapy vector does not result in germ cell transduction. *Human Gene Therapy* **11** 1705–1712. (doi:10.1089/10430340050111359)

Hendrickx R, Stichling N, Koelen J, Kuryk L, Lipiec A & Greber UF 2014 Innate immunity to adenovirus. *Human Gene Therapy* **25** 265–284. (doi:10.1089/hum.2014.001)

Ho NR, Usmani AR, Yin Y, Ma L & Conrad DF 2017 Multiplex shRNA screening of germ cell development by in vivo transfection of mouse testis. *G3* **7** 247–255. (doi:10.1534/g3.116.036087)

Hooley RP, Paterson M, Brown P, Kerr K & Saunders PT 2009 Intra-testicular injection of adenoviral constructs results in Sertoli cell-specific gene expression and disruption of the seminiferous epithelium. *Reproduction* **137** 361–370. (doi:10.1530/REP-08-0247)

Hu GX, Lin H, Chen GR, Chen BB, Lian QQ, Hardy DO, Zirkin BR & Ge RS 2010 Deletion of the Igf1 gene: suppressive effects on adult Leydig cell development. *Journal of Andrology* **31** 379–387. (doi:10.2164/jandrol.109.008680)

Ikawa M, Tergaonkar V, Ogura A, Ogonuki N, Inoue K & Verma IM 2002 Restoration of spermatogenesis by lentiviral gene transfer: offspring from infertile mice. *PNAS* **99** 7524–7529. (doi:10.1073/pnas.072207299)

Jackson NC, Jackson H, Shanks JH, Dixon JS & Lendon RG 1986 Study using in-vivo binding of 125I-labelled hCG, light and electron microscopy of the repopulation of rat Leydig cells after destruction due to administration of ethylene-1,2-dimethanesulphonate. *Journal of Reproduction and Fertility* **76** 1–10. (doi:10.1530/jrf.0.0760001)

Jimenez P, Saner K, Mayhew B & Rainey WE 2003 GATA-6 is expressed in the human adrenal and regulates transcription of genes required for adrenal androgen biosynthesis. *Endocrinology* **144** 4285–4288. (doi:10.1210/en.2003-0472)

Kanatsu-Shinohara M, Ogura A, Ikegawa M, Inoue K, Ogonuki N, Tashiro K, Toyokuni S, Honjo T & Shinohara T 2002 Adenovirus-mediated gene delivery and in vitro microinsemination produce offspring from infertile male mice. *PNAS* **99** 1383–1388. (doi:10.1073/pnas.022646399)

Kanatsu-Shinohara M, Toyokuni S & Shinohara T 2004 Transgenic mice produced by retroviral transduction of male germ line stem cells in vivo. *Biology of Reproduction* **71** 1202–1207. (doi:10.1095/biolreprod.104.031294)

Kerr JB, Donachie K & Rommerts FF 1985 Selective destruction and regeneration of rat Leydig cells in vivo. A new method for the study of seminiferous tubular-interstitial tissue interaction. *Cell and Tissue Research* **242** 145–156. (doi:10.1007/BF00225571)

Ketola I, Rahman N, Toppari J, Bielinska M, Porter-Tinge SB, Tapanainen JS, Huhtaniemi IT, Wilson DB & Heikinheimo M 1999 Expression and regulation of transcription factors GATA-4 and GATA-6 in developing mouse testis. *Endocrinology* **140** 1470–1480. (doi:10.1210/endo.140.3.6587)

Ketola I, Anttonen M, Vaskivuo T, Tapanainen JS, Toppari J & Heikinheimo M 2002 Developmental expression and spermatogenic stage specificity of transcription factors GATA-1 and GATA-4 and their cofactors FOG-1 and FOG-2 in the mouse testis. *European Journal of Endocrinology* **147** 397–406. (doi:10.1530/eje.0.1470397)

Kilcoyne KR, Smith LB, Atanassova N, Macpherson S, McKinnell C, van den Driesche S, Jobling MS, Chambers TJ, De Gendt K, Verhoeven G *et al*. 2014 Fetal programming of adult Leydig cell function by androgenic effects on stem/progenitor cells. *PNAS* **111** E1924–E1932. (doi:10.1073/pnas.1320735111)

Kim JM, Luo L & Zirkin BR 2000 Caspase-3 activation is required for Leydig cell apoptosis induced by ethane dimethanesulfonate. *Endocrinology* **141** 1846–1853. (doi:10.1210/endo.141.5.7444)

Kim TS, Choi HS, Ryu BY, Gang GT, Kim SU, Koo DB, Kim JM, Han JH, Park CK, Her S & Lee DS 2010 Real-time in vivo bioluminescence imaging of lentiviral vector-mediated gene transfer in mouse testis. *Theriogenology* **73** 129–138. (doi:10.1016/j.theriogenology.2009.07.028)

King SR, Rommerts FF, Ford SL, Hutson JC, Orly J & Stocco DM 1998 Ethane dimethane sulfonate and NNN′N′-tetrakis-(2-pyridylmethyl) ethylenediamine inhibit steroidogenic acute regulatory (StAR) protein expression in MA-10 Leydig cells and rat Sertoli cells. *Endocrine Research* **24** 469–478. (doi:10.3109/07435809809032635)

Kojima Y, Sasaki S, Umemoto Y, Hashimoto Y, Hayashi Y & Kohri K 2003 Effects of adenovirus mediated gene transfer to mouse testis in vivo on spermatogenesis and next generation. *Journal of Urology* **170** 2109–2114. (doi:10.1097/01.ju.0000092898.91658.08)

Krachulec J, Vetter M, Schrade A, Löbs AK, Bielinska M, Cochran R, Kyrönlahti A, Pihlajoki M, Parviainen H, Jay PY *et al*. 2012 GATA4 is a critical regulator of gonadectomy-induced adrenocortical tumorigenesis in mice. *Endocrinology* **153** 2599–2611. (doi:10.1210/en.2011-2135)

Kyrönlahti A, Euler R, Bielinska M, Schoeller EL, Moley KH, Toppari J, Heikinheimo M & Wilson DB 2011 GATA4 regulates Sertoli cell function and fertility in adult male mice. *Molecular and Cellular Endocrinology* **333** 85–95. (doi:10.1016/j.mce.2010.12.019)

LeCouter J, Lin R, Tejada M, Frantz G, Peale F, Hillan KJ & Ferrara N 2003 The endocrine-gland-derived VEGF homologue Bv8 promotes angiogenesis in the testis: localization of Bv8 receptors to endothelial cells. *PNAS* **100** 2685–2690. (doi:10.1073/pnas.0337667100)

Li T, Hu J, He GH, Li Y, Zhu CC, Hou WG, Zhang S, Li W, Zhang JS, Wang Z *et al*. 2012 Up-regulation of NDRG2 through nuclear factor-kappa B is required for Leydig cell apoptosis in both human and murine infertile testes. *Biochimica et Biophysica Acta* **1822** 301–313. (doi:10.1016/j.bbadis.2011.11.013)

Lobo MV, Arenas MI, Huerta L, Sacristan S, Perez-Crespo M, Gutierrez-Adan A, Diaz-Gil JJ, Lasuncion MA & Martin-Hidalgo A 2015 Liver growth factor induces testicular regeneration in EDS-treated rats and increases protein levels of class B scavenger receptors. *American Journal of Physiology – Endocrinology and Metabolism* **308** E111–E121. (doi:10.1152/ajpendo.00329.2014)

Machitani M, Sakurai F, Katayama K, Tachibana M, Suzuki T, Matsui H, Yamaguchi T & Mizuguchi H 2013 Improving adenovirus vector-mediated RNAi efficiency by lacking the expression of virus-associated RNAs. *Virus Research* **178** 357–363. (doi:10.1016/j.virusres.2013.09.021)

Manuylov NL, Zhou B, Ma Q, Fox SC, Pu WT & Tevosian SG 2011 Conditional ablation of Gata4 and Fog2 genes in mice reveals their

distinct roles in mammalian sexual differentiation. *Developmental Biology* **353** 229–241. (doi:10.1016/j.ydbio.2011.02.032)

Mazaud-Guittot S, Prud'homme B, Bouchard MF, Bergeron F, Daems C, Tevosian SG & Viger RS 2014 GATA4 autoregulates its own expression in mouse gonadal cells via its distal 1b promoter. *Biology of Reproduction* **90** 25.

Mitani K & Kubo S 2002 Adenovirus as an integrating vector. *Current Gene Therapy* **2** 135–144. (doi:10.2174/1566523024605591)

Molenaar R, de Rooij DG, Rommerts FF & van der Molen HJ 1986 Repopulation of Leydig cells in mature rats after selective destruction of the existent Leydig cells with ethylene dimethane sulfonate is dependent on luteinizing hormone and not follicle-stimulating hormone. *Endocrinology* **118** 2546–2554. (doi:10.1210/endo-118-6-2546)

O'Shaughnessy PJ & Fowler PA 2011 Endocrinology of the mammalian fetal testis. *Reproduction* **141** 37–46.

O'Shaughnessy PJ, Baker PJ, Heikkila M, Vainio S & McMahon AP 2000 Localization of 17beta-hydroxysteroid dehydrogenase/17-ketosteroid reductase isoform expression in the developing mouse testis–androstenedione is the major androgen secreted by fetal/neonatal leydig cells. *Endocrinology* **141** 2631–2637. (doi:10.1210/en.141.7.2631)

O'Shaughnessy PJ, Willerton L & Baker PJ 2002 Changes in Leydig cell gene expression during development in the mouse. *Biology of Reproduction* **66** 966–975. (doi:10.1095/biolreprod66.4.966)

O'Shaughnessy PJ, Morris ID & Baker PJ 2008 Leydig cell re-generation and expression of cell signaling molecules in the germ cell-free testis. *Reproduction* **135** 851–858. (doi:10.1530/rep-07-0529)

O'Shaughnessy PJ, Monteiro A, Fowler PA & Morris ID 2014 Identification of Leydig cell-specific mRNA transcripts in the adult rat testis. *Reproduction* **147** 671–682. (doi:10.1530/rep-13-0603)

Oka T, Maillet M, Watt AJ, Schwartz RJ, Aronow BJ, Duncan SA & Molkentin JD 2006 Cardiac-specific deletion of Gata4 reveals its requirement for hypertrophy, compensation, and myocyte viability. *Circulation Research* **98** 837–845. (doi:10.1161/01.RES.0000215985.18538.c4)

Padua MB, Jiang T, Morse DA, Fox SC, Hatch HM & Tevosian SG 2015 Combined loss of the GATA4 and GATA6 transcription factors in male mice disrupts testicular development and confers adrenal-like function in the testes. *Endocrinology* **156** 1873–1886. (doi:10.1210/en.2014-1907)

Pihlajoki M, Gretzinger E, Cochran R, Kyrönlahti A, Schrade A, Hiller T, Sullivan L, Shoykhet M, Schoeller EL, Brooks MD *et al*. 2013 Conditional mutagenesis of *Gata6* in SF1-positive cells causes gonadal-like differentiation in the adrenal cortex of mice. *Endocrinology* **154** 1754–1767. (doi:10.1210/en.2012-1892)

Pihlajoki M, Färkkilä A, Soini T, Heikinheimo M & Wilson DB 2016 GATA factors in endocrine neoplasia. *Molecular and Cellular Endocrinology* **421** 2–17. (doi:10.1016/j.mce.2015.05.027)

Qamar I, Park E, Gong EY, Lee HJ & Lee K 2009 ARR19 (androgen receptor corepressor of 19 kDa), an antisteroidogenic factor, is regulated by GATA-1 in testicular Leydig cells. *Journal of Biological Chemistry* **284** 18021–18032. (doi:10.1074/jbc.M900896200)

Qamar I, Ahmad MF & Narayanasamy A 2015 A time-course study of long term over-expression of ARR19 in mice. *Science Reports* **5** 13014. (doi:10.1038/srep13014)

Rahman NA, Kiiveri S, Rivero-Muller A, Levallet J, Vierre S, Kero J, Wilson DB, Heikinheimo M & Huhtaniemi I 2004 Adrenocortical tumorigenesis in transgenic mice expressing the inhibin alpha-subunit promoter/SV40 virus T-antigen transgene: relationship between ectopic expression of luteinizing hormone receptor and transcription factor GATA-4. *Molecular Endocrinology* **18** 2553–2569. (doi:10.1210/me.2002-0282)

Röhrig T, Pihlajoki M, Ziegler R, Cochran RS, Schrade A, Schillebeeckx M, Mitra RD, Heikinheimo M & Wilson DB 2015 Toying with fate: redirecting the differentiation of adrenocortical progenitor cells into gonadal-like tissue. *Molecular and Cellular Endocrinology* **408** 165–177. (doi:10.1016/j.mce.2014.12.003)

Rudigier LJ, Dame C, Scholz H & Kirschner KM 2017 Ex vivo cultures combined with vivo-morpholino induced gene knockdown provide a system to assess the role of WT1 and GATA4 during gonad differentiation. *PLoS ONE* **12** e0176296. (doi:10.1371/journal.pone.0176296)

Salva A, Hardy MP, Wu XF, Sottas CM, MacLaughlin DT, Donahoe PK & Lee MM 2004 Müllerian-inhibiting substance inhibits rat Leydig cell regeneration after ethylene dimethanesulphonate ablation. *Biology of Reproduction* **70** 600–607. (doi:10.1095/biolreprod.103.021550)

Schrade A, Kyrönlahti A, Akinrinade O, Pihlajoki M, Fischer S, Rodriguez VM, Otte K, Velagapudi V, Toppari J, Wilson DB & Heikinheimo M 2016 GATA4 regulates blood-testis barrier function and lactate metabolism in mouse Sertoli cells. *Endocrinology* **157** 2416–2431. (doi:10.1210/en.2015-1927)

Schrade A, Kyrönlahti A, Akinrinade O, Pihlajoki M, Häkkinen M, Fischer S, Alastalo TP, Velagapudi V, Toppari J, Wilson DB & Heikinheimo M 2015 GATA4 is a key regulator of steroidogenesis and glycolysis in mouse Leydig cells. *Endocrinology* **156** 1860–1872. (doi:10.1210/en.2014-1931)

Sher N, Yivgi-Ohana N & Orly J 2007 Transcriptional regulation of the cholesterol side chain cleavage cytochrome P450 gene (CYP11A1) revisited: binding of GATA, cyclic adenosine 3′,5′-monophosphate response element-binding protein and activating protein (AP)-1 proteins to a distal novel cluster of cis-regulatory elements potentiates AP-2 and steroidogenic factor-1-dependent gene expression in the rodent placenta and ovary. *Molecular Endocrinology* **21** 948–962. (doi:10.1210/me.2006-0226)

Shima Y & Morohashi KI 2017 Leydig progenitor cells in fetal testis. *Molecular and Cellular Endocrinology* **445** 55–64. (doi:10.1016/j.mce.2016.12.006)

Shima Y, Miyabayashi K, Haraguchi S, Arakawa T, Otake H, Baba T, Matsuzaki S, Shishido Y, Akiyama H, Tachibana T *et al*. 2013 Contribution of Leydig and Sertoli cells to testosterone production in mouse fetal testes. *Molecular Endocrinology* **27** 63–73. (doi:10.1210/me.2012-1256)

Shiraishi K & Ascoli M 2007 Lutropin/choriogonadotropin stimulate the proliferation of primary cultures of rat Leydig cells through a pathway that involves activation of the extracellularly regulated kinase 1/2 cascade. *Endocrinology* **148** 3214–3225. (doi:10.1210/en.2007-0160)

Smith L 2011 Good planning and serendipity: exploiting the Cre/Lox system in the testis. *Reproduction* **141** 151–161. (doi:10.1530/REP-10-0404)

Smith LB, O'Shaughnessy PJ & Rebourcet D 2015 Cell-specific ablation in the testis: what have we learned? *Andrology* **3** 1035–1049. (doi:10.1111/andr.12107)

Sodhi CP, Li J & Duncan SA 2006 Generation of mice harbouring a conditional loss-of-function allele of Gata6. *BMC Developmental Biology* **6** 19. (doi:10.1186/1471-213X-6-19)

Sriraman V, Sairam MR & Rao AJ 2003 Evaluation of relative roles of LH and FSH in regulation of differentiation of Leydig cells using an ethane 1,2-dimethylsulfonate-treated adult rat model. *Journal of Endocrinology* **176** 151–161. (doi:10.1677/joe.0.1760151)

Taylor MF, Woolveridge I, Metcalfe AD, Streuli CH, Hickman JA & Morris ID 1998 Leydig cell apoptosis in the rat testes after administration of the cytotoxin ethane dimethanesulphonate: role of the Bcl-2 family members. *Journal of Endocrinology* **157** 317–326. (doi:10.1677/joe.0.1570317)

Taylor MF, de Boer-Brouwer M, Woolveridge I, Teerds KJ & Morris ID 1999 Leydig cell apoptosis after the administration of ethane dimethanesulfonate to the adult male rat is a Fas-mediated process. *Endocrinology* **140** 3797–3804. (doi:10.1210/endo.140.8.6919)

Teerds KJ & Huhtaniemi IT 2015 Morphological and functional maturation of Leydig cells: from rodent models to primates. *Human Reproduction Update* **21** 310–328. (doi:10.1093/humupd/dmv008)

Teerds KJ, de Rooij DG, Rommerts FF, van den Hurk R & Wensing CJ 1989 Proliferation and differentiation of possible Leydig cell precursors after destruction of the existing Leydig cells with ethane dimethyl sulphonate: the role of LH/human chorionic gonadotrophin. *Journal of Endocrinology* **122** 689–696. (doi:10.1677/joe.0.1220689)

Tevosian S 2014 Transgenic mouse models in the study of reproduction: insight into GATA protein function. *Reproduction* **148** R1–R14. (doi:10.1530/REP-14-0086)

Tevosian SG, Jimenez E, Hatch HM, Jiang T, Morse DA, Fox SC & Padua MB 2015 Adrenal development in mice requires GATA4 and GATA6 transcription factors. *Endocrinology* **156** 2503–2517. (doi:10.1210/en.2014-1815)

Tremblay JJ 2015 Molecular regulation of steroidogenesis in endocrine Leydig cells. *Steroids* **103** 3–10. (doi:10.1016/j.steroids.2015.08.001)

Tremblay JJ & Viger RS 2001 GATA factors differentially activate multiple gonadal promoters through conserved GATA regulatory elements. *Endocrinology* **142** 977–986. (doi:10.1210/endo.142.3.7995)

Tsuzuki S, Tachibana M, Hemmi M, Yamaguchi T, Shoji M, Sakurai F, Kobiyama K, Kawabata K, Ishii KJ, Akira S *et al*. 2016 TANK-binding kinase 1-dependent or -independent signaling elicits the cell-type-specific innate immune responses induced by the adenovirus vector. *International Immunology* **28** 105–115. (doi:10.1093/intimm/dxv058)

Viger RS, Mertineit C, Trasler JM & Nemer M 1998 Transcription factor GATA-4 is expressed in a sexually dimorphic pattern during mouse gonadal development and is a potent activator of the Müllerian inhibiting substance promoter. *Development* **125** 2665–2755.

Virtanen HE & Toppari J 2014 Embryology and physiology of testicular development and descent. *Pediatric Endocrinology Reviews* **11** (Supplement 2) 206–213.

Watt AJ, Battle MA, Li J & Duncan SA 2004 GATA4 is essential for formation of the proepicardium and regulates cardiogenesis. *PNAS* **101** 12573–12578. (doi:10.1073/pnas.0400752101)

Wen Q, Cheng CY & Liu YX 2016 Development, function and fate of fetal Leydig cells. *Seminars in Cell and Developmental Biology* **59** 89–98. (doi:10.1016/j.semcdb.2016.03.003)

Wu HS, Lin HT, Wang CK, Chiang YF, Chu HP & Hu MC 2007 Human CYP11A1 promoter drives Cre recombinase expression in the brain in addition to adrenals and gonads. *Genesis* **45** 59–65. (doi:10.1002/dvg.20266)

Yan W, Kero J, Huhtaniemi I & Toppari J 2000 Stem cell factor functions as a survival factor for mature Leydig cells and a growth factor for precursor Leydig cells after ethylene dimethane sulfonate treatment: implication of a role of the stem cell factor/c-kit system in Leydig cell development. *Developmental Biology* **227** 169–182. (doi:10.1006/dbio.2000.9885)

Yang Y, Nunes FA, Berencsi K, Furth EE, Gonczol E & Wilson JM 1994 Cellular immunity to viral antigens limits E1-deleted adenoviruses for gene therapy. *PNAS* **91** 4407–4411. (doi:10.1073/pnas.91.10.4407)

Yang Y, Li Z, Wu X, Chen H, Xu W, Xiang Q, Zhang Q, Chen J, Ge RS, Su Z *et al*. 2017 Direct reprogramming of mouse fibroblasts toward Leydig-like cells by defined factors. *Stem Cell Reports* **8** 39–53. (doi:10.1016/j.stemcr.2016.11.010)

Zhang L, Wang H, Yang Y, Liu H, Zhang Q, Xiang Q, Ge R, Su Z & Huang Y 2013 NGF induces adult stem Leydig cells to proliferate and differentiate during Leydig cell regeneration. *Biochemical and Biophysical Research Communications* **436** 300–305. (doi:10.1016/j.bbrc.2013.05.098)

Zhang YF, Yuan KM, Liang Y, Chu YH, Lian QQ, Ge YF, Zhen W, Sottas CM, Su ZJ & Ge RS 2015 Alterations of gene profiles in Leydig-cell-regenerating adult rat testis after ethane dimethane sulfonate-treatment. *Asian Journal of Andrology* **17** 253–260. (doi:10.4103/1008-682X.136447)

Received 22 May 2017
First decision 13 June 2017
Revised manuscript received 9 July 2017
Accepted 14 July 2017